New approach for the treatment of pneumococcal diseases

Thesis submitted for the degree of

Doctor of Philosophy

at the University of Leicester

by

Mafalda Pires Damaso

Department of Infection, Immunity and Inflammation

University of Leicester

September 2010

À minha mãe, Antónia, ao meu pai, Joaquim, e ao meu paciente e carinhoso companheiro, Ricardo.

University of Leicester

Statement of Originality

The accompanying thesis submitted for the degree of PhD entitled "New approach for the treatment of pneumococcal diseases" is based on work conducted by the author in the Department of Infection, Immunity and Inflammation at the University of Leicester mainly during the period between September 2006 and September 2010.

All the work recorded in this thesis is original unless otherwise acknowledged in the text or by references.

None of the work has been submitted for another degree in this or any other University

Signed:_____ Date:_____

Name: MAFALDA PIRES DAMASO

Acknowledgements

I would first like to thank my supervisor Professor Peter Andrew for giving me the opportunity to work in this exciting and challenging project, and for his guidance during my research in his laboratory and throughout the writing-up period of my thesis.

I would also like to express my deepest and sincere gratitude to Dr. Rana Lonnen for her invaluable support, for sharing her knowledge with me and, especially, for our precious friendship. I am also grateful to Dr. James Lonnen for his positive words and for making sure that Rana and I would arrive safe at home after the long and late hours at work.

My sincere appreciation is extended to my co-supervisor Professor Christopher O'Callaghan and his team, Dr. Rob Hirst, Dr. Claire Smith and Norman Baker, for their tremendous support and guidance during the *ex vivo* work conducted at the Leicester Royal Infirmary.

I am also greatly indebted to the European Union for funding this project, PEUMOPEP, and to all partners of the PNEUMOPEP consortium, who contributed for the success of this work.

A special thanks goes to Dr. Fritz Frickel, who kindly contributed to this project with his expertise in the field of medicinal chemistry.

I would also like to thank all people in Lab 227, who have helped me during this project, in particular, Sandra Germano, Sarah Glenn and Vitor Fernandes; the members of the Division of Biomedical Services, specially, Ken White for his comprehension and assistance; Professor Leonor Faleiro, from the University of Algarve, for helping me to establish a link with the University of Leicester.

Last, but not least, I thank my family and my partner, Ricardo, for their unconditional love and for their words of encouragement.

Abstract

Pneumolysin (PLY) is a proven virulence factor of *Streptococcus pneumoniae*, deeply involved in the development of pneumococcal invasive diseases. The antibacterial and adjunctive therapies currently used in the management of pneumococcal infection do not address the pneumolysin-induced cytotoxicity. Therefore, even if patients survive the infection, they may suffer from long-term disabilities as a consequence of the exposure to the toxin. This research seeks to address this problem by developing new approaches to the treatment of pneumococcal diseases, based on peptides or small molecules that target pneumolysin and inhibit its activity. The peptides and small molecules were evaluated for their capacity to inhibit the haemolytic activity of pneumolysin *in vitro*. In total, four peptides and six small molecules were selected for *in vivo* tests. *In vivo* experiments were performed using a pneumonia model, where each animal was administered PBS or peptide / small molecule in PBS intranasally, every 6 hours after intranasal infection. One peptide (P1) and three small molecules (SM6, SM10 and SM14) improved significantly the outcome of the treatment group over the control group, when looking at the CFU in the blood, disease sign score and survival comparison. Moreover, two small molecules (SM10 and SM14) tested *ex vivo*, showed the capacity to abolish pneumolysin cytotoxic effect on the ciliary function of rat ependymal cells. The pneumolysin inhibitors identified in this work were pointed as potential candidates to further testing in drug discovery.

Abbreviations

Ala - Alanine

***Amp*^{r} -** gene for resistance to ampicillin

Å - Angstroms

AUC - Area under the curve

A_{λ} - Absorbance

BAB - Blood agar base

BHI - Brain heart infusion

BSA - Bovine serum albumin

CBF - Ciliary beat frequency

CDCs - Cholesterol-dependent cytolysins

CFU - Colony forming units

C_{max} - Highest plasma drug concentration

Cys - Cysteine

DMSO - Dimethyl sulfoxide

DNA - Deoxyribonucleic acid

dNTPs - Deoxynucleotides

FBS - Foetal bovine serum

GFP - Green Fluorescent Protein

His – Histidine

HTS - High throughput screening

HU - Haemolytic units

I.N. – Intranasal(ly)

I.P. – Intraperitoneal(ly)

I.V. - Intravenous(ly)

IMAC - Immobilized metal affinity chromatography

IPTG - Isopropyl β-D-1-thiogalactopyranoside

IR - Infrared

***Kan*^{r} -** gene for resistance to kanamycine

LA - Luria-agar

LB - Luria-Bertani

LDS - Lithium dodecyl sulphate

LMV - Large multilamellar vesicles

mA - milliampere

MEM - Minimum essential medium

OD_{λ} - Optical density

PBS - Phosphate Buffered Saline

PBS-T - PBS plus 0.05% (v/v) Tween 20

PCR - Polymerase chain reaction

PK - Pharmacokinetic

PLY - pneumolysin

POPC - Palmitoyloleoyl phosphatidylcholine

psi - pound *per* square inch

S - Siemens

SDS - Sodium dodecyl sulfate

SUV - Small unilamellar vesicles

TAE - Tris-Acetic Acid-EDTA

TB - Terrific-broth

TEMED - (N, N, N', N'- tetramethylethylenediamine)

TGS - Tris-Glycine-SDS

T_{max} - Time at which the C_{max} occurs

TMHs - Transmembrane β-hairpins

Trp - Tryptophan

UV- Ultraviolet

V- Volt

λ - Wavelength (nm)

Table of Contents

Chapter 1 - Introduction

1.1. *Streptococcus pneumoniae*

Streptococcus pneumoniae, also referred to as the pneumococcus, is a Gram-positive encapsulated, fermentative bacterium, which usually grows in pairs but can also be found in short chains in blood cultures (Figure 1.1) or liquid media (Alonso de Velasco *et al.*, 1995; Gray, 2000). Though it is carried asymptomatically in the upper respiratory tract of many individuals (Tuomanen *et al.*, 2004), it is a human pathogen of major importance (Berry *et al.*, 1995), causing serious invasive diseases such as pneumonia, meningitis, and bacteraemia, in addition to otitis media and acute sinusitis. The incidence of these pneumococcal diseases is highest in infants under 2 years of age and in people over 60 years of age (Alonso de Velasco *et al.*, 1995).

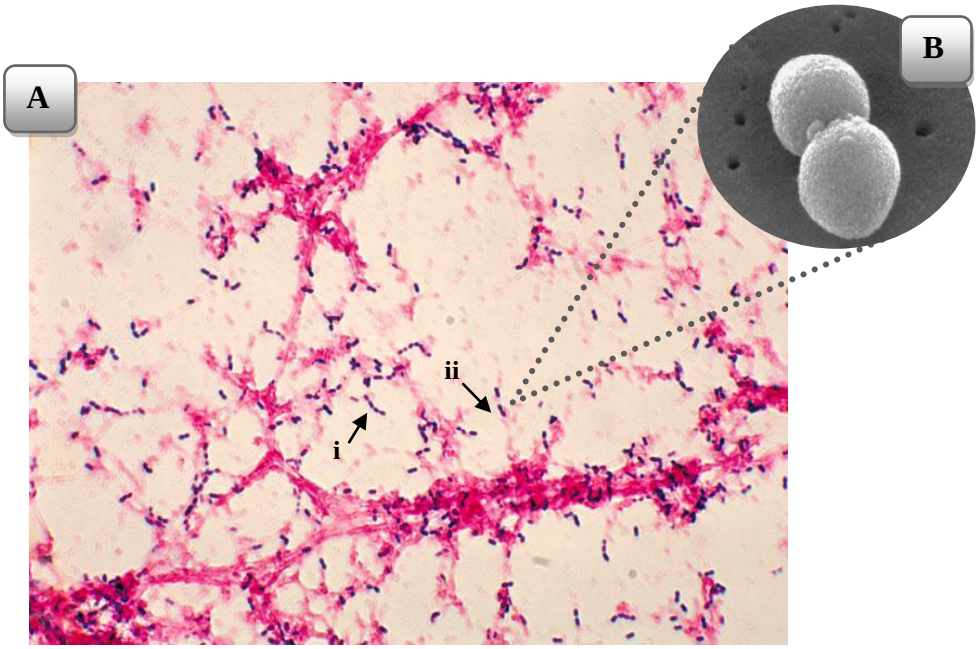

Figure 1.1- *S. pneumoniae* (A) grown from a blood culture: i) Gram-positive cocci chain; ii) Gram-positive diplococci. (B) Scanning electron micrograph of a pair of diplococci. Images obtained and modified from CDC Public Health Image Library.

1.1.1. Epidemiology and serotype distribution

Although all age groups may be affected, the incidence of invasive pneumococcal diseases (IPD) is greater among the very young and elderly groups. Even though the rates of cases are similar between these groups, the elderly are more likely to die from invasive infections (e.g. Figure 1.2), probably because of underlying medical conditions and age related immune dysfunction (Tuomanen *et al.*, 2004).

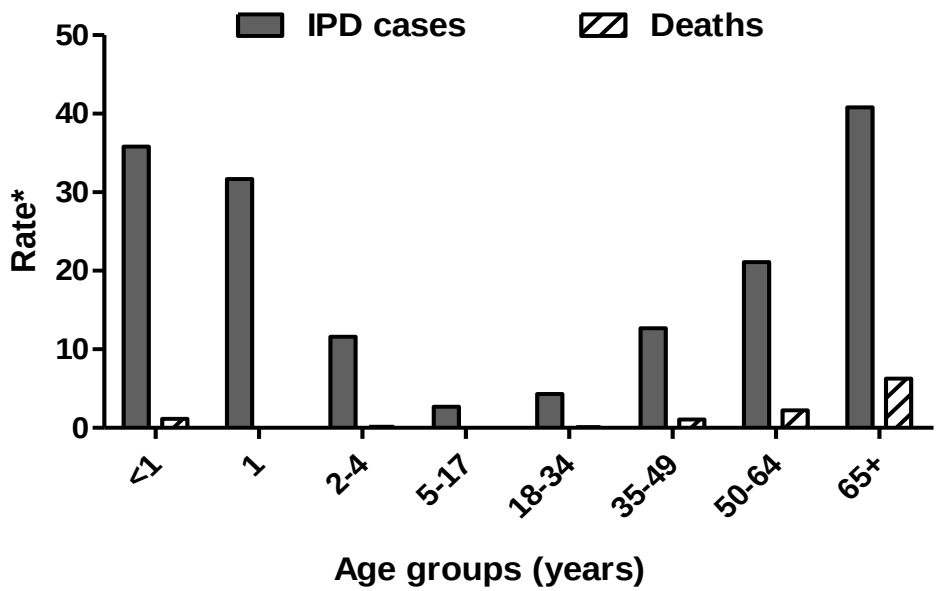

Figure 1.2 – Incidence of cases and deaths caused by invasive pneumococcal diseases by age (*Cases/100,000 population), USA, provisional 2008. Source: Active Bacterial Core Surveillance/EIP Network (CDC - Centers for Disease Control and Prevention, 2008).

Pneumococcal infections also impose an increased risk to groups with chronic medical conditions and immune deficiencies, such as sickle cell anaemia, asplenia and HIV infection (WHO, 2009).

There are several population-based surveillance reports which seem to show considerable differences on the incidence and mortality rates of IPD across the globe, in particular between industrialised and developing countries. For instance, a global surveillance study in children aged 1-59 months, in 2000, estimated the occurrence of

approximately 14.5 million invasive pneumococcal disease episodes. About 826,000 deaths resulted, of which 91,000 occurred in HIV-positive and 735,000 in HIV-negative children. Of the deaths in children without underlying medical conditions, over 61% occurred in ten African and Asian countries (O'Brien *et al.*, 2009).

Although less severe, other forms of pneumococcal disease such as middle-ear infection (otitis media), sinusitis or recurrent bronchitis occur among children. For instance, in the USA alone, seven million cases of otitis media are attributed to *S. pneumoniae* each year (WHO, 2009).

In industrialized countries, the reported annual incidence of IPD in persons over 65 ranges from 24-85 cases per 100,000 population (WHO, 2008). Pneumococcal pneumonia is estimated to account for at least 30% of all cases of community-acquired pneumonia (CAP) requiring hospitalisation, with a case fatality rate of 11% to 44%. For instance, the annual incidence of community-acquired pneumonia in 2002, in the USA, was approximately 18 cases per 100,000 elderly people and the incidence of pneumococcal pneumonia was at least 5.5 cases per 100,000 elderly population (WHO, 2009). Pneumococcal bacteraemia occurs in more than 25% of patients with pneumococcal pneumonia (Afessa *et al.*, 1995; Riley, 2000), and is responsible for up to 60% of case fatalities among elderly people (WHO, 2007).

The incidence of IPD in the general adult population in developing countries is not clear. Few studies conducted in these areas have been undertaken to evaluate the impact of HIV infection on pneumococcal disease. In a study on the HIV-infected adult population conducted in Uganda in 2002 (French *et al.*, 2000), an annual incidence of 1700 cases of IPD per 100,000 population was reported. In another study among HIV-positive commercial sex workers in Kenya, an annual incidence of pneumococcal disease of 4250 per 100,000 population was reported (Gilks *et al.*, 1996). Studies like

these provide clear evidence of the strong influence of HIV- infections on the increase of IPD rates.

In addition, there seems to be a seasonal pattern in the incidence of IPD. Every year, an increase in rates of IPD is registered during the winter and early spring months in temperate areas (e.g. Figure 1.3), when respiratory viral infection, more particularly caused by influenza A, are more common (Dowell *et al.*, 2003).

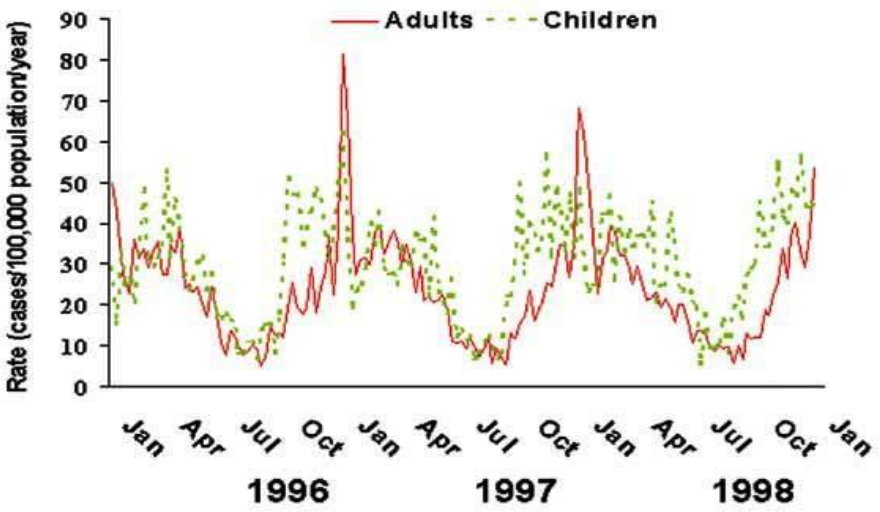

Figure 1.3 - Weekly rates of invasive pneumococcal disease in children (dotted line; ages 0–17 years) and adults (solid line; age >18 years) in the United States, 1996–1998. Data obtained from Dowell *et al.*, 2003.

On the basis of the differences in capsular polysaccharide structure on the surface of *S. pneumoniae*, which constitutes a primary virulence factor, it is possible to divide the pneumococci into 90 serotypes (Henrichsen, 1999). Nevertheless, the majority of invasive pneumococcal infections are caused by strains representing only a small number of serotypes. Although the distribution of serotypes isolates varies among age groups and geographic location (Scott *et al.*, 1996), it is possible to recognise some trends. The predominant serotypes among adults are 1, 3, 4, 5, 6A, 6B, 7F, 8, 9N, 9V, 11A, 12F, 14, 18C, 19A, 19F, 22F and 23F. Within this group, types 3, 7F, 9V, 14 and 23F are the ones that occur with more frequency and types 3, 6B and 19F are commonly

associated with fatal cases (Henriques *et al.*, 2000). In children, the most predominant serotypes causing invasive diseases are 1, 4, 5, 6A, 6B, 9V, 14, 18C, 19A, 19F and 23F (CDC - Centers for Disease Control and Prevention, 1997). Serotype 3 strains occur frequently in cases of otitis media but rarely cause invasive diseases in children.

1.1.2. Virulence factors

Streptococcus pneumoniae expresses different virulence factors, which contribute to its pathogenicity. Most of the expressed virulence factors are situated on its cell surface, whereas the rest of them are located in the cytoplasm. These factors are involved in direct interactions with host tissues or in concealing the bacterial surface from the host defense mechanisms (Jedrzejas, 2001). Some of the main virulence factors of *S. pneumoniae* are shown in Figure 1.4 and they are briefly described below.

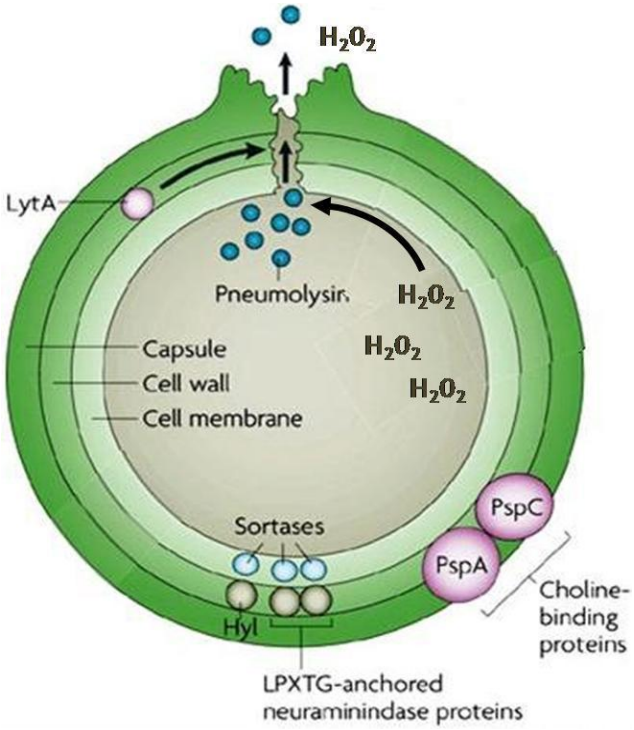

Figure 1.4- Main virulence factors of *S. pneumoniae*. The capsule; the cell wall; choline-binding proteins PspA and PspC (pneumococcal surface protein A and C, respectively); the LPXTG-anchored neuraminidase proteins; (Hyl) hyaluronidase; (LytA) autolysin A; (Ply) Pneumolysin; (H_2O_2) hydrogen peroxide. Image obtained and modified from Kadioglu *et al.*, 2008.

The **capsule** is an essential pneumococcal virulence factor (Watson & Musher, 1990). The capsule consists of high molecular weight polymers which may be classified as linear heteropolymers, composed of ≥2 monosaccharides, or multichained heteropolymers, composed of 2-5 monosaccharides with additional residues (Van Dam *et al.*, 1990; Gillespie, 1989). The chemical structure and the quantity of capsular polysaccharide produced determine the ability of the different serotypes to cause invasive diseases (Alonso de Velasco *et al.*, 1995). All serotypes are antigenic (Gillespie, 1989) but are in general poor immunogens, since they incite a weak primary antibody response and give no memory response (Van Dam *et al.*, 1990). The capsule constitutes a primary mechanical barrier against host immune cells by preventing (i) complement component C3b, deposited on the cell wall, becoming opsonically active (Angel *et al.*, 1994; Hostetter, 1986) and (ii) phagocytosis of bacteria by neutrophils (Matthay *et al.*, 1981; Chudwin *et al.*, 1985).

The **cell wall** is mainly composed of peptidoglycan with **cell wall polysaccharide,** a complex teichoic acid containing phosphorylcholine residues, attached to it via N-acetylmuramic acid (Jennings *et al.*, 1980). In contrast to the capsular polysaccharide, the cell wall polysaccharide is common to all pneumococcal serotypes (Alonso de Velasco *et al.*, 1995). This cell wall component is involved in the activation of host inflammatory response, by the activation of the alternative complement pathway (Winkelstein & Tomasz, 1978). During this stage, the anaphylatoxins C3a and C5a are produced, resulting in the (i) enhancement of vascular permeability, (ii) mast cell degranulation and (iii) recruitment and activation of neutrophils at the inflammation site (Johnston & R.B, 1991). The cell wall polysaccharide stimulates the production of the cytokine interleukin-1 (IL-1) (Riesenfeld-Orn *et al.*, 1989) and it also plays a role as a mediator of pneumococcal attachment to endothelial cells (Geelen *et al.*, 1993).

The **pneumococcal surface protein A** (PspA) is a surface protein found in all pneumococcal strains but with structural and antigenic variability between them (Crain *et al.*, 1990). Structural studies of PspA showed that its highly electronegative properties stabilise the pneumococcal capsular charge, which interferes with the fixation of the complement component C3 to its surface, so preventing complement-mediated opsonisation (Tu *et al.*, 1999; Kadioglu *et al.*, 2008). PspA also binds to the glycoprotein lactoferrin, an important component of innate immunity. It is thought that through this binding PspA blocks the active site(s) of apolactoferrin (iron-depleted form of lactoferrin), protecting bacterium from its bactericidal activity (Shaper *et al.*, 2004). There are some studies on the *in vivo* effect of deleting the *pspA* gene, using serotype 3 and 4 strains, which showed the importance of PspA for *in vivo* growth (McDaniel *et al.*, 1987; Hava & Camilli, 2002). However, similar experiments involving serotype 2 strains failed to show an effect (Berry & Paton, 2000).

The **pneumococcal surface protein C** (PspC) is associated with the adherence of pneumococci to host tissues. This is may be due with the ability of PspC to bind glycoconjugates on the surface of epithelial cells of the host (Rosenow *et al.*, 1997; Smith & Hostetter, 2000; Kadioglu *et al.*, 2008). PspC also binds the polymeric immunoglobulin receptor, which plays a crucial role in the mucosal immunity by transporting the polymeric IgA across the mucosal epithelium. This ability could be the first stage of the translocation of pneumococci across human nasopharyngeal epithelial cells (Zhang *et al.*, 2000a; Dave *et al.*, 2004; Kadioglu *et al.*, 2008). An additional property of this surface protein is its ability to bind complement factor H, thereby inhibiting alternative complement activation and phagocytosis (Quin *et al.*, 2005; Kadioglu *et al.*, 2008).

Autolysin A (LytA) or N-acetylmuramoyl-L-alanine amidase is an enzyme involved in the growth of *S. pneumoniae* by allowing cell division by cleavage of the N-acetylmoranoyl-L-alanine bond of pneumococcal peptidoglycan (Giudicelli & Tomasz, 1984; Alonso de Velasco *et al.*, 1995; Kadioglu *et al.*, 2008). However, during the stationary phase of growth, pneumococcal cells release the Forssman antigen (lipoteichoic acid which contains phosphorylcholine residues), a powerful inhibitor of LytA (Horne & Tomasz, 1985; Alonso de Velasco *et al.*, 1995). As a consequence, in the absence of Forssman antigen the enzyme undergoes unrestrained activity which induces bacterial lysis and enhances inflammation through the release of pneumococcal cytoplasm contents (e.g. pneumolysin) (Alonso de Velasco *et al.*, 1995). *S. pneumoniae* isogenic mutants not expressing autolysin A (*lyt A*$^-$) were shown to have reduced virulence in murine models of pneumonia, bacteraemia and meningitis (Canvin *et al.*, 1995; Berry & Paton, 2000; Hirst *et al.*, 2008).

To the date, there are three known types of pneumococcal **neuraminidases**: NanA, NanB and NanC. All pneumococcal strains express NanA and most of them also express NanB, however, only about 50% of strains express NanC (Kadioglu *et al.*, 2008). These enzymes are secreted from the cells but only NanA contains a C-terminal sequence LPXTGX, which allows it to covalently bind to peptidoglycan (Camara *et al.*, 1994). Neuraminidases cleave terminal sialic acid residues from cell surface glycolypids and glycoproteins. This activity is thought to result in the exposure of host cell surface receptors for possible interaction with pneumococci, contributing to increased adhesion and other processes (Paton *et al.*, 1993, Manco *et al.*, 2006). On the other hand, it has been shown that sialic acid itself is a signaling molecule that induces the expression of NanA and NanB and results in an enhanced capacity of pneumococci to adhere to host surfaces and/or survive within a biofilm environment (Trappetti *et al.*, 2009). There is

not yet an experimental proof of the biological role of NanC, however it may have a tissue-specific role, as it is more common to find NanC in isolates from CSF rather than in carriage isolates (Pettigrew *et al.*, 2006).

Hyaluronidase (Hyl) is produced by most strains of *S. pneumoniae* (Humphrey, 1948). The enzyme may facilitate host invasion by *S. pneumoniae* by degrading hyaluronan (also known as hyaluronic acid), an important component of connective tissues (Gillespie & Balakrishnan, 2000; Feldman *et al.*, 2007). Studies have been made in order to understand the importance of the role of hyaluronidase in the pathogenesis of pneumococcal infections. It has been demonstrated that pneumococcal strains with higher hyaluronidase activity breach the blood-brain barrier and disseminate more effectively (Kostyukova *et al.*, 1995). In addition, pneumococcal strains isolated from patients with meningitis and meningoencephalites have been shown to have significantly higher hyaluronidase activity than strains causing purulent otitis media (Volkova *et al.*, 1994). Another study has suggested that this enzyme may also contribute to pneumolysin-mediated damage and dysfunction of respiratory epithelium (Feldman *et al.*, 2007).

Pneumolysin (Ply) is a major virulence factor of *S. pneumoniae* (Canvin *et al.*, 1995, Rubins *et al.*, 1996; Hirst *et al.*, 2004a; Hirst *et al.*, 2008). It is a pore forming toxin produced in the cytoplasm of pneumococci (Jonhson, 1977). Details of the toxin's mechanisms of action and role in the pneumococcal pathogenesis are discussed in section 1.2.

Hydrogen peroxide produced by pneumococcus was found to have toxic effects on rat alveolar epithelial cells *in vitro*, which suggested that this factor may contribute to lung injury in cases of pneumococcal pneumonia (Dowell *et al.*, 2003). Hydrogen peroxide has also been demonstrated to cause mitochondrial damage and apoptosis of human

neuronal cells *in vitro* (Braun *et al.*, 2002), and to induce cell toxicity by inhibiting ependymal ciliary beat frequency on rat brain slices (Hirst *et al.*, 2000). In addition, hydrogen peroxide has been shown to contribute to neuronal damage in a rabbit model of pneumococcal meningitis (Braun *et al.*, 2002). This virulence factor was also shown to have a bactericidal effect against other common inhabitants of the host respiratory tract (e.g. *Haemophilus influenzae, Neisseria meningitidis*), during co-culture *in vitro* (Pericone *et al.*, 2000; Pericone *et al.*, 2003).

1.1.3. Pneumococcal pathogenesis

In Figure 1.5 some of the aspects of pneumococcal pathogenesis are represented.

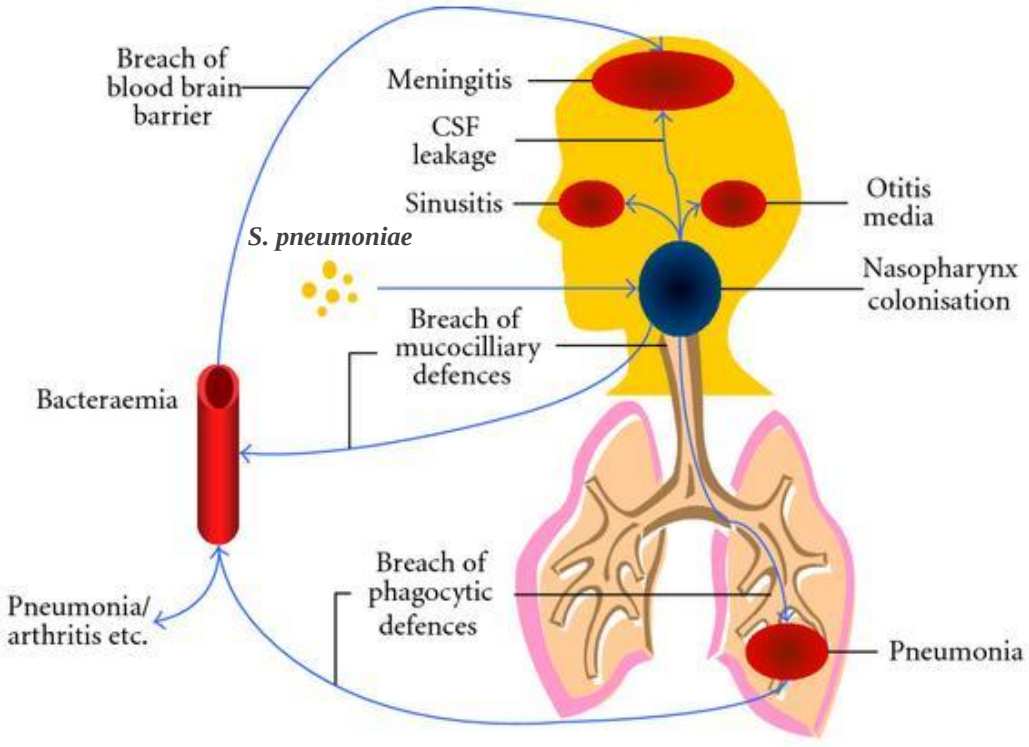

Figure 1.5- Schematic representation of the routes of host invasion by *S. pneumoniae*, which may lead to the development of invasive disease. Image obtained and modified from Goonetilleke et al., 2009.

Transmission of *S. pneumoniae* occurs through direct contact with the respiratory droplets from individuals with pneumococcal infections or, more often, individuals asymptomatically carrying the microorganism in the nasopharynx (Tuomanen *et al.*, 2004). Once established in the nasopharynx, many pneumococcal strains may be carried for long periods of time, without the occurrence of infections (Kadioglu *et al.*, 2008). Nevertheless, it is still not clear how effective colonisation is as an immunising event. Colonisation is most common in early childhood, beginning shortly after birth, and starting to decline with increasing age (Gillespie, 1989; Kadioglu *et al.*, 2008). Most infants acquire one or more strains sequentially or simultaneously, with rates of carriage varying widely among the known pneumococcal capsular serotypes (Kadioglu *et al.*, 2008). Among adults, the probability of pneumococcal carriage depends on the frequency of contact with children (Gillespie, 1989). Colonisation increases in frequency during the "colder" months in temperate areas, when viral infection are most common (Gillespie, 1989; Dowell *et al.*, 2003,). In this regard, it has been shown that adherence of pneumococci to the epithelial cells of the upper respiratory tract can be enhanced by preceding viral infections (Plotkowski *et al.*, 1986).

Most infections do not occur after long periods of carriage but rather are believed to take place following the acquisition of a new serotype (Richard B. Johnston, Jr., 1991). The confinement or not of pneumococci to the nasopharynx, is determined by the immune status of the host and by the virulence of the colonising strain (Alonso de Velasco *et al.*, 1995). A breach in the specific and nonspecific host defences of the upper respiratory tract, induced by some of the virulence factors described before, may facilitate the invasion of pneumococcus to the lower respiratory tract, nasal sinuses or middle ear. Epithelial damage may also facilitate direct access of pneumococcus to the bloodstream (Boulnois, 1992, Musher, 1992).

Once in the lungs, there is an inflammatory response by the host but it appears that in many cases this does not halt progression of the pneumococci to the blood. From the blood, *S. pneumoniae* may migrate to the meninges and there disrupt the blood-brain barrier to reach the subarachnoid space. Alternatively, they may reach the meninges directly from the nasopharynx (Boulnois, 1992).

1.1.4. Current strategies employed in the prevention and treatment of pneumococcal diseases and the problems associated with their use

1.1.4.1. Pneumococcal vaccines

At the present, there are two types of pneumococcal vaccines available on the market, based on purified *S. pneumoniae* capsular polysaccharides: the pneumococcal polysaccharide vaccines (PPV23) and the pneumococcal conjugated vaccine (PCV7). These vaccines were developed to induce the production of type-specific antibodies against pneumococcal capsular polysaccharides that would activate and fix the complement, promoting bacterial opsonisation and phagocytosis, and therefore, help in the prevention of pneumococcal diseases (WHO, 2009).

The PPV23, licensed in 1983, has been used to vaccinate people over 65 years of age, and people aged 2-64 years who have a chronic illness (e.g. cardiovascular or pulmonary disease, sickle cell disease, diabetes) or a weakened immune system due to an illness (e.g. HIV infection, Hodgkin's disease, chronic renal failure) (Schrag *et al.*, 2001; NFID, 2009). These vaccines are currently manufactured by Merck (Pneumovax 23) and by Sanofi Pasteur (Pneumo 23) (Siber *et al.*, 2008). A 0.5 ml dose of these vaccines contain 25 µg of purified capsular polysaccharides from each of 23 different pneumococcal serotypes (1, 2, 3, 4, 5, 6B, 7F, 8, 9N, 9V, 10A, 11A, 12F, 14, 15B, 17F, 18C, 19A, 19F, 20, 22F, 23F and 33F) and contains no adjuvant. These serotypes

account for most cases of invasive pneumococcal diseases (approximately 90%) in industrialised countries (e.g. Europe, North America) (WHO, 2008). The unavailability of reliable serotype data from developing countries may mean that the vaccine will be less efficient than predicted, if the serotype distribution there differs markedly from those in industrialised countries (Gillespie, 1989).

Pneumococcal polysaccharides are T-cell independent antigens (Gillespie, 1989; Siber *et al.*, 2008). Therefore, the pneumococcal polysaccharide vaccine is poorly immunogenic in (i) immunocompromised patients (e.g. patients with sickle cell disease, chronic renal failure, immunoglobulin deficiency, Hodgkin's disease, leukemia) (Shapiro *et al.*, 1991; Niederman *et al.*, 2001), (ii) elderly people, in particular those with chronic illnesses (Huss *et al.*, 2009), and (iii) children less < 2 years old (WHO, 2008). PPV23 is also unable to elicit immune memory, so that a second dose does not boost antibody levels (WHO, 2009). Following a single dose of PPV23 serotype specific IgM, IgA and IgG2 are, in decreasing order, produced (Gillespie, 1989). In addition, PPV23 does not provide protection against mucosal infections, and therefore, it is unable to reduce pneumococcal carriage in the nasopharynx (WHO, 2008).

The limitations of PPV23 contributed for the development and subsequent introduction of the hepta-valent pneumococcal conjugated vaccine (Prevnar; Wyeth), in 2000. The PCV7 contains polysaccharides from seven pneumococcal serotypes (4, 6B, 9V, 14, 18C, 19F and 23F), each one conjugated to a protein carrier. In Prevnar this carrier is the genetically detoxified diphtheria toxin CRM_{197} (Siber *et al.*, 2008). The vaccine is adsorbed onto aluminium phosphate to enhance the antibody response (Siber *et al.*, 2008). The use of this vaccine is particularly recommended in routine vaccination programmes of children < 2 years old (Siber *et al.*, 2008). Despite the remarkable effectiveness of the vaccine in reducing the incidence of pneumococcal diseases caused

by the vaccine-serotypes (Lopalco, 2007), there are certain disadvantages associated with its use. For instance, the serotypes included in the PCV7 provide between 65%-80% coverage of the serotypes associated with IPD among children, in industrialised countries. However, the prevalence of pneumococcal serotypes varies geographically, and as a consequence, the coverage provided by PCV7 in developing countries is much lower (WHO, 2007). In addition, since the introduction of the vaccine in 2000, serotype replacement has been observed among populations of children, with an increase in the cases of pneumococcal diseases caused by non-vaccine serotypes (Eskola *et al.*, 2001; O'Brien *et al.*, 2007). Finally, but not less importantly, there is also the high-cost of the vaccine, which makes its use restricted to "third world" countries (Lopalco, 2007).

1.1.4.2. Treatment of pneumococcal diseases

The selection of antibiotics employed in the treatment of pneumococcal diseases depends on the location of infection and on the age of the patient (Tuomanen *et al.*, 2004). The treatment is generally based on the use of penicillins, third generation cephalosporins (such as cefotaxime and ceftriaxone) and macrolides (such as erythromycin, azithromycin and clarithromycin) (Tuomanen *et al.*, 2004). Vancomycin has also been used in the treatment of penicillin-resistant and cephalosporin-resistant pneumococcal meningitis (Klugman, 1994; MERCK, 2009). Due to its poor CSF penetration when used as a sole agent, vancomycin is commonly administered along with other antibiotics, such as ceftriaxone, cefotaxime (MERCK, 2009). Fluoroquinolones, a family of synthetic broad-spectrum antibiotics, have been also used for the treatment of pneumococcal pneumonia in adults (Tuomanen *et al.*, 2004).

There has been a marked increase in the number of drug resistant *S. pneumoniae*, primarily against beta-lactam antibiotics and macrolides (Reinert, 2009). For instance, in a study undertaken in Hong Kong, the prevalence of penicillin-resistance *S.*

pneumoniae isolates rose from 6.6% in the first quarter of 1993 to 55.8% of isolates in the second quarter of 1995; and most of the isolates were also resistant to co-trimoxazole, tetracycline, chloramphenicol and erythromycin (Lyon *et al.*, 1996). Also, in a surveillance study on antibiotic resistance in invasive pneumococcal disease (Reinert *et al.*, 2002), conducted in Germany between 1992 and 2000, an increase in both macrolide and penicillin resistance was observed. The percentage of strains exhibiting reduced susceptibility to penicillin increased from 1.8% in 1992 to 5.8% in 2000. A marked increase in resistance was observed with erythromycin, where the resistance rate rose from 3.0% in 1992 to 15.3% in 2000 (Reinert *et al.*, 2002).

Numerous studies have shown the close link between the increase in antibiotics consumption and the emergence of resistant pneumococcal strains (WHO, 2009). For example, in the study by Reinert and colleagues (Reinert *et al.*, 2002), analysis of antibiotic consumption data showed that erythromycin resistance was highly correlated with the consumption of total macrolides (Figure 1.6).

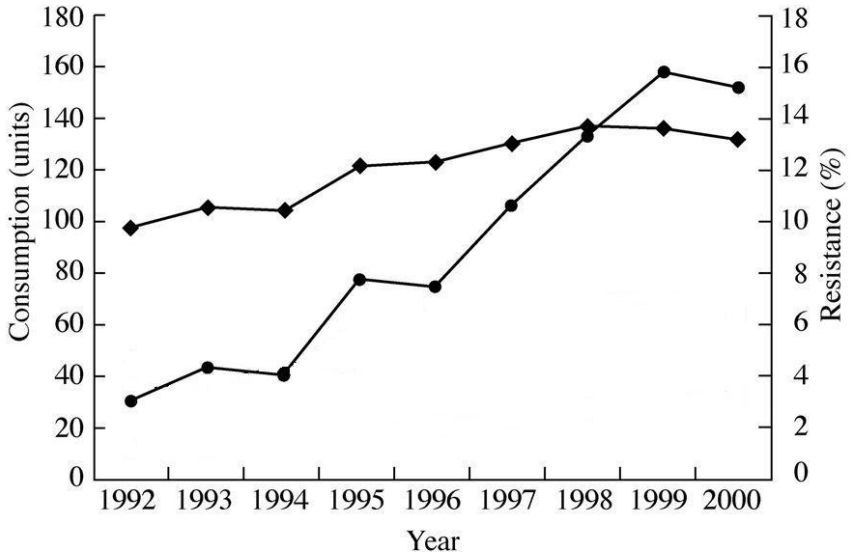

Figure 1.6 – Correlation between the consumption total macrolides (♦) and the increased resistance of pneumococci to erythromycin (•) in Germany (1992-2000). Data obtained from Reinert *et al.*, 2002.

Similarly, a longitudinal analysis of invasive *S. pneumoniae* in the United States found that increases in the prevalence of penicillin-resistant pneumococci in the early 1990s correlated with increased prescription rates for certain β-lactam agents, while a fairly constant prevalence of tetracycline-resistant pneumococci was associated with slight decreases in the prescription rate for tetracycline (Butler *et al.*, 1996).

Even when the right antibacterial therapy is employed, the consequent release of the pneumococcal toxins, in particular pneumolysin, may lead to irreversible neurological-sequelae or death (Rani *et al.*, 2005; Saha *et al.*, 2009).

1.1.4.3. Use of corticosteroids as adjunctive therapy in the management of pneumococcal meningitis

The administration of corticosteroids, such as dexamethasone, along with antibiotics has been used in the treatment of pneumococcal meningitis, in order to reduce the mortality rates and neurologic sequelae associated with the disease (Van De Beek *et al.*, 2007). The major sequelae of meningitis consist of motor lesions, and behavioral disturbances (Santana-Arciaga, 1996). Motor lesions include seizures, spasticity and paresis; whereas the cognitive deficits seem to be in the areas of motor integrity, perceptual motor skill, new learning, and the ability to process several stimuli simultaneously (Santana-Arciaga, 1996). Hearing loss is another important complication of bacterial meningitis (Santana-Arciaga, 1996). In developing countries, 12–50% of individuals with pneumococcal meningitis die, compared with 5% in developed countries. Sequelae are reported in 15–20% of children in developed countries, whereas in developing countries the rate of sequelae is not well-known and it is probably under-reported (Molyneux *et al.*, 2002).

It is believed that the release of bacterial components such as pneumolysin, upon the use of antibiotics, can directly cause damage or can stimulate the expression of inflammatory cytokines within the central nervous system (Santana-Arciaga, 1996). These cytokines affect adversely the capillary endothelial cell function, arachidonic acid metabolism, and cerebral blood flow (Santana-Arciaga, 1996). This results in an increase in permeability of the blood-brain barrier, cytotoxic and vasogenic cerebral oedema, and increased intracranial pressure (Santana-Arciaga, 1996; Molyneux *et al.*, 2002). These alterations may then lead to local hypoxia and focal ischemia of brain tissue, possibly manifested as neurologic sequelae, learning or developmental disabilities, or communication disorders (Santana-Arciaga, 1996).

The reason for adding corticosteroids to the regimen of treatment of pneumococcal meningitis is that steroids, such as dexamethasone, modulate production of inflammatory cytokines which, in turn, may attenuate the host's inflammatory response and thereby may prevent an adverse outcome.

Nevertheless, the use of dexamethasone as an adjunctive therapy in the treatment of acute pneumococcal meningitis is controversial (Van De Beek *et al.*, 2007; Greenwood, 2007). Some studies have shown no significant improvement of the disease outcome among meningitis patients, whereas, other studies have shown the contrary. For instance, a trial involving 598 Malawian children provided convincing evidence of a lack of any benefit (Molyneux *et al.*, 2002). Of the 598 children included in this study, 307 (51%) were assigned to dexamethasone and 295 (49%) to placebo. 238 (40%) of the 598 patients had *S. pneumoniae*, 170 (28%) *Haemophilus influenzae* type b, 67 (11%) *Neisseria meningitidis*, and 29 (5%) *Salmonella* spp. Negative culture was found in 78 (13%) of the patients. The number of overall deaths was the same in the two treatment groups. At final outcome, neurological sequelae were identified in 84 (28%)

of children on steroids and in 81 (28%) on placebo. The number of children dying in hospital did not differ between groups.

A similar outcome was observed in another a trial of dexamethasone, involving 465 Malawian patients 16 years of age or older with acute bacterial meningitis (Scarborough *et al.*, 2007). Here, overall mortality at 40 days after enrolment was high (54%) and did not differ significantly between patients treated with dexamethasone (56%) and those from placebo group (53%). The rates of neurological handicap or mortality or clinically detectable hearing loss after enrollment were not different between the groups.

In contrast, a study by Girgis et al. came to a different conclusion (Girgis *et al.*, 1989). In this trial a significant reduction in the mortality rate was observed in the group that received dexamethasone (13.5% vs. 40.7%, $p < 0.01$). In addition, a significant reduction in neurologic handicap (hearing impairment and paresis) was observed in the surviving patients receiving dexamethasone. None of the patients receiving steroids had hearing loss whereas 12.5% patients from placebo group had severe hearing loss ($p < 0.05$).

1.2. Pneumolysin

Pneumolysin (PLY), the central object of interest in this project, is a 53 kDa protein consisting of 471 amino acids residues (Walker *et al.*, 1987). PLY belongs to a large family of structurally and antigenically related pore-forming toxins, the cholesterol-dependent cytolysins (CDCs). Members of this family are produced by different species of Gram-positive bacteria belonging to the genera *Streptococcus*, *Clostridium*, *Listeria*, *Bacillus* and *Arcanobacterium*, and include streptolysin O from *Streptococcus pyogenes* and perfringolysin O from *Clostridium perfringens* (Tweten, 2005) (Table 1.1). The majority of CDCs, including PLY, require the presence of membrane cholesterol for their cytolytic activity (Gilbert, 2002; Nollmann *et al.*, 2004; Tweten, 2005).

Table 1.1 – The family of cholesterol-dependent cytolysins. Table adapted from Palmer, 2001.

Bacterial genus	Species	Toxin name
Streptococcus	*S. pyogenes*	
	S. equisimilis	Streptolysin O
	S. canis	
	S. pneumoniae	Pneumolysin
	S. suis	Suilysin
	S. intermedius	Intermedilysin
Bacillus	*B. cereus*	Cereolysin O
	B. alvei	Alveolysin
	B. thuringiensis	Thuringiolysin O
	B. laterosporus	Latersporolysin
Clostridium	*C. tetani*	Tetanolysin
	C. botulinum	Botulinolysin
	C. perfringens	Perfringolysin O
	C. septicum	Septicolysin O
	C. histolyticum	Histolyticolysin O
	C. novyi	Novyilysin
	C. chauvoei	Chauveolysin
	C. biofermentans	Bifermentolysin
	C. sordellii	Sordellilysin
Listeria	*L. monocytogenes*	Listeriolysin O
	L. ivanovii	Ivanolysin
	L. seeligeri	Seeligerolysin
Arcanobacterium	*A.pyogenes*	Pyolysin

Cholesterol has been considered to be a receptor for the members of this family, based on the evidence that CDCs are not cytolytically active on cholesterol-deficient membranes and also that the depletion of cholesterol from membranes reduces the extent of binding and interferes with the cytolytic mechanism of these toxins (Johnson *et al.*, 1980; Waheed *et al.*, 2001; Giddings *et al.*, 2003).

In addition, it has been shown that apoptotic responses to pneumolysin are dependent on the cytolytic properties of the molecule, as demonstrated by an experiment where a

point mutant in the domain required for cytolytic activity of pneumolysin (W433F) failed to induce apoptosis, whereas a pneumolysin defective mutant for complement activation (D385N) induced apoptosis at the same extent as the wild-type pneumolysin (Braun *et al.*, 2002). Furthermore, based on the evidence that macrophages from wild-type mice are more prone to pneumolysin-induced apoptosis than cells from TLR4-deficient mice and that these mice are more susceptible to invasive disease that wild-type mice, it has been suggested that the apoptotic response to pneumolysin is mediated by Toll-like receptor 4 (TLR4) and confers protection against pneumococcal invasive disease (Srivastava *et al.*, 2005; Malley *et al.*, 2003).

Contrary to the other members of the CDC family, pneumolysin is not actively secreted during pneumococcal growth (Walker *et al.*, 1987). Instead, pneumolysin is found in the cytoplasm of the bacterial cells (Jonhson, 1977), which is associated with there being no signal peptide at the N-terminus of the protein (Walker *et al.*, 1987). It is believed that the release of this toxin, in the form of a soluble monomer (Tilley *et al.*, 2005), is mediated by the action of the pneumococcal autolysin A (Alonso de Velasco *et al.*, 1995) or it is resultant from the use of antibiotics for the treatment of pneumococcal infections (Mohammed *et al.*, 1999). A more recent study detected the presence of active pneumolysin at the cell wall of *S. pneumoniae*, which is intriguing given that pneumolysin lacks not only a signal peptide but also any of the cell wall anchoring motifs known in Gram-positive bacteria (Price & Camilli, 2009).

1.2.1. Role of pneumolysin in pneumococcal diseases

Pneumolysin has been studied in a wide range of *in vitro* and *in vivo* systems in order to define its role in the pathogenesis of pneumococcal diseases. Evidence of the importance of pneumolysin in the virulence of pneumococcus *in vivo* was first

demonstrated by Paton and colleague in 1983. When they immunised mice with a partially inactivated form of pneumolysin they observed a considerable increase in the survival time of mice challenged intranasally with pneumococcus (Paton *et al.*, 1983). Later, the cloning and characterisation of pneumolysin gene (Walker *et al.*, 1987; Paton *et al.*, 1986) allowed the construction of isogenic pneumolysin-negative mutants (Berry *et al.*, 1989), which were employed in further studies for a better understanding of the role of the toxin *in vivo*. In an early study (Berry *et al.*, 1989), the intranasal challenge of mice with a pneumolysin-negative mutant, designated PLN-A, revealed a reduction in the virulence. In addition, when given intravenously to mice, PLN-A survived significantly less well than the wild-type strain (Berry *et al.*, 1989). Another study reported that after the intranasal administration of PLN-A to mice, it was observed that there was a reduction in the severity of the inflammatory response, a decrease in bacterial growth rate within the lungs and a delayed invasion of bacteria into the blood stream, in comparison to the infection with the wild-type strain (Canvin *et al.*, 1995). In a bacteraemia model in mice, the growth rate of PLN-A was shown to be enhanced by co-infection with wild-type pneumococci (Benton *et al.*, 1995). This observation suggests the influence of pneumolysin on the ability of the bacteria to multiply. Benton and co-workers also showed that intravenous challenge of mice with PLN-A resulted in chronic bacteraemia rather than acute sepsis (Benton *et al.*, 1995).

Pneumolysin has been also shown to influence the recruitment pattern of inflammatory cells into the loci of infection, during experimental pneumococcal pneumonia in mice using wild-type pneumococci and the mutant strain PLN-A (Kadioglu *et al.*, 2000). In this study, the absence of pneumolysin was associated with significantly less intense and delayed influx of leukocytes, whereas the presence of pneumolysin was implicated in the early recruitment of neutrophils and bacterial dissemination in the lungs. In

addition, the maximum accumulation of lymphocytes in the lungs was found to be significantly less intense and delayed in the absence of pneumolysin.

More recently, it was shown that other pneumolysin-deficient mutant, designated ΔPly (Berry *et al.*, 1999), employed in a rat meningitis model, has reduced virulence compared with wild-type bacteria (Hirst *et al.*, 2008). This study also showed that the CSF infection with this mutant did not cause ependyma disruption.

In a different experimental approach, García-Suarez and colleagues (Del Mar Garcia-Suarez *et al.*, 2004) tested the ability of three anti-pneumolysin monoclonal antibodies (De Los Toyos *et al.*, 1996) to affect the progress of pneumococcal pneumonia in mice. It was observed that mice treated with two of these monoclonal antibodies (on their own or combined), prior to infection with *S. pneumoniae,* exhibited prolonged survival periods in comparison to the control groups.

In addition, Alexander et al. have demonstrated that the immunization of mice with PdB, a pneumolysin toxoid carrying the mutation W433F, confers non-serotype-specific protection against *Streptococcus pneumoniae* (Alexander *et al.*, 1994). In this study, the immunized mice exhibited significantly increased levels of anti-pneumolysin antibodies, in particular of IgG1, eliciting a degree of protection against twelve pneumococcal strains representing nine serotypes.

Several studies have been undertaken in order to analyse the interactions of purified pneumolysin or whole pneumococci with isolated cells or tissues *in vitro*. These revealed the multi-functional character of this toxin. At high concentrations, pneumolysin causes lysis of cells containing cholesterol in their membranes (Boulnois *et al.*, 1991). At sublytic concentrations the toxin has several effects on the cells of the immune system. It has been seen that pneumolysin: stimulates the production of inflammatory cytokines, such as tumor necrosis factor alpha (TNF-α) and interleukin-

1beta (IL-1β), by human monocytes (Houldsworth *et al.*, 1994); inhibits the cilia beating of respiratory epithelial cells (Feldman *et al.*, 1990) and of cerebral ependymal cells (Mohammed *et al.*, 1999); disrupts the monolayers of cultured epithelial cells from the upper respiratory tract (Feldman *et al.*, 1990) and from the alveoli (Rubins *et al.*, 1993); inhibits the bactericidal activity and random migration of neutrophils (Paton & Ferrante, 1983), and inhibits proliferation and antibody production by human lymphocytes (Ferrante *et al.*, 1984). In addition, pneumolysin activates the classical complement pathway in the absence of anti-pneumolysin specific-antibody, possibly by its ability to bind the Fc portion of IgG antibody (Mitchell *et al.*, 1991).

1.2.2. Homology of the primary amino acid sequence of pneumolysin and other CDCs

The amino acid sequence of pneumolysin was aligned with other CDCs and aerolysin (Rossjohn *et al.*, 1998) (Figure 1.7). The alignment between the CDCs family and aerolysin does not seem very plausible, considering the numerous insertions and deletions observed. The sequence identity between aerolysin and PLY is only 16.6%, with the longest stretch of sequence identity corresponding to two amino acid residues.

In contrast, there is a striking similarity between PFO and PLY. The proteins share 48% sequence identity and 60% sequence similarity, extending over the entire length of the two sequences. The longest stretch of sequence identity (ECTGLAWEWWR) is between residues 427 and 437 (458-468 in PFO), a loop at the bottom of domain 4 that contains the Trp-rich motif and a single cysteine residue.

In addition, as it was expected, the primary sequence of PLY does not contain a signal sequence for secretion.

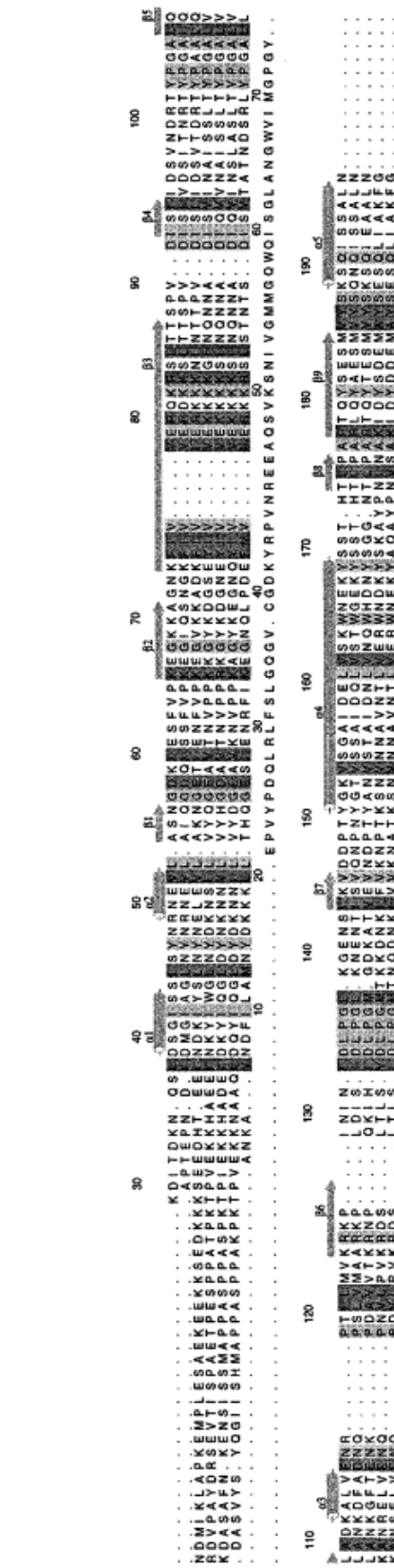

Figure 1.7- Sequence alignment of the CDCs and aerolysin. The light shades refer to the identical regions of the sequence, while the dark shades refer to the similar areas of the sequence. The Trp-rich motif is shown inside the red box. Secondary structure elements are shown above the sequence. Residue numbering referring to PFO and PLY are displayed above and below the aligned CDCs, respectively. Figure obtained and modified from Rossjohn *et al.*, 1998.

1.2.3. Mutagenesis studies

Over the past three decades, several mutagenesis studies have been made in the attempt to comprehend the molecular basis of the function of pneumolysin, in particular the importance of the Trp-rich motif and of the single Cys428 for the haemolytic and complement-activating activities of the toxin. For a more clear understanding, the mutagenesis data are summarised in Table 1.2.

Table 1.2 – Summary data on the *in vitro* activity of mutants of pneumolysin.

	Mutation	Effect of mutation		Reference
		Haemolytic Activity (% of wild-type)	**Complement activation** (% of wild-type)	
	C428A	100	100	(Saunders *et al.*, 1989)
	C428S	15	100	
	C428G	1	100	
	D385N	100	0	(Mitchell *et al.*, 1991)
	Y384F	100	30	
	W379F	100	80	
	W397F	100	85	
	W433R	1	nd	(Hill *et al.*, 1994)
	W433F	1	nd	(Korchev *et al.*, 1998)
	W435F	20	nd	
	W436F	50	nd	
	H367R	0	nd	(Mitchell, 1999)
	E434Q	20	100	
	E434D	50	100	
Domain 4	P462S	73	nd	(Owen *et al.*, 1994)
	Deletion a.a. 419-471	0	nd	
	Deletion a.a. 430-471	0	nd	
	Deletion a.a. 441-471	0	nd	
	Deletion a.a. 450-471	0	nd	
	Deletion a.a. 465-471	0.2	nd	
	Deletion a.a. 460-471	0	nd	
	Deletion of a.a. 471	100	nd	
	Deletion of domain 4	0	nd	(Baba *et al.*, 2001)
Domain 3	H156T	2	nd	(Hill *et al.*, 1994)
Domain 2	R31C	75	nd	
Domain 1	L75F	100	nd	
	V127G	75	nd	

'nd' - not determined

1.2.4. Homology-based structural properties of pneumolysin monomer

The crystal structure of pneumolysin monomer has not been reported. However, a homology model of pneumolysin was initially constructed (Sowdhamini *et al.*, 1997) based on the crystal structure of the pore-forming toxin aerolysin, produced by the Gram-negative *Aeromonas hydrophila* (Parker *et al.*, 1994). A representation of the X-ray crystal structure of proaerolysin can be seen in Figure 1.8. Despite the sequence identity between pneumolysin and aerolysin being only 16.6%, the homology model was undertaken because electron microscopy data from the pneumolysin monomer (Morgan *et al.*, 1994) revealed an asymmetric molecule composed of four domains, with similar shape and domain arrangement to aerolysin.

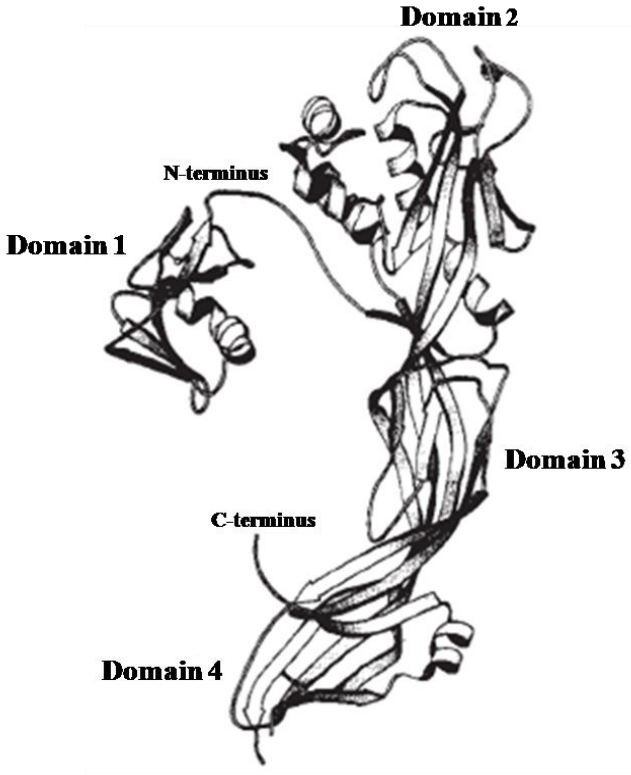

Figure 1.8 - Ribbon representation of the X-ray crystal structure of proaerolysin (Parker *et al.*, 1994)**.** The molecule has an elongated shape and is constituted of four domains.

This homology model was abandoned when the crystal structure of perfringolysin O, produced by *Clostridium perfringens*, was resolved (Rossjohn *et al.*, 1997). Pneumolysin and perfringolysin O share 48% sequence identity and 60% sequence similarity, and also are believed to have the same mechanism of pore-formation. Therefore, it was possible to establish a new homology model based on the crystal structure of perfringolysin (Rossjohn *et al.*, 1998). According to this model (Figure 1.9), pneumolysin is an elongated rod-shaped molecule, 11 nm in length and 5 nm in width, with four domains consisting of 41% β-sheet and 21% α-helices, which is consistent with the electron microscopy and the circular dichroism data of Morgan and co-workers (Morgan *et al.*, 1994). Domain 1, 2 and 4 are linearly disposed, while domain 3 is loosely packed against domain 2 (Rossjohn *et al.*, 1998). In domain 4 a Trp-rich motif is located, which consists of an 11-amino acid conserved sequence (section 1.2.2), containing three tryptophan residues and the single Cys residue. In addition, domain 3 comprises four β-sheets connected to two sets of helices, TMH1 and TMH2, with each set containing three short α-helices, which are thought to be involved in pore formation and function (El-Rachkidy, 2003).

Several studies of domain 4 and 3 have been undertaken for pneumolysin and other cytolysins, such as perfringolysin O and streptolysin O, in order to understand their involvement in the pore formation. These studies suggested that domain 4 mediates binding and shallow insertion into the membrane (De Los Toyos *et al.*, 1996; Shepard *et al.*, 1998; Gilbert, 2002). Domain 3, on the other hand, is thought to be involved in the process of oligomerisation (Palmer, 2001), and also to play a "key" role in the toxin insertion and pore formation (Shepard *et al.*, 1998; Gilbert, 2002; Tilley *et al.*, 2005). Domain 2 provides a structural connection between domains 1 and 4, while domain 1 is believed to play an important role in oligomerisation (De Los Toyos *et al.*, 1996;

Rossjohn *et al.*, 1997). An overview of the proposed mechanism of pore formation by pneumolysin will be presented next.

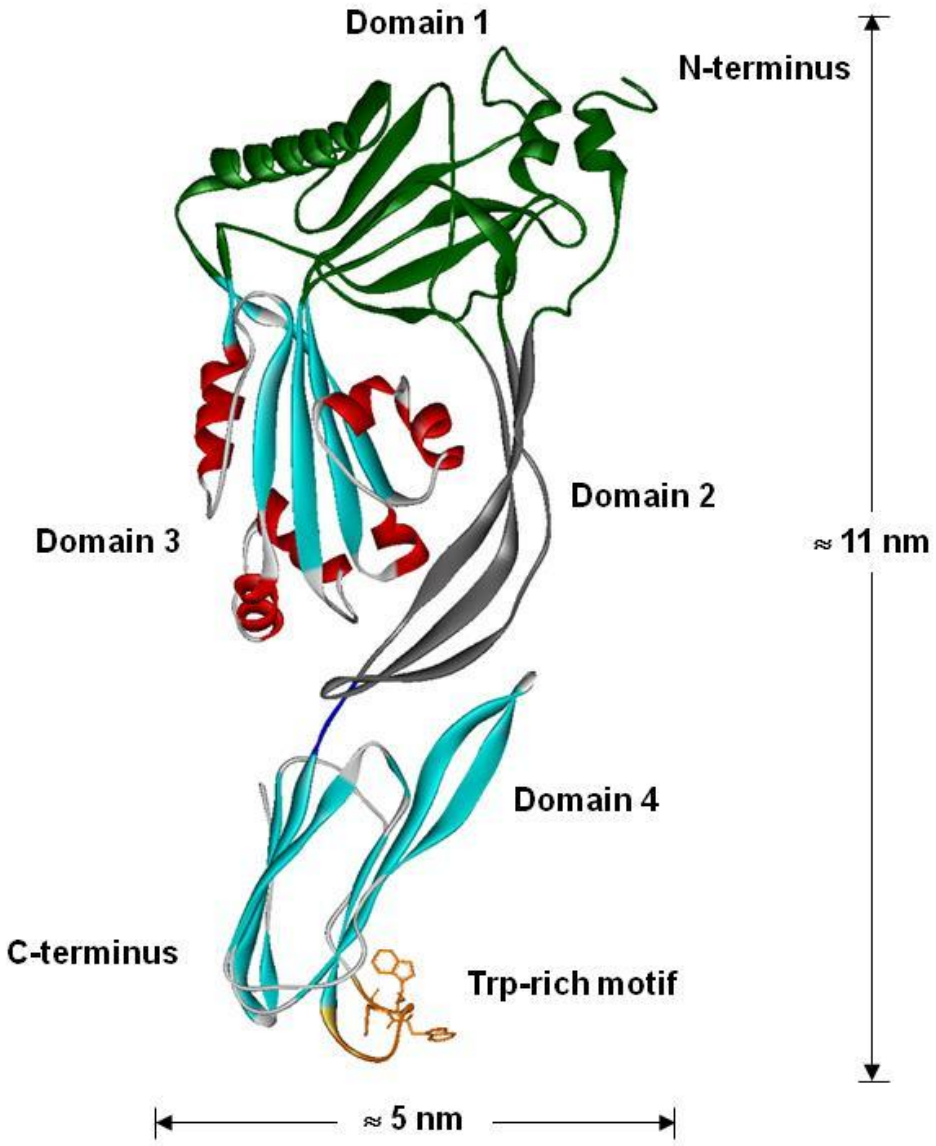

Figure 1.9 - Homology model of pneumolysin based on the crystal structure of perfringolysin O. The pneumolysin monomer is an elongated rod-shape molecule, composed of 4 domains. Located in domain 4, is the Trp-rich motif (yellow). The small α-helices shown in domain 3 (red) have been predicted to refold into β-hairpins (TMH1 and TMH2) and enter the membrane during the pore formation. Image obtained and modified from El-Rachkidy, 2003.

1.2.5. Overview of the mechanism of pore formation

In the past few years, the mechanism of pore formation of the cholesterol-dependent cytolysins have been subject of intensive studies, employing negative stain electron microscopy (EM), cryo-EM, atomic force microscopy (AFM), imaging processing, three-dimensional (3D) reconstruction, fluorescence and kinetic assays (Palmer *et al.*, 1996; Rossjohn *et al.*, 1997; Shepard *et al.*, 1998; Czajkowsky *et al.*, 2004; Tilley *et al.*, 2005). As a result, two mechanisms of pore assembly have been proposed for the CDCs family. The initial proposal, based on studies with streptolysin O, suggested that monomers bind to the membrane and insert before oligomerisation takes place to form a transmembrane pore (Palmer *et al.*, 1998). On the other hand, studies involving perfringolysin O suggested that monomers bind to the membrane and oligomerise on the surface to form a prepore structure, and only then do the oligomers insert into the membrane to form the pore (Shepard *et al.*, 2000; Heuck *et al.*, 2003). Later, it also was demonstrated that streptolysin O also forms prepore structures (Heuck *et al.*, 2003). These findings suggested a common mechanism of pore formation shared by the members of the CDCs family.

Tweten had described a possible mechanism of pore formation for the CDCs family (Tweten, 2005), which can be seen in Figure 1.10. According to this description, a soluble CDC monomer binds to the cholesterol-rich host membrane in a perpendicular orientation, via the undecapeptide conserved region present in domain 4. After binding, monomers move laterally to initiate the formation of the oligomers. The interaction of domain 4 with the membrane apparently triggers structural changes within domain 3 which promotes oligomeric contacts with adjacent monomers. The resultant oligomeric complex constitutes the prepore structure, in which insertion of the oligomers into the membrane to create a pore has not occurred. The conversion from prepore-to-pore

occurs when the prepore complex reaches a large size (most likely a complete ring structure). At this point, the α-helical bundles in domain 3 of each monomer are thought to unravel, forming two extended amphipathic transmembrane β-hairpins (TMH1 and TMH2). During this stage, the domain 2 structure appears to collapse, bringing domains 1 and 3 closer to the membrane, which allows the transmembrane β-barrel to insert across the lipid bilayer.

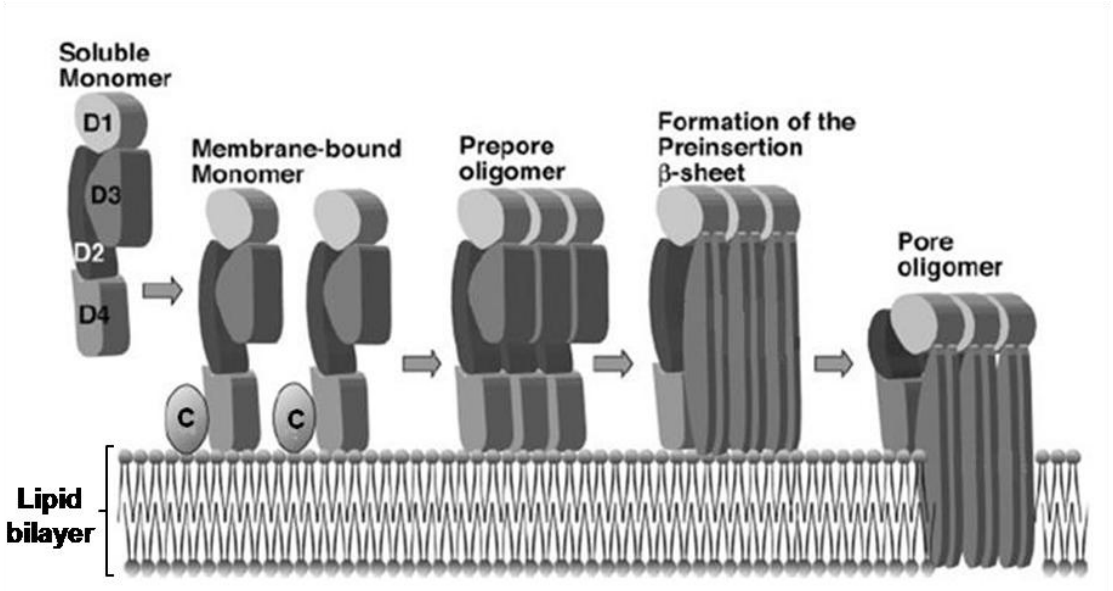

Figure 1.10 – Mechanism of pore formation currently accepted for the members of CDCs family. D1, D2, D3 and D4 represent the four domains comprised by the soluble form of the CDC monomer. C represents the cholesterol receptor present at the host membranes. Image obtained and modified from Tweten, 2005.

A study by Czajkowsky and collegues (Czajkowsky *et al.*, 2004) contributed with a piece of evidence supporting the prepore-to-pore theory regading the cytolytic mechanism of the CDCs. By using atomic force microscopy, they showed a significant difference in the height by which the prepore and pore structures of perfringolysin O project from the membrane surface. Time-lapse images of the prepore-to-pore conversion obtained during that study (Czajkowsky *et al.*, 2004) can be seen in Figure 1.11. In each image, it is possible to observe oligomeric complexes with two different

heights: the taller complexes extend out approximately 113 Å from the membrane surface while the shorter complexes project approximately 73 Å. It is noticeable that almost all of the taller complexes become progressively shorter with time. These observations appear to be associated with the vertical collapse of the prepore structure which re-enforces the prepore-to-pore theory.

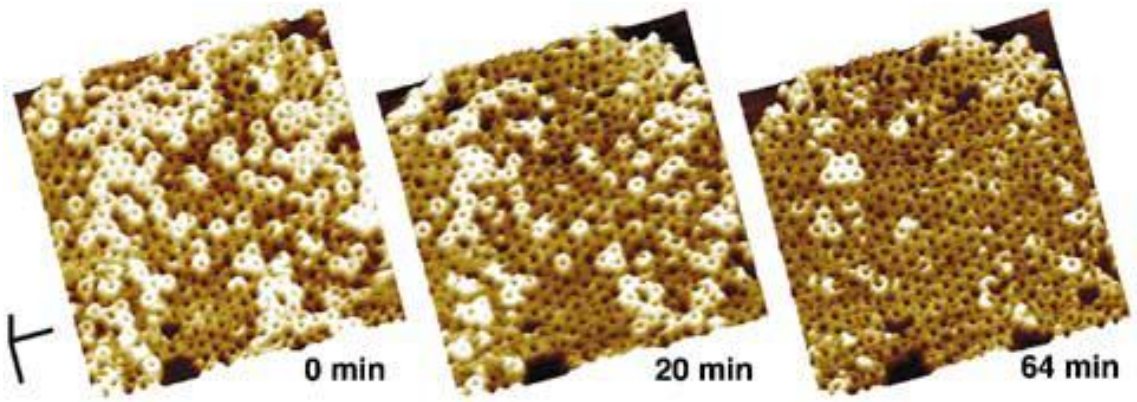

Figure 1.11 - Time-lapse series of images of perfringolysin O oligomeric complexes showing alterations in height upon conversion from prepores to pores. From left to right: complexes that are initially at a height of ≈113 Å (brighter-yellow oligomeric structures) gradually decrease to a height of ≈73 Å (darker-yellow oligomeric structures) over time. (Scale bar: x, y, 100 nm; z, 10 nm). Image obtained from Czajkowsky *et al.*, 2004.

More recently, Tilley and co-workers (Tilley *et al.*, 2005) presented a 3D reconstruction of cryo-EM structures of the prepore and pore complexes of pneumolysin, combined with the atomic structures of the domains of perfringolysin O (Figure 1.12). Based on this study, pneumolysin oligomerises first into a prepore structure. Then, upon the prepore-to-pore transition, domain 2 suffers a vertical collapse (shown by the reduction of the oligomer height and by the appearance of a protruding ridge on the outside of PLY pore structure), which brings domain 3 30 Å closer to the membrane and allows the insertion of the TMHs across the lipid bilayer.

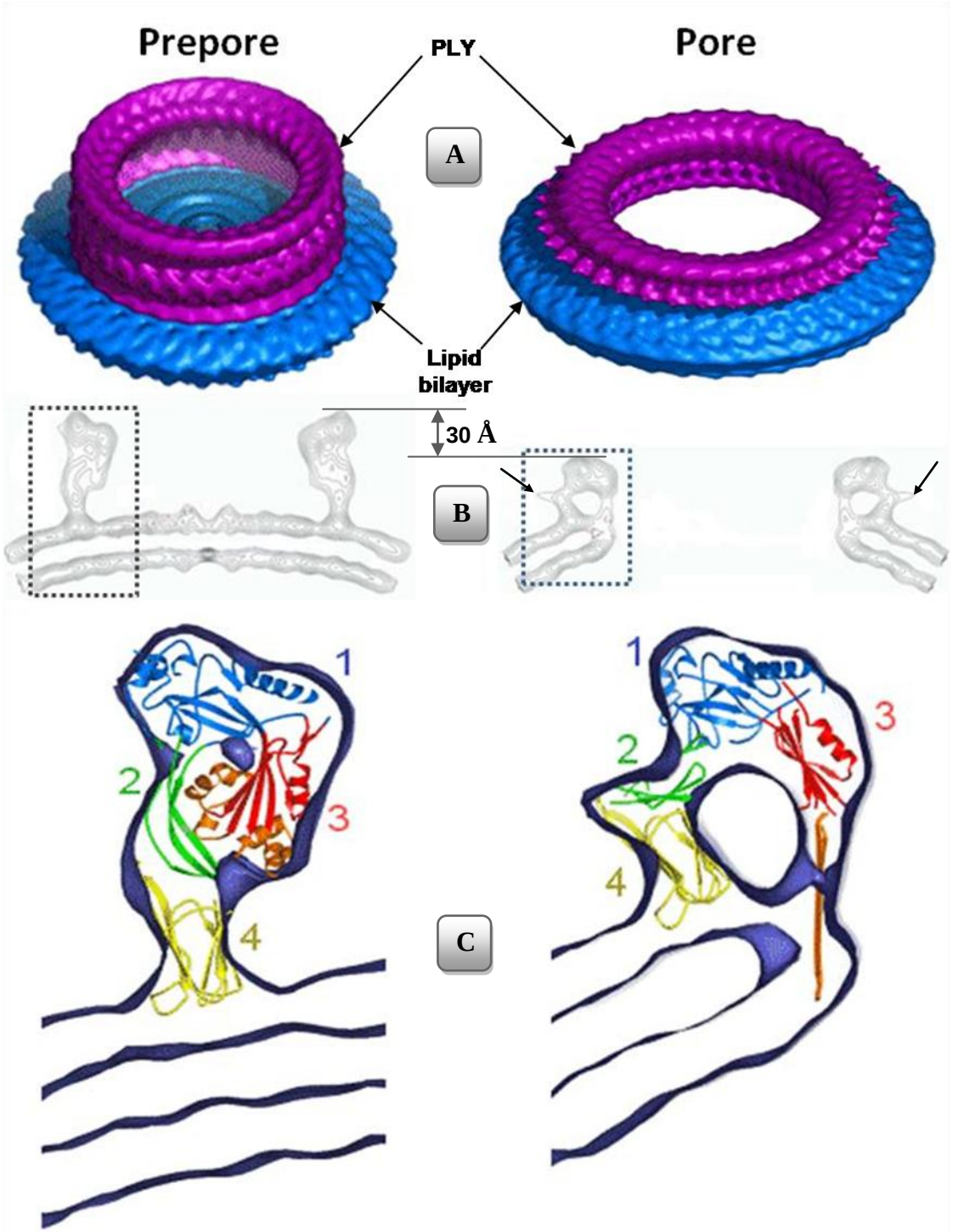

Figure 1.12 - 3D reconstruction of the cryo-EM structures of prepore and pore forms of pneumolysin (PLY). (A) Surface-countered views of the prepore and pore structures on the extracted disks of liposome membrane. (B) Cross-sections through the prepore and pore density maps. Here are signalised (i) the reduction of 30 Å in the oligomer height and (ii) the appearance of a protruding ridge, at the level of domain 2, on the outside of the pore structure. (C) Cross-sections through one side of prepore and pore density maps, with fitted domains of the crystal structure of perfringolysin O monomer. Images obtained and modified from Tilley *et al.*, 2005.

1.2.5.1. Functional characterisation of CDCs pores

Transmembrane channels formed by cholesterol-dependent cytolysins interfere with membrane permeability, allowing the free flow of material in and out of the host cells and leading ultimately to their lysis (Bashford, 2001; Alouf, 2003; El-Rachkidy *et al.*, 2008).

Early studies regarding the electrophysiological properties of the transmembrane channels induced by CDCs were conducted on synthetic membranes rather than eukaryotic cells, the real targets of the members from this family. Studies conducted by Menestrina (Menestrina *et al.*, 1990) and Slatin (Slatin *et al.*, 1990) detected the formation of transmembrane pores in planar lipid bilayers by perfringolysin O and δ-endotoxins (CryIAc and CryIIIA), respectively, exhibiting a wide spectrum of conductances (perfringolysin O: 2-30 nS; δ-endotoxins: 200-4000 pS). Korchev and colleagues (Korchev *et al.*, 1992, Korchev *et al.*, 1998) described the occurrence of multiple-conductance channels (small < 30 pS; 30 pS < medium < 1 nS; large > 1nS) across planar lipid bilayers exposed to pneumolysin. Shepard and colleagues (Shepard *et al.*, 2000), on the other hand, reported the observation of homogeneous large conductance channels in planar lipid bilayers exposed to perfringolysin O.

More recently, El-Rachkidy (El-Rachkidy *et al.*, 2008) described the generation of pneumolysin-induced multiple conductance pores in inside-out patches of Chinese hamster ovary (CHO) cells membranes. The ion-conducting channels formed across the membranes exhibit small (<200 pS), medium (>200 pS and <1 nS) and large (>1 nS) conductance steps. The occurrence of medium conductance channels was registered more frequently, displaying an average conductance of about 700 pS. Small conductance channels were observed with much less frequency than medium channels and were generally open for only a short period of time. On the other hand, large

conductance channels, despite being observed less often than small and medium channels, were open for longer periods of time. The detection of channels with a wide spectrum of conductances in this work is consistent with the observations from previous studies conducted on planar lipid bilayers (Menestrina *et al.*, 1990; Slatin *et al.*, 1990, Korchev *et al.*, 1992; Korchev *et al.*, 1998). It is then likely that the difference in the results obtained by Shepard and colleagues (Shepard *et al.*, 2000) is associated with technical variations rather than differences in the behaviour of the conductance channels of the toxins.

One possible explanation for the occurrence of channels with different conductance steps may be related with differences in the physical dimensions of oligomeric structures inserting the membranes. Some studies reported the presence of arc and ring structures in membranes exposed to cholesterol-dependent cytolysins (Gilbert, 2002; Menestrina *et al.*, 1990; Korchev *et al.*, 1998). However, these studies did not provide evidence of significant differences in the diameter of ring-shape pores that would explain the observations of a wide-spectrum of conductance channels. On the other hand, some believe that the arc-shape structures are incomplete oligomers inserted across lipid bilayers, functioning as channels. This concept would help to explain the observation of channels with different conductances, based on the differences between arc and ring structures.

Another hypothesis is that the oligomeric structures inserted in the membranes produce more than just simple and inert holes that lead to the lysis of cells. Instead, the pores may have a more complex and dynamic internal structure, which control of the flux of ions and molecules through the membrane, generating channels of differing conductances, without any apparent changes of their external structure. Some studies reported the observation of electrophysiological changes in the pores formed by a lytic-

deficient mutant of pneumolysin, W433F, in comparison with the ion-conducting channels formed by the wild-type toxin (i.e. changes in the frequency at which small, medium and large conductance-channels occur) (Korchev *et al.*, 1998; El-Rachkidy *et al.*, 2008). In addition, electron-microscopy data revealed that this mutant formed oligomeric arc and ring structures with dimensions identical to those of wild-type toxin, and that the ratio of arcs to rings formed was the same for both wild-type and mutant toxin (Korchev *et al.*, 1998).

1.2.6. Application of phage-displayed peptide libraries and high-throughput screening of small molecules as strategies to identify potential inhibitors of pneumolysin

1.2.6.1. Phage-displayed peptide libraries

Phage-display of random peptide libraries was used in this work as a tool for the identification of peptides with the ability to bind to pneumolysin. This technique was first described by Smith in 1985 (Smith, 1985). Its main advantages over other technologies (e.g. synthetic peptides libraries) are the ability to screen libraries containing a vast number of unique peptides/protein sequences and maintenance of a link between the displayed peptide/protein and the DNA sequence encoding it (Devlin *et al.*, 1990; Azzazy & Highsmith Jr, 2002; Willats, 2002; Mullen *et al.*, 2006). In addition, it is a simple method, inexpensive to set up and it has a wide range of applications (Cortese *et al.*, 1995) such as epitope mapping and development of mimotope-based vaccines (Folgori *et al.*, 1994; Buchwald *et al.*, 2005; Beninati *et al.*, 2009; Smith *et al.*, 2009). Similarly to the work presented here, this technology has been also employed in the identification of potential inhibitors of tetanus toxin and the botulinum neurotoxins A, B, C and E (Zdanovsky *et al.*, 2001).

Escherichia coli filamentous phage M13 was used in this work for the display of peptide libraries. The key feature of M13 and its closely related phages (fd and f1) is that they can accumulate to high titrers, because their production does not cause cell lysis (Russel *et al.*, 2004). Consequently the intermediate phage purification steps between rounds of panning become considerably simplified (NEB, 2007). Other advantages of the use of filamentous phages are that their genomes are small and tolerate insertions into non-essential regions; cloning and library construction are facilitated by the ability to isolate both single- and double-stranded DNA; coat proteins can be modified with retention of infectivity; and they are stable at a broad range of stringent selection conditions (Russel *et al.*, 2004).

The libraries used in this work carried random DNA inserts encoding peptides (8-12 amino acids residues) fused to the N-terminal region of pVIII, the major coat protein of the M13 filamentous phage. From the five coat proteins that compose filamentous phages, pIII and pVIII are by far the most commonly used in phage-display (Russel *et al.*, 2004; Mullen *et al.*, 2006). Typically, peptides fused to pIII are displayed at low valency (3-5 copies per phage particle), whereas pVIII fusions are displayed at high valency (around 270 copies per phage particle) (Russel *et al.*, 2004; NEB, 2007). The valency of display is an important factor to take into account when choosing the appropriate strategy for phage-display, given that it influences the selection of peptides of differing binding-affinities. The high affinity (avidity) conferred by the high valency of pVIII display allows the selection of very low-affinity ligands, while low valency pIII display limits selection to higher affinity ligands (NEB, 2007). In this work, where *de novo* selection of peptides binding to pneumolysin was made, the high valency characteristic of pVIII display was of great interest for the construction of the peptide libraries, as it increased the chances of isolating clones with differing affinities,

including weakly-binding clones, which otherwise could have been missed if the pIII display had been used.

1.2.6.2. High-throughput screening of small molecules

High-throughput screening was used in this work as a tool for the identification of small molecules with the ability to inhibit pneumolysin's haemolytic activity. High-throughput screening (HTS) is a widely used method in drug discovery in which a large number of compounds can be rapidly tested against defined targets (Cho & Juliano, 1996; Drug & Market Development, 2001; HTS Research, 2010). An HTS campaign comprise of many components, three of which are listed below:

- Screening libraries: They can comprise millions of compounds, selected for drug-like characteristics such as solubility, partition coefficient (logP), molecular weight, number of hydrogen bond donors/acceptors (Lipinski's rule of 5) (HTS Research, 2010) and, most importantly, they should include compounds or families of compounds of great structural diversity (Personal Communication). High-throughput screening of compounds' libraries (run in 96-, 384-, or 1536-well formats) generally employs modern robotic equipment, sophisticated control software, advanced liquid handling, and sensitive detection methods (HTS Research, 2010). Thus, it requires a beforehand adaptation of the biological/chemical screening assays to this automated system.
- Target: The screened compounds mentioned above can act as inhibitors of target enzymes/proteins, as competitors for binding of a natural ligand to its receptor, as agonists or antagonists for receptor-mediated intracellular processes, and so forth. Of these targets, cell membranes receptors, mostly G-protein coupled receptors, make up the largest group (45% of the total), enzymes make up the next largest

group (28%), followed by hormones (11%), unknowns (7%), ion-channels (5%), nuclear receptors (2%), and finally DNA (2%) (Martis *et al.*, 2011).

- Biological assays: In order to assess whether a compound interacts with its target the availability of suitable assay is essential for an HTS. Screening assays can be divided into two categories: functional or non-functional. Functional assays measure the capacity of a compound to alter the original function of a target molecule (e.g., inhibition of the haemolytic activity of the pore-forming toxin pneumolysin). Non-functional assays frequently simply measure binding of a compound to the defined target or use some indirect method to measure the target's activity (e.g., tritrated binding assays; quantification of fluorescence activity associated with calcium signaling). Functional assays are generally preferred as they are less likely to generate false positive hits (HTS Research, 2010). The positive results obtained during the HTS campaign are usually called hits. The compounds resulting in hits are then collected ("cherry-picked") for confirmation. The confirmed hits are further tested for the potency of their activity or for their binding affinity to a receptor. The hits identified during HTS can then be used as the starting point for a drug discovery program. At this stage, some basic indicators of toxicity or bioavailability may be considered in an attempt to eliminate potential failures as early in the discovery process as possible (Drug & Market Development, 2001).

1.3. Aim of the project

Evidence provided by several *in vitro* and *in vivo* studies point clearly to a vital role for pneumolysin in invasive pneumococcal diseases. The antibactericidal and adjunctive therapies currently available do not address the cytotoxicity induced by pneumolysin. Therefore the aim of this research project was the development of a new approach to the treatment of pneumococcal diseases that targets pneumolysin. This new approach was to (i) select peptides that bind pneumolysin from phage-display peptide libraries and (ii) identify small molecules from a commercial library that exhibit inhibitory properties against the toxin. These peptides and small molecules would be evaluated for their capacity to inhibit the toxin's haemolytic activity *in vitro*. Those that pass the initial screening would be tested in *in vivo* models of pneumonia and/or bacteraemia and *ex vivo* studies of damage to brain. The most promising peptides or small molecules could be good candidates for development towards new drugs.

Chapter 2 - Materials and Methods

2.1. Materials

All the chemicals and reagents used in this work were supplied by Oxoid (UK), Fisher Scientific (UK), Sigma (UK) and Merck (UK) unless otherwise stated in the text. DNA primers were manufactured by MWG (Germany).

2.2. Media

Luria-Bertani (LB) and Luria-agar (LA) media, with appropriate addition of antibiotic, were used for the growth of recombinant strains of *Escherichia coli*. Brain heart infusion (BHI) broth and blood agar base (BAB) supplemented with 5% (v/v) of horse blood were used for the growth of *Streptococcus pneumoniae*. Tryptone soya agar (TSA) was used for the growth *Pseudomonas aeruginosa*. Overnight express instant terrific broth (TB), with required antibiotic, was used for targeted protein expression by recombinant strains of *E. coli*. All media were autoclaved at 121ºC, 15 psi for 20 minutes. A full list of media used in this work and their composition is described in Table 2.1.

2.3. Antibiotics

All antibiotics were prepared as described in Table 2.2, filtered-sterilised through a 0.2µm acrodisc syringe filter (PALL- Life Sciences), aliquoted and stored at -20ºC. For use, the antibiotics were thawed at room temperature and added to autoclaved medium after it had been cooled to approximately 50ºC.

Table 2.1- Bacterial growth media

Media	Composition	Reference
Brain heart infusion	- 14.8 g BHI powder - 400 ml distilled H_2O	Oxoid / Merck
Blood agar base	- 16 g BAB powder - 400 ml distilled H_2O	Oxoid
Overnight Express Instant TB Medium	- 6% (w/v) Overnight Express Instant TB - 1% (v/v) Glycerol - §Antibiotic - Distilled H_2O	Novagen
Luria-agar	- Same as Luria-Bertani broth with addition of 1.5%(w/v) of agar	(Sambrook & Russel, 2001)
Luria-Bertani broth	- 4 g tryptone - 2 g yeast extract - 2 g NaCl - 400 ml distilled H_2O	(Sambrook & Russel, 2001)
Tryptone soya agar	- 16 g TSA powder - 400 ml distilled H_2O	Oxoid
SOC medium	**SOB medium:** - 4 g tryptone -1 g yeast extract - 0.1 g NaCl - 200 ml distilled H_2O **Plus:** - 50 µl 2M $MgCl_2$ - 200 µl 1M glucose Filter-sterilised through 0.2 µm acrodisc syringe filter and added to 10 ml of SOB medium immediately before use.	(Sambrook & Russel, 2001)

§ The final concentration of required antibiotic is described in Table 2.2

Table 2.2 - Antibiotics solutions

Antibiotic	Stock	Final concentration
Ampicillin	100 mg/ml in distilled H_2O	100 μg/ml
Erythromycin	100 mg/ml in Ethanol	1 mg/ml
Kanamycin	10 mg/ml in distilled H_2O	25 μg/ml

2.4. Plasmids and bacterial strains

2.4.1. Plasmids and bacterial strains used in molecular cloning

The plasmid pKK-*ply* is based on pkk233-2 vector (Brown, 1991) and it carries the wild-type pneumolysin gene (*ply*) (Walker *et al.*, 1987), a resistance gene for ampicillin and an IPTG inducible promoter. The plasmid was used in this work as DNA template for the cloning of the *ply* gene and for protein expression.

The plasmid pAcGFP1-C In-Fusion Ready (Clontech) carries the gene for Green Fluorescent Protein (*gfp*) from *Aequorea coerulescens* and a gene conferring resistance to kanamycin (Clontech, 2006b). The vector was used to fuse the *ply* gene with the *gfp* gene. This fusion retains the fluorescent properties of the GFP and allows monitoring of the fusion product localization *in vitro* and *in vivo*. The vector also provides a pUC origin of replication for propagation in *E. coli*.

The In-Fusion Ready pEcoli-Nterm 6xHN (Clontech) is a highly inducible bacterial expression plasmid that carries a resistance gene for ampicillin and codeing sequences for an N-terminal 6-histidine (His) tag, which allows the purification of the expressed products by immobilized metal affinity chromatography (Clontech, 2006a). This vector was used for expression of the fused protein GFP-PLY. The bacterial plasmids and the *E. coli* strains used in this work are respectively summarised in Table 2.3 and Table 2.4.

Table 2.3 – Summary of bacterial plasmids

Plasmid	Description	Reference
pKK-*ply*	- pKK233-2 carrying wild-type *ply* gene - IPTG inducible promoter - *Amp*^{r}	- (Brown, 1991) - (Walker *et al.*, 1987)
pAcGFP1-C In-Fusion Ready	- *gfp* gene - pUC origin of replication - *Kan*^{r}	(Clontech, 2006b)
In-Fusion Ready pEcoli-Nterm 6xHN	-highly inducible bacterial expression - N-terminal 6xHis tag - *Amp*^{r}	(Clontech, 2006a)

Table 2.4 - Summary of *E. coli* strains

Escherichia coli **strains**	**Description**	**Source**
BL21-Gold (DE3)pLysS	Harbouring pKK-*ply* recombinant plasmid.	Frozen stocks, lab 227 Department of Infection, Immunity and Inflammation (III); University of Leicester
	BL21-Gold (DE3)pLysS chemically competent cells, provide a tighter control of protein expression. Cells were used in this work for heat-pulse transformation with the plasmid pEcoli-Nterm 6xHN carrying the *GFP-ply* gene.	Stratagene
Fusion-Blue™ competent cells	These chemically competent cells were used in this work for heat-pulse transformation with the plasmids pAcGFP1-C and pEcoli-Nterm 6xHN carrying respectively the *ply* and *gfp-ply* genes.	Clontech

2.4.2. Summary of bacterial strains used in biological assays

The biological assays were focused in the use of wild-type *S. pneumoniae* serotype 2 strain D39. Other species were used in anti-microbial activity tests. These were *Streptococcus pyogenes*, *Staphylococcus aureus*, Methicillin-resistant *Staphylococcus aureus* (MRSA), *Clostridium perfringens*, *Bacillus cereus*, *Escherichia coli*, *Pseudomonas aeruginosa* and *Enterobacter aerogenes*, All the strains were from the frozen stocks of laboratory 227 (Department of Infection, Immunity and Inflammation; University of Leicester), with the exception of MRSA and *P. aeruginosa* which were clinical isolates from the Leicester Royal Infirmary.

2.5. Primers

The sequences of the specific primers used in this work are listed in Table 2.5.

Table 2.5 – Sequence of the specific primers.

Primer	Sequence
PLY_F*	**5'AAG GCC TCT GTC GAC ATG GCA AAT AAA GCA GTA AAT GAC3'**
PLY_R*	**5'AGA ATT CGC AAG CTT CTA GTC ATT TTC TAC CTT ATC CTC3'**
GFP_F**	**5'AAG GCC TCT GTC GAC ATG GTG AGC AAG GGC GCC GAG CTG3'**

Notes: The underlined sequences correspond to the overhangs of the specific primers.

*** PLY_F and PLY_R were the forward and reverse primers of *ply* gene. PLY_R was also used to amplify the fused product *gfp-ply* and for its sequencing.**

**** GFP_F was the forward primer used in the amplification of *gfp-ply* and its sequencing**

2.6. General DNA manipulation techniques

2.6.1. Small-scale plasmid extraction (Miniprep)

Small-scale plasmid extraction was done using two commercially available kits NucleoSpin® Plasmid (Macherey-Nagel, UK) and QIAprep Spin Miniprep (Qiagen, UK), depending on availability in the lab. Both procedures used the modified alkaline lysis method of Birnboim and Doly (Birnboim & Doly, 1979). All buffers and purification columns were provided with the kits. All centrifugation steps were carried out in a standard benchtop microcentrifuge at 11,000 – 17,900 ×g, depending on the kit in use. Ten millilitres of an overnight culture of *E. coli* in LB plus required antibiotic were transferred to microfuge tubes and centrifuged for 30 seconds at room temperaure. Following harvesting, the pelleted cells were resuspended in a buffer containing RNase A (provided with the kit and added to the buffer to a final concentration of 0.1 mg/ml and 0.4 mg/ml in the case of the QIAprep Spin Miniprep kit and NucleoSpin® Plasmid kit, respectively). The SDS (sodium dodecyl sulfate) /alkaline lysis buffer from the kit was then added and the tubes mixed thoroughly. After 5 minutes of incubation at room temperature, the resultant clear and viscous lysate was neutralized by the addition of a guanidine hydrochloride containing buffer to precipitate denatured proteins, cell debris and other remaining products and centrifuged after for 10 minutes. The supernatant was then loaded onto a silica-membrane spin column and centrifuged for 1 minute to bind the plasmid DNA. The membrane was washed with an “ethanolic” buffer, centrifuging for 1 minute, and then dried with an additional step of centrifugation to remove the residual washing buffer. 50 µl of Tris-HCl (pH 8.5) buffer were added to the column and left incubating at room temperature for 1 minute, in order elute the DNA. The column was centrifuged for 1 minute and the plasmid DNA collected in a clean and sterile microfuge tube.

2.6.2. Polymerase chain reaction (PCR)

PCR was done according to the method described by Saiki and colleagues (Saiki *et al.*, 1988). The reactions were prepared in 50 µl using the following reagents:

- 5 µl 10× NH_4 reaction buffer: 160 mM $(NH_4)_2SO_4$, 670 mM Tris-HCI (pH 8.8 at 25°C), 0.1% (v/v) Tween-20 (Bioline).
- 1.5 µl 50 mM $MgCl_2$ solution (Bioline).
- 1 µl deoxyribonucleotides triphosphate mix (dNTPs): 10 mM of each dATP, dTTP, dCTP, dGTP (Bioline). The mixture was prepared by adding 10 µl of each dNTP (100 mM) to 60 µl UV-treated nanopure H_2O. The dNTPs solution was mixed well, aliquoted and stored at -20ºC.
- 25 pmol of each forward and reverse primers (Table 2.5).
- DNA template was used up to 100 ng. In the negative control no DNA was added.
- Nanopure H_2O, UV treated for 10 minutes, up to a final volume of 50 µl.
- 1 µl (5 units) of thermostable Biotaq^{TM} DNA polymerase (Bioline).

The PCR tubes containing the mixture were pulse-centrifuged for 10 seconds and then placed in a T-Gradient Thermal Cycler (Biometra, Germany). The thermal cycling was performed using the following cycling parameters:

DNA template: *ply*			
95ºC		1 minute	
94ºC	30 cycles	30 seconds	Denaturation
65ºC		30 seconds	Annealing
72ºC		2 minutes	Extension
72ºC		10 minutes	

DNA template: *gfp-ply*			
95ºC		1 minute	
94ºC	30 cycles	30 seconds	Denaturation
68ºC		30 seconds	Annealing
72ºC		2 minutes	Extension
72ºC		10 minutes	

The PCR products were analysed by agarose gel electrophoresis (section 2.6.4).

2.6.3. Colony PCR

Colony PCR was applied in the selection of transformants. The reactions were prepared in 50 µl using the following reagents:

- 5 µl 10× NH_4 reaction buffer: 160 mM $(NH_4)_2SO_4$, 670 mM Tris-HCI (pH 8.8 at 25°C), 0.1% (v/v) Tween-20 (Bioline).
- 1.5 µl 50 mM $MgCl_2$ solution (Bioline).
- 1 µl deoxyribonucleotides triphosphate mix (dNTPs): 10 mM of each dATP, dTTP, dCTP, dGTP (Bioline). The mixture was prepared by adding 10 µl of each dNTP (100 mM) to 60 µl UV-treated nanopure H_2O. The dNTPs solution was mixed well, aliquoted and stored at -20ºC.
- 25 pmol of each forward and reverse primers.
- Sweep of colonies. In the negative control no DNA was added.
- 41 µl nanopure H_2O, UV treated for 10 minutes.
- 1 µl (5 units) of thermostable Biotaq^{TM} DNA polymerase (Bioline).

The PCR tubes containing the mixture were pulse-centrifuged for 10 seconds and then placed in a T-Gradient Thermal Cycler (Biometra, Germany). The thermal cycling was performed using the cycling parameters described in section 2.6.2 and the PCR products analysed by agarose gel electrophoresis (section 2.6.4).

2.6.4. Agarose gel electrophoresis

PCR products were run on 0.9% (w/v) agarose gels which are suitable to separate fragments with sizes ranging 0.5-7 Kb (Sambrook & Russel, 2001). Gels were prepared by adding 0.9 g agarose (Bioline) to 100 ml 1× TAE buffer, pH 7.7 (50× TAE buffer:

242 g Tris base, 57.1 ml glacial acetic acid, 100ml of 0.5 M EDTA (pH 8.0)). The agarose was heated in a microwave for few minutes, until it was completely dissolved, and then it was cooled to approximately 50ºC, before the addition of ethidium bromide to a final concentration of 0.2 μg/ml. The gel was then poured into a sealed casting tray, with a comb in place and left to solidify. Afterwards, the casting tray containing the gel was transferred to an electrophoresis tank, containing TAE buffer, and the comb was carefully removed. Each DNA sample was mixed with 1× DNA loading dye (6× DNA loading dye - Fermentas, UK) and loaded into the wells, alongside a 1 Kb DNA ladder (MBI Fermentas, UK) as a reference to determine the size of the fragments. In general, the electrophoresis was performed by applying a constant voltage of 70 V. The DNA fragments were visualized using an UV transilluminator.

2.6.5. Purification of PCR products

PCR products were purified using the QIAquick PCR purification kit (Qiagen, UK). This step was to remove unwanted primers and impurities such as salts, enzymes and unincorporated nucleotides, which could affect the success of further cloning steps. The protocol provided by the manufacturer was followed. All buffers and purification columns were supplied with the kit. All centrifugation steps were done in a standard benchtop microcentrifuge at 17,900 ×g. Five volumes of binding buffer were added to 1 volume of PCR sample and mixed. The mixture was loaded onto a silica-membrane spin column and centrifuged for 30 seconds to bind DNA. The membrane was then washed with an "ethanolic" buffer, centrifuging for 1 minute, and dried with an additional step of centrifugation. Tris-HCl (pH 8.5) buffer was added to the column and left to incubate at room temperature for 1 minute. The column was centrifuged for 1 minute and the purified PCR product collected into a clean and sterile microfuge tube.

2.6.6. Cloning of targeted gene sequences

Cloning was done using the In-Fusion™ Dry-Down PCR Cloning Kit (Clontech) and the TALON® Express Bacterial Expression & Purification Kit (Clontech). The plasmids used are shown in Table 2.3. The ligation reactions were performed according to the manufacturer's instructions. Lyophilised reaction mixtures (In-Fusion™ Dry-Down mix) were provided with the kits, in sealed 8-well strips. The DNA inserts were mixed with the correspondent vectors at a molar ratio 2:1 in 10 µl of UV treated nanopure H_2O and then added to the reaction tubes provided. The reaction mixtures were incubated for 30 minutes, at room temperature for cloning of *ply* and at 42ºC in the subcloning of *gfp-ply*. Once the reaction was finished, the tubes were transferred to ice. The resultant recombinant vectors were used in the transformation of chemically competent cells (section 2.6.7).

2.6.7. Heat-pulse transformation of chemically competent bacterial cells

2.6.7.1. Transformation into Fusion-Blue™ competent cells

Plasmids were transformed into a chemically competent *E. coli* strain – the Fusion-Blue™ competent cells (Table 2.4). Cells were supplied by Clontech in 50 µl frozen vials. The reaction mixtures (section 2.6.6) were diluted with 40 µl of UV treated nanopure H_2O. The transformation steps were carried out according to the manufacturer's instructions. Frozen vials of competent cells were thawed on ice. Once thawed, the tubes were gently tapped to ensure complete suspension of cells. 2.5 µl of the diluted reaction mixtures were then added to the cells. The tubes were gently mixed and left on ice for 30 minutes. Cells were then heat-shocked in a water bath at 42ºC for

45 seconds and placed immediately on ice for 1 minute. After heat-pulse transformation, 450 µl SOC medium (Table 2.1) were added to the cells and these were subsequently incubated at 37ºC for 1 hour with shaking at 220rpm. Then the transformation products were plated onto LA (Table 2.1) plus appropriate antibiotic (Table 2.2) and incubated overnight at 37ºC. Next day, colonies were randomly selected for colony PCR screening (section 2.6.3) and patched onto fresh LA (plus appropriate antibiotic) plates for subsequent isolation of plasmid DNA (section 2.6.1). Once the presence of the insert of interest was confirmed, the isolated plasmid DNA was lyophilised and sent for sequencing at MWG.

2.6.7.2. Transformation into BL21-Gold (DE3)pLysS competent cells

Escherichia coli BL21-Gold (DE3)pLysS (Table 2.4) is an easy inducible *E. coli* strain that promotes high levels of protein expression. Cells were supplied in 100 µl frozen vials by Stratagene. The transformation protocol recommended by the manufacturer was followed. The vials were thawed on ice. Once thawed, the cells were gently mixed and aliquoted into prechilled 14 ml falcon polypropylene round-bottom tubes (BD, UK). 1–2 µl (≈ 50 ng) of transforming DNA were then added to the aliquots, while 1 µl of pUC18 control plasmid was added into a separate vial of *E. coli*. The transformation reactions were gently swirled and incubated on ice for 30 minutes. Each transformation reaction was then heat-pulsed in a 42ºC water bath for 20 seconds and placed immediately on ice for 2 minute. Afterwards, 900 µl of pre-warmed (42ºC) SOC medium were added to the cells and these were subsequently incubated at 37ºC for 1 hour with shaking at 220rpm. Then, the transformation products were plated out onto LA plus ampicillin and incubated overnight at 37ºC. Next day, colonies were randomly selected and patched onto fresh LA plus ampicillin plates, which were subsequently

incubated overnight at 37ºC. Plasmid DNA isolated from the selected transformants was lyophilised and sent for sequencing at MWG.

2.7. Small-scale protein expression

Small-scale protein expression was done according to the method described in Sambrook & Russel, 2001. The appropriate recombinant *E. coli* (Table 2.4) was inoculated into 10 ml of LB with required antibiotic (Table 2.2) and incubated overnight at 37ºC, with shaking at 220 rpm. Next day, 1 ml of the overnight culture was added into 10 ml of fresh LB with appropriate antibiotic (Table 2.2) and incubated at 37ºC, with shaking at 220 rpm. When the culture reached an OD_{600} of approximately 0.5-0.6, protein expression was induced by the addition of 1 mM filtered-sterilised IPTG (Melford laboratories, UK) and the culture was incubated until it reached an OD_{600} of approximately 1.5-1.6. At this stage, the cells were harvested in a PK131R Refrigerated Centrifuge (ALC International), at 2,324 ×g for 15 minutes, at 4ºC. The pellet was then resuspended in 250 µl ice cold phosphate buffer saline (PBS: 136 mM NaCl, 8 mM Na_2HPO_4, 1.5 mM KH_2PO_4, 2.7 mM KCl, pH 7.3) and transferred to a clean and sterile eppendorf tube. The cells were then sonicated with a small sonicator probe (Soniprep), in order to produce a crude cell extract containing pneumolysin. The tube containing the cells' suspension was kept all time in a beaker filled with ice, to prevent overheating. Sonication was performed at 1 minute intervals, by a applying a 5 seconds pulse with an amplitude of 6 microns, followed by a "cooling" period of 55 seconds. The procedure was repeated 5-6 times or until the bacterial sonicate became clearer and less viscous. Then, the cell lysate was centrifuged at 15,115 ×g in a bench-top centrifuge, for 10 minutes at 4ºC. The supernatant was transferred into a clean and sterile tube and checked afterwards for activity using a haemolytic assay (section 2.10.1).

2.8. Large-scale protein expression and purification

The scaled-up expression of the wild-type and recombinant pneumolysin was performed by means of the conventional IPTG induced protein expression method (El-Rachkidy, 2003) or by using an overnight express autoinduction system (Novagen).

The purification procedures were performed by Dr. Rana El-Rachkidy (Department of Infection, Immunity and Inflammation; University of Leicester) using two FPLC systems (Pharmacia, UK and GE healthcare, UK). All the buffers employed in the purification steps were filtered through 0.2 µm filter-vacuum units (Nalgene), prior to their use.

2.8.1. IPTG induced large-scale protein expression

A 1:100 dilution of a recombinant *E. coli* (Table 2.4) overnight culture was made in 2 L flasks containing 1000 ml LB with ampicillin (Table 2.2). The flasks were incubated at 37ºC with shaking at 220 rpm until the culture attained an OD_{600} of approximately 0.5-0.6. At this stage the protein expression was induced with 1 mM of filtered-sterilised IPTG (Melford laboratories, UK) and the flasks re-incubated for approximately 2-3 hours or until the culture reached an OD_{600} of 1.5-1.6. The culture was then transferred into 500 ml polypropylene bottles, which were centrifuged at 4,000 rpm in an Avanti® J-E refrigerated centrifuge (Beckman Coulter) with a F10 BCI rotor for 40 minutes at 4ºC. When the sonication step was not performed in the same day, the harvested cells were stored at -80ºC and thawed on ice before use. Then, the pellet was resuspended in 5 ml of 250 mM ice-cold PBS (8 mM Na_2HPO_4, 1.5 mM KH_2PO_4, 2.5 mM KCl, 250 mM NaCl, pH 7.2) and lysed by sonication using a large sonicator probe. This step was performed in 2 minutes intervals, by a applying a 10 seconds pulse, with at an amplitude

of 7 microns, followed by a "cooling" period of 1 minute 50 seconds. The procedure was repeated approximately 10 times or until the bacterial sonicate became clearer and less viscous. The cell lysate was transferred into 50 ml polypropylene tubes and centrifuged at 20,000 rpm in an Avanti® J-E refrigerated centrifuge (Beckman Coulter) with a JA 25.50 rotor for 30 minutes at 4ºC, in order to remove the cell debris. The supernatant obtained was filtered through a 0.45 μm acrodisc syringe filter (PALL- Life Sciences) and checked for haemolytic activity (section 2.10.1). The crude extract containing pneumolysin was stored at -20ºC.

2.8.2. Large-scale protein expression using an overnight express autoinduction system

The Overnight Express Instant TB Medium (Novagen) was alternatively used in the large-scale expression of pneumolysin. The culture medium was formulated as described in section 2.2, Table 2.1. The guidelines provided by the supplier were followed. 10 ml of overnight express instant TB medium plus ampicillin (Table 2.2) were inoculated with 0.1% (v/v) recombinant *E. coli*, from glycerol stocks, and incubated overnight at 37ºC with shaking at 300 rpm. Next day, 5% (v/v) inocula were generated at two different stages with increasing volumes of culture. In the first stage, 0.001 volume of the overnight culture was transferred into 4 ml of fresh TB medium containing ampicillin (Table 2.2) and the cultures were incubated at 37ºC with shaking at 300 rpm. When the OD_{600} attained 0.5, 5% (v/v) of inoculum produced in the first stage was transferred into 20 ml of fresh TB medium containing ampicillin (Table 2.2). The cultures were incubated at 37ºC with shaking at 300 rpm until attained an OD_{600} of approximately 0.5. Finally, 5% (v/v) inocula were transferred into 2 L flasks containing 500 ml of fresh TB medium with ampicillin (Table 2.2). The flasks were incubated

overnight at 37ºC with shaking at 300 rpm. Next day, the cultures were transferred into 500 ml polypropylene bottles, which were centrifuged at 4,000 rpm in an Avanti® J-E refrigerated centrifuge (Beckman Coulter) with a F10 BCI rotor, for 40 minutes at 4ºC. The harvested cells were then resuspended in an extraction reagent (Bugbuster® protein extraction reagent from Novagen) at room temperature, using approximately 5 ml of reagent per gram of wet paste. The cell suspensions were subsequently incubated at a slow setting on a shaking platform, for 20 minutes at room temperature. The cell lysate was transferred into 50 ml polypropylene tubes and centrifuged at 16,000 rpm in an Avanti® J-E refrigerated centrifuge (Beckman coulter) with a JA 25.50 rotor for 40 minutes at 4ºC, in order to remove the cell debris. The supernatant was filtered through a 0.45 μm acrodisc syringe filter (PALL- Life Sciences) and checked for its haemolytic activity (section 2.10.1). The crude extract containing pneumolysin was stored at -20ºC.

2.8.3. Purification of the recombinant wild-type pneumolysin

The recombinant wild-type pneumolysin was purified employing a modified version of that described by Gilbert and co-workers (Gilbert *et al.*, 1998). The method consisted of a two-stage purification, starting with a hydrophobic interaction chromatography, characterised by the binding of the hydrophobic region of pneumolysin to a phenyl group linked to the sepharose beads in the chromatography column, followed by an ion exchange chromatography, where the pneumolysin present in the purified fraction from the previous step, was eluted by applying a salt gradient (El-Rachkidy, 2003).

2.8.3.1. Hydrophobic interaction chromatography

The crude extract from the preceding step (section 2.8.1 or section 2.8.2) was loaded onto a 20 ml HiLoad Phenyl Sepharose High Performance column (GE Healthcare) that was previously equilibrated with at least one column volume of elution buffer (buffer B: nanopure H_2O) and two column volumes of binding buffer (buffer A: 8 mM Na_2HPO_4, 1.5 mM KH_2PO_4, 2.5 mM KCl, 250 mM NaCl, pH 7.2), at a flow rate of 1 ml/min. The column was initially washed thoroughly with 100% buffer A, until all the unbound proteins were washed off the column and, consequently, the peak of absorbance at 280 nm returned to the baseline. The column was then washed with 100% buffer B to elute pneumolysin. The fractions under the pick of absorbance were checked for their haemolytic activity (section 2.10.1) and then stored at -20ºC.

2.8.3.2. Ion exchange chromatography

The fractions containing pneumolysin from the preceding purification stage (section 2.8.3.1) were loaded onto a 1 ml Source 15Q column (GE Healthcare) which was pre-equilibrated with at least eight column volumes of high ionic strength elution buffer (buffer B: 8 mM Na_2HPO_4, 1.5 mM KH_2PO_4, 2.5 mM KCl, 1 M NaCl, pH 7.5) and forty column volumes of binding buffer (buffer A: buffer B lacking NaCl, pH 7.5), at a flow rate of 1 ml/min. The column was initially washed thoroughly with 100% buffer A, until all the unbound proteins were washed off the column and, consequently, the peak of absorbance returned to the baseline. Then, a linear gradient of salt from 0 to 200 mM NaCl (buffer B) was applied and pneumolysin was eluted at approximately 130 mM NaCl. The collected fractions were checked for their haemolytic activity (2.10.1) and purity (section 2.9.2). The fractions containing pure pneumolysin were stored at -80ºC.

2.8.4. Purification of the recombinant fusion protein GFP-PLY

The recombinant fusion protein GFP-PLY with a 6×His-tag at the N-terminus was purified by means of immobilized metal affinity chromatography (IMAC). The concept of this method has first been introduced by Porath *et al.* in 1975 and it is based on the natural ability of certain amino acids (histidine, cysteine and tryptophan) to form complexes with transition metal ions such as Ni^{2+}, Co^{2+}, Cu^{2+}, Zn^{2+} around neutral pH (Block *et al.*, 2009; Hu & Seeley, 2010). The complexes formed can then be broken by reducing the pH and increasing the ionic strength of the buffer or by including EDTA or imidazole in the buffer (Hu & Seeley, 2010). This way, it was possible to reversibly bind the 6×His-tagged recombinant fusion protein to the metal ion Ni^{2+} immobilised on the resin of the chromatography column. Finally, by increasing the concentration of the imidazole in the elution buffer, the complex formed between the histidine residues and the metal group was broken, allowing the elution of the recombinant fusion pneumolysin.

2.8.4.1. Immobilized metal affinity chromatography

The crude extract from the preceding step (section 2.8.2) was loaded onto a 5 ml HisTrap High Performance column (GE Healthcare) that was pre-equilibrated with at least five column volume of binding buffer (buffer A: 20 mM Na_2HPO_4, 0.5 M NaCl, 40 mM imidazole, pH 7.4), at a flow rate of 1 ml/min. The column was initially washed thoroughly with 100% buffer A, until all the unbound proteins were washed off the column and, consequently, the peak of absorbance returned to a steady baseline. The column was then washed with 100% buffer B (20 mM Na_2HPO_4, 0.5 M NaCl, 500 mM imidazole, pH 7.4) to elute pneumolysin. The fractions under the peak of absorbance at 280 nm were checked for their haemolytic activity (section 2.10.1) and purity (section 2.9.2). The fractions containing pure GFP-PLY were stored at -80ºC.

2.9. General techniques for protein manipulation

2.9.1. Determination of protein concentration by UV spectroscopy

The concentration of purified protein present in the fractions collected (section 2.8.3 and section 2.8.4) was determined by measuring the A_{280}. For this, 1:20 dilutions of a 2 mg/ml bovine serum albumin solution (Amersham) and purified toxin were prepared in 1 ml of nanopure H_2O. To the blank only nanopure H_2O was added. The A_{280} of each sample were measured in quartz cuvettes, with a 1 cm pathlength. Finally, the concentration (mg/ml) of purified protein in the fractions was determined by the following equation

$$\text{Concentration}\left(\text{mg/ml}\right) = \frac{A_{280}}{\varepsilon_{280} \times (\text{cuvette path length in cm})} \times \text{dilution factor.}$$

ε_{280} - extinction coefficient (cm^2mg^{-1}). The ε_{280} value predicted for pneumolysin is 1.36 cm^2mg^{-1} (Solovyova *et al.*, 2004).

2.9.2. SDS polyacrylamide gel electrophoresis (SDS-PAGE)

A discontinuous SDS polyacrylamide gel electrophoresis system was employed in this work by using a 5% (w/v) stacking gel and 12% (w/v) resolving gel (Sambrook & Russel, 2001). SDS-PAGE was performed using the Mini-PROTEAN 3 cell (Bio-rad).

2.9.2.1. Gel preparation

Before casting the gels, the glass plates were assembled, evenly aligned and secured by a casting frame. The assembly was then placed on a casting stand that had sealing

casting gaskets on the bottom. Then, a 15 ml 12% (w/v) resolving gel was prepared (Sambrook & Russel, 2001) using the components in Table 2.6.

Table 2.6 - Solutions for preparation of 12% (w/v) resolving gels for SDS-PAGE.

Component	Volume (ml)
Nanopure H_2O	4.9
30% (w/v) acrylamide (Ultrapure protogel – National Diagnostics, UK)	6.0
1.5 M Tris-HCl , pH 8.8	3.8
10% (w/v) SDS	0.15
10% (w/v) ammonium persulfate	0.15
TEMED (Bio-rad)	0.006

Once the ammonium persulfate and TEMED were added, the mix was quickly vortexed and smoothly poured into the assembled cassettes, up to approximately 1 cm below the level of the comb teeth. The resolving gels were immediately overlaid with nanopure H_2O to prevent dehydration, and allowed to polymerise for approximately 45 minutes. At this stage, 1× running buffer was prepared by adding 100 ml of 10× Tris-glycine-SDS (TGS) electrophoresis grade buffer (National Diagnostics) in 1L of distilled H_2O. After polymerisation of the resolving gels, the overlaying nanopure H_2O was removed and the excess absorbed with filter paper. At this point, 5 ml of 5% (w/v) stacking gel were prepared (Sambrook & Russel, 2001) using the components in Table 2.7.

Table 2.7 - Solutions for preparation of 5% (w/v) stacking gels for SDS- PAGE.

Component	Volume (ml)
Nanopure H_2O	3.4
30% (w/v) acrylamide (Ultrapure protogel – National Diagnostics, UK)	0.83
1.0 M Tris-HCl , pH 6.8	0.63
10% (w/v) SDS	0.05
10% (w/v) ammonium persulfate	0.05
TEMED (Bio-rad)	0.005

After the ammonium persulfate and TEMED were added, the solution was quickly vortexed and smoothly poured on the top of the resolving gels. The comb was inserted immediately into the settled stacking gel before polymerisation began. If the gels were to be used same day, they were transferred into the electrophoresis tank, half-filled with 1× TGS buffer, otherwise they were stored in 1× TGS buffer at 4ºC.

2.9.2.2. Sample preparation

The protein samples were treated by briefly heating them in the presence of a reducing buffer (Roe, 2001). A beaker filled with H_2O was heated to boiling. While this was taking place, 4× NuPAGE® LDS (lithium dodecyl sulphate) sample buffer (Invitrogen) was added to the samples to 1× final concentration. The lids of the samples tubes were punctured with a needle, in order to release the pressure generated during the heating process. When the boiling temperature was attained, the tubes were placed in a floating rack and transferred to the boiling H_2O for 5 minutes.

2.9.2.3. Electrophoresis

After the preparation of the samples, the moulding combs were carefully removed and the wells filled with 1× TGS buffer. The samples were smoothly loaded into the wells alongside the protein markers (Precision plus protein standard – all blue; Bio-rad), and the electrophoresis chambers were filled with 1× TGS buffer. The lid was then placed on the mini-tank, in the correct orientation of the electrodes. The gels were set to run at a constant current of 40 mA, until the dye present in the loading buffer reached the bottom. Once the electrophoresis was completed the gel cassette was gently separated and the gel carefully removed into a large Petri dish. The gel was briefly rinsed with distilled H_2O and subsequently incubated overnight in a Coomassie blue staining solution, prepared by adding 1 part ethanol to 9 parts Protoblue safe – colloidal Coomassie blue G-250 stain (National Diagnostics). Next day, the gel was washed in water and analysed. In other cases, the gels were transblotted for later immunodetection (section 2.9.3).

2.9.3. Western blotting

Immunoblotting was performed using a mouse anti-pneumolysin antibody, PLY-4 (De Los Toyos *et al.*, 1996), kindly provided by Dr. Fernando Vázquez Valdés (Universidad de Oviedo, Spain).

2.9.3.1. Protein transfer

Protein samples were electrophoresed through a 12% (w/v) SDS-PAGE (section2.9.2). After electrophoresis, a gel sandwich was constructed in a plastic blotting cassette. The gel was placed on the negative (dark) side of the blotting cassette and a nitrocellulose membrane (Amersham) on the positive (clear) side, intercalated between a blotting pad

and two layers of thick filter paper (Bio-rad) from each side, as described in (Sambrook & Russel, 2001). The cassette was then placed in the mini trans-blot tank (Bio-rad), filled with ice-cold transfer buffer (5.9 g Tris, 2.9 g glycine, 200 ml methanol, 3 ml 10% (w/v) SDS, 800 ml distilled H_2O, pH 8.3) and placed in ice bucket. The transfer was performed at 250 mA for 1 hour. Once the blotting was completed, the membrane was blocked overnight at 4ºC, with 5% (w/v) skimmed milk in PBS.

2.9.3.2. Immunodetection

Next day, the membrane was washed 3 times (10 minutes each wash) with PBS containing 0.05% (v/v) Tween 20 (PBS-T), and incubated with the primary monoclonal antibody PLY-4 (1:1000 dilution in PBS-T plus 2% (w/v) skimmed milk), at room temperature and shaking for 90 minutes. The membrane was then washed 4 times with PBS-T (10 minutes each wash), and incubated with the secondary antibody, goat anti-mouse IgG (Sigma) alkaline phosphatase conjugate (1:2000 dilution in PBS-T plus 2% (w/v) skimmed milk), at room temperature and shaking for 1 hour. Finally, the membrane was washed 4 times with PBS-T (10 minutes each wash). The detection of the antibody complex was done by incubating the membrane with approximately 5 ml of BCIP/NBT liquid substrate system (Sigma) until the bands were completely developed.

2.10. Biological assays

2.10.1. Haemolytic assay

Haemolytic assays were performed to assess the biological activity of pneumolysin using the method described by Owen and collaborators (Owen *et al.*, 1994). 50 µl of serial two-fold dilutions of the toxin in PBS were done across 12 wells of a round bottomed 96-wells microtiter plate (Nunc, Denmark). For the negative control, PBS was used. 50 µl of a 4% (v/v) sheep red blood cells suspension was added. To prepare sheep red blood cells, 10 ml of sheep blood (Oxoid, UK) were centrifuged at 1,734 ×g in an Allegra^{TM} X-22R refrigerated centrifuge (Beckman Coulter), for 15 minutes at 4ºC. The supernatant was carefully removed with a Pasteur pipette and 400 µL of the pelleted red blood cells transferred into 10 ml of PBS, to make a suspension with a concentration of 4% (v/v) sheep red blood cells. After addition of blood, the plate was incubated at 37ºC for 30 minutes. The activity of the toxin (HU/ml) was determined by assessing by eye the dilution where 50% lysis of the erythrocytes occurred. For this it was necessary to calculate the number of haemolytic units (HU) present in all wells up to where 50% lysis occurred. The undiluted toxin was established to contain 1 HU. When diluted in the first well this 1 HU was divided in 2 HU, in the second well in 4 HU and so on. Finally, the number of haemolytic units required to produce 50% lysis within a total volume of 100 µl, were converted to HU/ml and used to express the haemolytic activity of the toxin, as illustrated in Figure 2.1.

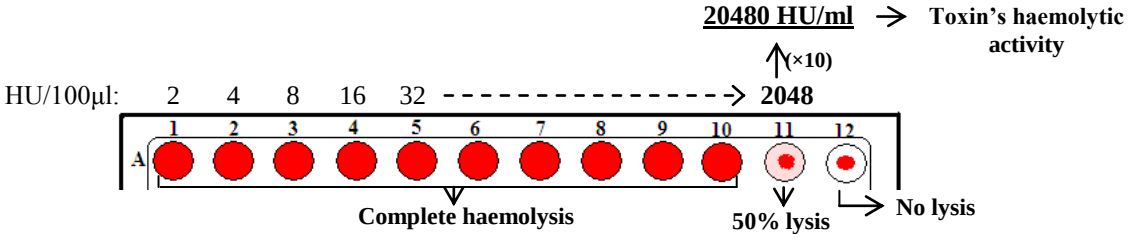

Figure 2.1- Determination of the biological activity of pneumolysin.

2.10.2. Preparation and storage of anti-pneumolysin peptides and small molecules stocks

Peptides (Table 2.8) were obtained from Severn Biotech Ltd. (UK). The peptides were provided in a lyophilised form and were resuspended in nanopure H_2O to a final concentration of 2 mg/ml.

Small molecules from Maybridge (Fisher, UK), were also provided in a lyophilised form and resuspended in absolute DMSO (Sigma), at a final concentration of 50 mM. A 1:100 dilution of "stock 1" in PBS was prepared for use in *in vitro* inhibition assays of pneumolysin.

The stocks were kept at 4ºC for short periods of time and for longer periods of time they were stored at -20ºC.

Table 2.8 – Anti-pneumolysin peptides.

Peptide ID	Sequence
P1	A E G E F S R R T R A G F G D P A K
P2	A E G E F D I D H Y L E Y I G A G G D P A K
P3	A E G E F R R W C C T R C R V L P P D P A K
P4	A E G E F T E T K W T C R R Q V W G D P A K
P5	A E G E F A G K N L K H G N H T V G D P A K
P6	A E G E F S R Q A H G V R R G G R G D P A K

2.10.3. *In vitro* inhibition assays

50 µl of peptides or small molecules (section 2.10.2) were added to the first wells of round-bottomed 96-wells microtiter plates (Nunc, Denmark) and 25 µl were two-fold serial diluted in PBS across 12 wells. This was followed by the addition of 80 ng of pneumolysin to each well and incubation at 37ºC, for 45 minutes. After the incubation period, 50 µl of 4% (v/v) sheep red blood cells suspension was added to each well and the plates were incubated once more at 37ºC, for at least 30 minutes. Controls with only red blood cells in PBS or red blood cells plus pneumolysin and also of peptides/small molecules plus red blood cells were prepared following the same procedure.

2.10.4. Procedures for *in vivo* experiments

All *in vivo* procedures were performed according to the standard operating procedures under the project license 80/2111, following the regulations from the Animal Scientific Procedure Act 1986 of the United Kingdom Home Office.

The mice used in this work were specific pathogen free (SPF) outbred MF1 females, 8 weeks old or more, weighing 25-30 g obtained from Harlan (Bicester, UK). The animals were maintained in groups of five under controlled conditions of temperature, humidity and day length. They were given tap water and pelleted food.

2.10.4.1. Preparation of *S. pneumoniae* passaged frozen stocks

Standardized virulent wild-type *S. pneumoniae* D39 stocks were prepared by a modification of a previous method (Canvin *et al.*, 1995). 10 ml of a pneumococcal overnight culture in BHI broth (Table 2.1) were centrifuged at 1,734 ×g in an Allegra™ X-22 centrifuge (Beckman Coulter) for 15 minutes, and the pellet resuspended in 5 ml

of PBS to give an OD_{500} 1.4-1.6. The identity of the strain was confirmed by an Optochin sensitivity test (section 2.10.4.2). Two mice were intraperitoneally challenged (section 2.10.4.5) with 100 µl of D39 suspension. Approximately 24 hours later, if the mice were scored 1+ lethargic (section 2.10.4.4) the animals were anaesthetised with 5% (v/v) of inhaled isoflurane in 1.6-1.8 L O_2/minute inside an anaesthetic box. When anaesthesia was confirmed by reduction of breathing rate and loss of joint reflex, blood samples were collected from each mouse by cardiac puncture (section 2.10.4.9). Without allowing recovery from anaesthesia, the animals were culled by cervical dislocation.

The collected samples were individually processed by inoculating 50 µl of blood into 10 ml of BHI broth and incubating statically, overnight at 37ºC. On the following day, the supernatants were removed without disturbing the loose sediment of red blood cells, and spun at 1,734 ×g in an Allegra^{TM} X-22 centrifuge (Beckman Coulter) for 15 minutes. The resulting pellets were resuspended in 1 ml of serum broth (80% BHI (v/v) + 20% (v/v) heat-inactivated foetal bovine serum (FBS; Sigma). Then, 700 µl of this suspension were added in 10 ml of serum broth to give an OD_{500} 0.7. The culture was incubated statically for approximately 5 hours at 37 ºC, until the OD_{500} was 1.6. Aliquots of 500 µl were made and stored at -80ºC until further use.

To evaluate the quality of the stocks, 24 hours after storage at -80ºC one aliquot was thawed and centrifuged at 15,115 ×g in a benchtop centrifuge for 2 minutes. The supernatant was removed and remaining pellet resuspended in 400 µl of sterile PBS. The concentration of colony forming units (CFU) was determined (section 2.10.4.3) and the identity of the strain confirmed by the Optochin sensitivity test (section 2.10.4.2). The stocks could be stored for at least 3 months at -80ºC with no significant loss of viability.

2.10.4.2. Optochin sensitivity test for identification of *S. pneumoniae*

Determination of optochin sensitivity was done by a method previously described (Bowers & Jeffries, 1955). A streak of the organism to be tested was made on blood agar base (Table 2.1) supplemented with 5% (v/v) horse blood (Oxoid, UK). A paper disc impregnated with Optochin (Oxoid, UK) was then placed in the centre of the inoculum, followed by overnight incubation in CO_2 gas jars at 37ºC. After incubation, the appearance of a zone of inhibition at least 5 mm from the edge of the disc indicated the organism was optochin sensitive.

2.10.4.3. Viable count

Viable count was performed by the method described by Miles and Misra (Miles *et al.*, 1938). 20 µl of sample were serially diluted in 180 µl PBS in round-bottomed 96-wells microtitre plates (Nunc, Denmark), up to a dilution of 10^6. Blood agar plates were divided into six sectors and 30 µl of a single dilution plated onto one sector. The plates were incubated in CO_2 gas jars overnight at 37ºC. The following day, colonies were counted in the sector where 30-300 colonies were visible. The concentration of colony forming units (CFU) per millilitre was determined by using the following equation

$$\text{CFU per ml} = \frac{\text{Number of colonies in sector}}{30\ \mu\text{l}\ (\text{Volume plated per sector})} \times \text{Dilution} \times 1000\ (\text{conversion factor})$$

2.10.4.4. Scoring of the signs of the disease after infection

After infection with *S. pneumoniae* D39, the signs of disease were frequently assessed and scored until the end of the experiment, based on the scheme of Morton *and* co-workers (Morton & Griffiths, 1985) and described in Table 2.9. The mice were not

allowed to reach a moribund state, and mice found to have a score of 6 were culled by cervical dislocation.

Table 2.9 - Disease scoring scheme.

Sign	Description	Score
Normal	Healthy appearance. Highly active.	**0**
1+/2+ Hunched	Slight (1+) or pronounced (2+) convex curvature of the upper spine.	**1; 2**
1+/2+ Starey coat (Piloerection)	Slight (1+) or pronounced (2+) piloerection of the coat.	**3; 4**
1+/2+ Lethargic	Pronounced hunching and piloerection accompanied by a considerable (1+) or severe (2+) reduction of activity.	**5; 6**
Moribund	Complete inertia. Drastic reduction of breathing rate. Drop of the body temperature.	**N/A**

N/A – Not applicable

2.10.4.5. Intraperitoneal injection of mice

For intraperitoneal infection or treatment, each mouse was restrained by grasping the scruff of the neck firmly between the thumb and forefinger. The tail was held in place by using the fourth and fifth fingers of the same hand against palm in order to stretch the animal gently. The hand was then turned to position the mouse tilted at a 45º angle,

head-downwards, showing its ventral side, so that the internal organs would be slightly displaced forward, avoiding their puncture. Using a 0.5 ml insulin syringe, the dose, in up to 100 µl sterile PBS, was injected after careful insertion of the needle into the lower right quadrant of the abdominal cavity at an approximate 45º angle.

2.10.4.6. Intranasal administration to mice

Mice were lightly anaesthetised with 2.5% (v/v) isoflurane (Animalcare Ltd., UK) over 1.6-1.8 L O_2/minute. The confirmation of effective anaesthesia was made by observation of no pedal reflex. A mouse was held by the scruff of the neck in a vertical position with its nose upward. The dose was then administered in up to 50 µl sterile PBS, given drop by drop into the nostrils, allowing the animal to inhale it in between drops. Once the dose was given, the mouse was returned to its cage, placed on its back, to recover from the effects of anaesthetic.

2.10.4.7. Intravenous injection of mice

Mice were placed in a cage inside an incubator at 37ºC, for 20 minutes, to dilate their veins. After incubation, the cage was brought outside and the mice were kept warm under an infra-red (IR) lamp. A mouse was then placed inside a restrainer, leaving the tail of the animal exposed. The tail was disinfected with 70% (v/v) Hibitane (5% (w/v) chlorhexidine gluconate from Regent Medical Ltd.; UK) in ethanol. Then, with a 0.5 ml insulin syringe, containing the dose in up to 100 µl sterile PBS, was carefully inserted into one of the lateral veins and the plunge slowly pulled back to confirm the presence blood from the vein entered the chamber and the dose was then gently injected into the vein.

2.10.4.8. Oral administration to mice

Oral dosing was done with the aid of 20 G × 30 mm rounded tip gavage tubes. The length of the tube was measured from the tip of the animal's head to the last rib and it was marked at the length of the mouse's nose, to avoid perforation the stomach during execution of the procedure. Each mouse was restrained by grasping the scruff of the neck firmly between the thumb and forefinger. The tail was held in place by using the fourth and fifth fingers of the same hand against palm to stretch the animal gently, creating a straight line through the neck and oesophagus. The mouse was hold in an upright position, slightly tilted back. The gavage tube attached to a 1 ml syringe, containing the required dose in up to 100 µl sterile PBS, was placed in the side of the mouth, over the tongue. The tube was then moved forward through the pharynx, gently pressing it to the roof of the mouth, and carefully passed down the oesophagus. When the tube reached the stomach, the dose was smoothly injected. Once the procedure was finished the animal was returned to its cage and monitored for 5 minutes for potential complications.

2.10.4.9. Cardiac puncture of mice

Mice were first anaesthetised inside an anaesthetic box with 5% (v/v) isoflurane (Animalcare Ltd., UK) over 1.6-1.8 L O_2/minute. When they were deeply anaesthetised, a mouse was placed on its back, with its whole head inside the cone of an anaesthetic mask. The appropriate level of anaesthesia was then confirmed by lack of pinch reflex. At this point, the base of the ribcage was gently compressed on each side with the thumb and forefinger, lifting it slightly. A 21 G × 5/8" needle attached to a 2 ml syringe was then inserted at approximately 30º angle, 5-10 mm towards the chin from below the ribs, to penetrate the heart. The required volume of blood was collected slowly.

Normally, the volume of blood obtained never exceeded 1 ml. After collecting the required volume of blood, the mouse was immediately culled by cervical dislocation.

2.10.4.10. Tail bleed of mice

Mice were placed in a cage inside an incubator at 37ºC, for 20 minutes to promote vasodilatation. Once outside the incubator, the mice were kept warm under an IR lamp. A mouse was then placed inside a restrainer and the lid closed, leaving the tail of the animal exposed. The tail was disinfected with 70% (v/v) Hibitane (5% (w/v) chlorhexidine gluconate from Regent Medical Ltd.; UK) in ethanol. The needle of a 0.5 ml insulin syringe was placed parallel to the tail and carefully introduced into a located vein and the blood was drawn into the chamber. Alternatively, the vein was punctured with a syringe needle and the blood collected from the bleeding.

2.10.4.11. Anti-pneumococcal toxicity tests

Assays were performed in order to test the effect of selected peptides or small molecules on wild-type D39 viability. For that, 10 ml of BHI broth (Table 2.1) were inoculated with D39 and incubated statically overnight, at 37ºC. Next day, the overnight cultures were centrifuged at 1,734 ×g in an Allegra^{TM} X-22 centrifuge (Beckman Coulter) for 15 minutes, and the pellet resuspended in 5 ml sterile PBS. Then, D39 was mixed with peptide or small molecule in PBS, at the same concentrations planned to be administered *in vivo*. For this, approximately 1×10^7 CFU D39 were mixed with 0.3 mg of peptide or 0.12 mg of small molecule in PBS, in a final volume of 300 µl. In the control the peptide and small molecule were replaced by water and 2% (v/v) DMSO,

respectively. The viable count (section 2.10.4.3) of the control and test groups was determined at t_{zero} and 2 hours after static incubation at 37ºC.

2.10.4.12. *In vivo* assays of anti-pneumococcal efficacy of peptides in a pneumonia model

In vivo experiments employing a pneumonia model (Kadioglu *et al.*, 2000) were performed using a control and a test group with ten mice in each. In these experiments, each mouse from the control group was intranasally challenged (section 2.10.4.6) with D39 in PBS ($\approx 2\times10^6$ CFU/50 µl), while the test group was administered intranasally D39 ($\approx 2\times10^6$ CFU/50 µl/mouse) mixed with peptide (50 µg/50 µl/mouse) in PBS. After completing the procedure, the viable count (section 2.10.4.3) of the given dose was determined. Thereafter, each animal was administered PBS or peptide in PBS intranasally every 6 hours, as appropriate. The CFU in the blood (section 2.10.4.3) was determined every 12 hours by tail bleeding (section 2.10.4.10), and the progress of the signs of disease (section 2.10.4.4) assessed every 6 hours. After approximately 72 hours the experiments were ended. Using the statistical software GraphPad Prism v.5.00, the survival rates of control and test groups were statistically compared by means of a log-rank test, while the CFU in the blood and signs of disease were compared by means of a Mann-Whitney test. The statistical significance was taken as a P value < 0.05.

2.10.4.13. *In vivo* assays of anti-pneumococcal efficacy of small molecules in a pneumonia model

The *in vivo* experiments were performed using 5 mice *per* group, employing a pneumonia model. Each mouse from the control and test groups was intranasally challenged (section 2.10.4.6) with D39 ($\approx 2\times10^6$ CFU/50 µl). CFU of the given dose

was determined as previously described (section 2.10.4.3). One hour post-infection, each animal was intranasally administered PBS or small molecule (20 μg/50 μl) in PBS, as appropriate treatments. Procedures then followed the scheme previously described in section 2.10.4.12.

2.10.4.14. Collection of serum samples for use in pharmacokinetic (PK) studies

Pharmacokinetic (PK) studies were performed with serum samples collected after intravenous (section 2.10.4.7) or oral (section 2.10.4.8) administration of selected small molecules to mice.

Mice were intravenously administered with small molecule in PBS at a concentration of 20 μg/100 μl/mouse. Then at pre-selected times, pre-selected groups of three mice were exsanguinated by cardiac puncture (section 2.10.4.9). The collected blood was centrifuged at 11,290 ×g in a refrigerated Mikro 22R centrifuge (Hettich) for 3 minutes at 4ºC. The serum was then transferred to another tube and kept on dry ice until storage at -80ºC. The same procedures were applied after the oral administration of the small molecules in PBS at a concentration of 200 μg/100 μl/mouse.

2.10.5. Assessment of the direct anti-microbial activity of small molecules *in vitro*

Paper disks (Oxoid) were impregnated with the small molecules (20 mg/ml in DMSO) or DMSO. The impregnated disks were placed onto different agar plates (Table 2.10) containing streaks of *S. pneumoniae*, *S. pyogenes*, *S. aureus*, MRSA, *C. perfringens*, *B. cereus*, *E. coli*, *P. aeruginosa* and *E. aerogenes* (section 2.4.2). The plates were then incubated as shown in Table 2.10 and observed the next day. The diameters of zones of clearance were measured.

Table 2.10 – Growth conditions of the bacterial strains used in the assessment of the direct anti-microbial activity of small molecules *in vitro*.

	Agar plate (Table 2.1**)**	**Growth conditions**
S. pneumoniae	BAB plus 5%(v/v) horse blood	37ºC; anaerobic
S. pyogenes	BAB plus 5%(v/v) horse blood	37ºC; anaerobic
E. coli	LA	37ºC; aerobic
S. aureus	LA	37ºC; aerobic
MRSA	LA	37ºC; aerobic
P. aeruginosa	TSA	37ºC; aerobic
E. aerogenes	LA	37ºC; aerobic
C. perfringens	LA	37ºC; aerobic
B. cereus	TSA	37ºC; aerobic

2.10.6. *Ex vivo* assays

2.10.6.1. Inhibition of the effect of pneumolysin on the ciliary function of ependymal cells

Ependymal cell cultures were prepared based on the method described by (Hirst *et al.*, 2008). Eight-well tissue culture trays (Nunc) were coated with 40 µl (≈ 1 µg/cm^2) of bovine fibronectin (Sigma) and incubated at 37°C in 5% (v/v) CO_2 for 2 hours before use. The growth medium was minimum essential medium (MEM: GIBCO Life Technologies, UK) with added penicillin (100 IU/ml), streptomycin (100 µg/ml), fungizone (2.5µg/ml), BSA (5 µg/ml), insulin (5 µg/ml), transferrin (10 µg/ml) and selenium (5µg/ml), stored at 4ºC.

Neo-natal (0-1 day old) Wistar rats (Division of Biomedical Services; University of Leicester) were culled by cervical dislocation, and their brains were removed by careful dissection. The cerebellum was removed along with (≈ 3 mm) edge regions of the left and right cortical hemispheres and the frontal cortex. The remaining brain areas (containing ependymal cells and ventricles) were mechanically dissociated in 4 ml of growth medium, by passing the tissue through a 21-gauge needle into a 5 ml syringe. Dissociated tissue from two brains were added (500 μl/well) into eight-well tissue culture trays, containing 2.5 ml of growth medium (at room temperature) *per* well. The medium was replaced 3 days after seeding. From then onwards, the adherent ependymal cells were fed every two days with 2 ml of fresh growth medium supplemented with thrombin.

After approximately two weeks, when the cells were fully ciliated, the inhibition experiments with pneumolysin and small molecules were performed. Ciliated ependymal cell areas were identified using an inverted light microscope (Nikon, UK) and the growth medium replaced by 1 ml *per* well of medium M199 containing 25 mM HEPES, pH 7.4 (GIBCO Life Technologies, UK). The tissue culture trays were covered by extra thick cling film and placed inside a thermostatically controlled incubation chamber surrounding the stage of an inverted light microscope (Nikon, UK). The cell cultures were allowed to equilibrate until the temperature of the assay medium attained 37ºC. At this point, pneumolysin (5.4 HU/ml) with and without small molecule (to a final concentration of 3 μM), pre-incubated together in 1ml of medium M199 at 37ºC for 45 minutes, was added to the wells containing the ciliated cells in 1 ml of medium M199. To the control cells, 1 ml of M199 medium was added instead. Beating cilia were recorded before and after exposure (1, 5, 10, 15 and 30 minutes), with a digital high-speed video camera (Fastec imaging, model TSHRMS) at a rate of 500 frames/s.

The recorded video sequences were played back at reduced frame rates using the software Midas player v.2.2.0.0 (Xcitex). Ciliary beat frequency (CBF) was determined by the following equation

$$\text{CBF (FPS}^{*}) = \frac{500 \text{ frames / s}}{(\text{frames elapsed for 5 ciliary beat cycles})} \times 5 \left(\text{conversion per beat cycle}\right).$$

*FPS – Frames *per* second

Statistical analysis was done by one-way ANOVA, using the statistical software GraphPad Prism v.5.00. The statistical significance was taken as a P value of <0.05.

2.10.6.2. Inhibition of the effect of pneumolysin on the ciliary function of rat brain slices

The experiments were performed with the kind collaboration of Dr. Rob Hirst (Department of Infection, Immunity and Inflammation; University of Leicester).

Wistar rats (14-17 days old) were culled by cervical dislocation and their brains were removed by careful dissection. The cerebellum was removed and mounted on a vibratome under ice-cold M199 medium containing 25mM HEPES (pH 7.4), penicillin (100 IU/ml) and streptomycin (100 μg/ml). The brain was sliced (250 μm thick) through the medulla oblongata and pons into the floor of the fourth ventricle so that the ciliated V-shaped floor was clear. Before use, the slices were mounted in 1 ml of 37ºC pre-warmed M199 medium containing 25mM HEPES (pH 7.4) and then placed in a thermostatically controlled incubation chamber surrounding the stage of an inverted light microscope (Nikon, UK). The ciliated edges were recorded with a high-speed video camera (Fastec imaging, model TSHRMS) at 30 frames per second, before and

during the exposure of the ependymal tissue to pneumolysin or pneumolysin pre-incubated with small molecule (as described in section 2.10.6.1).

2.11. Preliminary study of the mode of action of the small molecules

This work was developed based on a method described before (El-Rachkidy, 2003), in which unilamellar lipid vesicles were used as a model to study the time course of release of a fluorescent dye (calcein) from the vesicles, after exposure to pneumolysin.

2.11.1. Liposome manufacture

Liposomes were prepared by mixing thoroughly 7 mg of palmitoyloleoyl phosphatidylcholine (POPC) with 7 mg of cholesterol (Avanti® Polar Lipids, inc.; Alabama; USA) in 1 ml of chloroform (El-Rachkidy, 2003). The organic solvent was then evaporated under a nitrogen stream for approximately 1 hour. The weight of the eppendorf tube was checked in order to confirm the production of a fully dried film (the desired final weight was the weight of the empty tube plus the weight of added lipids). Any extra weight indicated the presence of chloroform and further drying was required. Afterwards, the lipid film was hydrated with a solution containing calcein (80 mM calcein, 50 mM NaCl in 1M NaOH, pH 7.0) and vortexed vigorously for 1 hour (for that, the Eppendorf tube was place inside an universal tube packed with tissue paper to stabilise the Eppendorf tube, and then the universal tube containing the eppendorf tube was sellotaped in a horizontal position to the shaker of the vortex). The resultant suspension of large multilamellar vesicles (LMV) was then left overnight at room temperature. The conversion of the LMV to small unilamellar vesicles (SUV) was done by sonication in a bath sonicator for 15 minutes. At this point, unilamellar vesicles entrapping calcein were formed. The free calcein was removed from the vesicle

suspension by centrifugation at 45,000 rpm in a Beckman TL-100 ultracentrifuge with a TLA 100.2 rotor for 1 hour at room temperature. The resultant pellet was then washed 4-5 times with 1 ml of NaCl buffer (160 mM NaCl, 10 mM HEPES, pH 7.0) until the colour of the suspension became more clear. Finally, the liposomes pellet was resuspended in 5 ml of NaCl buffer and stored at 4ºC up to 1 week.

2.11.2. Determination of calcein release

Fluorescence of released calcein was measured using a Varioskan® Flash spectrofluorometer (Thermo-Electron Corporation). 50 µl of the liposome suspension (section 2.11.1) were mixed with 150 µl of NaCl buffer and the mixture was transferred into the wells of a flat bottomed 96-wells microfluor 1 black plate (Thermo scientific). Calcein fluorescence was excited at 470 nm and the emission was monitored at 509 nm. After 50 seconds of excitation, 50 µl of pneumolysin (final concentration ≈ 5 HU/ml) pre-incubated with different concentrations of small molecule (for 45 minutes at 37ºC) was added to the wells, whereas only pneumolysin and NaCl buffer were added to the control wells. The fluorescence emission was monitored for further 500 seconds.

2.11.3. Detection of binding of pneumolysin to the liposomes

The content of the wells from section 2.11.2 was collected and centrifuged at 19,000 ×g in a refrigerated Mikro 22R centrifuge (Hettich) for 15 minutes at 4ºC. The supernatant retained and the pellet was resuspended in NaCl buffer and re-centrifuged to remove unbound pneumolysin. The presence of pneumolysin on the supernatant and pellet was assayed by Western blotting (section 2.9.3).

Chapter 3 - Results

This research project sought the development of a new approach for the treatment of pneumococcal diseases through the identification of lead peptides or small molecules that would inhibit pneumolysin activity. This chapter will present the results obtained at the different stages of the strategies involving the use of anti-pneumolysin peptides (section 3.1) and small molecules (section 3.2), starting with the *in vitro* evaluation of their capacity to inhibit pneumolysin's haemolytic activity. This is followed by the assessment of the efficacy of a selection of peptides and small molecules in *in vivo* models. Additionally, the outcome of the use of a selection of small molecules on the effect of pneumolysin on the ciliary function of rat ependyma will be presented. Finally, data from preliminary studies towards the understanding of the mode of action of the inhibitory small molecules will be shown (section 3.3).

3.1. Anti-pneumolysin peptides

3.1.1. Summary of the strategies in the screening for pneumolysin-binding peptides

The selection of peptides was undertaken by a collaborator, Prof. Franco Felici, in the University of Messina (Italy). The screening of four phage displayed random peptide libraries was done by means of a biopanning technique. Briefly, filamentous phage M13 displaying peptides on its surface coat (pVIII coat protein) was passed through magnetic beads with pneumolysin attached to them. The non-specific binders were removed by washing and the specific binders were recovered in a subsequent elution step. Because the position in the phage genome of the DNA coding for each peptide was known, DNA sequencing revealed the translated amino acid sequence of the binding peptide. Peptides were synthesised by a commercial company (see section 2.10.2). From this screening stage, twenty peptides were found to bind pneumolysin and were further evaluated for their capacity to inhibit pneumolysin haemolytic activity *in vitro*. The amino acid sequences and the identification codes corresponding to each of the twenty peptides are presented in Table 3.1. The random peptide inserts (in bold) have different lengths (from 8 up to 12 amino acid residues) and levels of constrain, that is, contain cysteine residues into, or flanking, some of the inserts (e.g. peptides P3 and P7).

Table 3.1 – Pneumolysin-binding peptides selected from the screening of the phage display peptide libraries.

Peptide ID	Sequence[Ψ]
P1	A E G E F **S R R T R A G F** G D P A K
P2	A E G E F **D I D H Y L E Y I G A G** G D P A K
P3	A E G E F **R R W C C T R C R V L P** P D P A K
P4	A E G E F **T E T K W T C R R Q V W** G D P A K
P5	A E G E F **A G K N L K H G N H T V** G D P A K
P6	A E G E F **S R Q A H G V R R G G R** G D P A K
P7	A E G E F **W C W G G V E W R L C P** P D P A K
P8	A E G E F **I R K S D R F S R H V S** G D P A K
P9	A E G E F **W R R T W F C R S M S** P D P A K
P10	A E G E F **T K S R T R F W G G G R** G D P A K
P11	A E G E F **G R R W W C T R V G** P D P A K
P12	A E G E F **K K A D T H R V M V E N** G D P A K
P13	A E G E F **F T S R F W F C K L Q A** P D P A K
P14	A E G E F **K K G A M S P V V Q N A** G D P A K
P15	A E G E F **R C W A C R R A S C G Q** P D P A K
P16	A E G E F **E G R V W Q C K V R S** P D P A K
P17	A E G E F **N H N R G P P V A G G** G D P A K
P18	A E G E F **F K R S S V R D N L G R** G D P A K
P19	A E G E F **P K R A P E I V G H I H** P D P A K
P20	A E G E F **G P Y G N F Y A M D Y** W D P A K

[Ψ] The peptide sequences were presented so that the amino group (NH_2-) was at the left and the carboxyl group (-COOH) was at the right. The first and last five amino acids (not in bold) are constant in the identified sequences, as they belong to the pVIII coat protein sequence in the phagemid vectors used for the construction of the libraries.

3.1.2. *In vitro* evaluation of the capacity of the selected pneumolysin-binding peptides to inhibit pneumolysin activity

The twenty pneumolysin-binding peptides, identified in the earlier screening stage, were tested *in vitro* according to the method described in section 2.10.3. The results obtained with these peptides are summarised in Table 3.2. From the twenty peptides tested *in vitro*, only four (P1, P2, P5 and P6) inhibited pneumolysin's haemolytic activity. All four peptides were inhibitory at the exact same concentrations.

Table 3.2 – Summary of *in vitro* inhibition of haemolytic activity by pneumolysin-binding peptides.

Peptide ID	Effect observed on PLY activity	*Lowest concentration causing 100% inhibition (mg/ml)	Peptide ID	Effect observed on PLY activity	*Lowest concentration causing 100% inhibition (mg/ml)
P1	**Inhibition**	**0.0625**	**P11**	No inhibition	—
P2	**Inhibition**	**0.0625**	**P12**	No inhibition	—
P3	No inhibition	—	**P13**	No inhibition	—
P4	No inhibition	—	**P14**	No inhibition	—
P5	**Inhibition**	**0.0625**	**P15**	No inhibition	—
P6	**Inhibition**	**0.0625**	**P16**	No inhibition	—
P7	No inhibition	—	**P17**	No inhibition	—
P8	No inhibition	—	**P18**	No inhibition	—
P9	No inhibition	—	**P19**	No inhibition	—
P10	No inhibition	—	**P20**	No inhibition	—

*In cases where inhibition was observed, the lowest concentration of peptide able to cause complete inhibition of pneumolysin's (PLY) haemolytic activity is also presented.

An example of the data that gave rise to Table 3.2 is shown in Figure 3.1 with peptides P1, P2, P5, P6, P8, P9 and P10. In the control with pneumolysin and red blood cells (control 1), full haemolysis resultant from the toxin activity is seen, translated by the presence of a transparent red coloured supernatant in the wells. On the other hand, in the control wells with red blood cells alone (control 2) haemolysis did not occur, which is seen by the formation of pelleted cells and clear supernatant. This control also is an indicator of the integrity of the cells. In the same figure, inhibition of pneumolysin activity was identified at 0.125 mg/ml (well n.º 3) and 0.0625 mg/ml (well n.º 4) of the peptides P1, P2, P5 and P6 (indicated by the solid line boxes), whereas with peptides P8, P9 and P10 inhibition was not observed at any of the tested concentrations. As it can be seen in the wells with peptides and red blood cells (control 3), haemolysis was detected at the highest peptide concentrations (0.5 mg/ml and 0.25 mg/ml) but it did not occur at the inhibitory concentrations of the peptides P1, P2, P5 and P6 (indicated by the dashed line boxes). Thus, these inhibitory concentrations of the peptides did not compromise the integrity of the red blood cells.

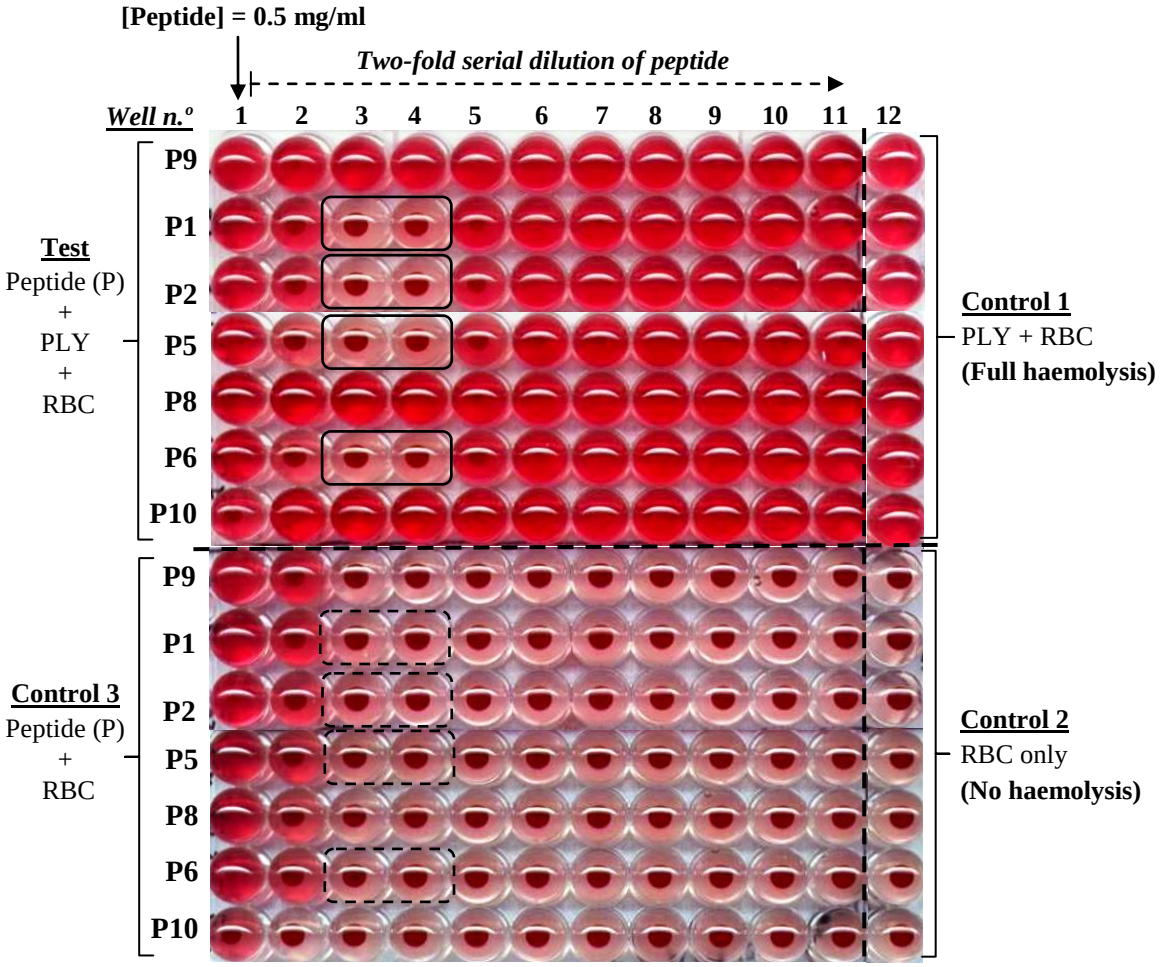

Figure 3.1- *In vitro* assay of inhibition of pneumolysin's haemolytic activity with pneumolysin-binding peptides P1, P2, P5, P6, P8, P9 and P10. Peptides were two-fold serially diluted between wells 1 and 11. Column 12 contains assay positive (full haemolysis) and negative (no haemolysis) controls. The solid line boxes at test wells indicate where full inhibition of pneumolysin's haemolytic activity was observed. The dashed line boxes at control 3 indicate the integrity of the red blood cells (RBC) in presence of inhibitory concentrations of the corresponding peptides in the test wells.

The results obtained *in vitro* with the remaining thirteen peptides can be seen in Table 3.2 and in Figure 3.2, which shows data in form of OD_{595} measurements. In each graph two controls are shown, corresponding to the OD_{595} values obtained with the red blood cells alone (top dash dotted green line) and with pneumolysin plus red blood cells (bottom dashed red line). The solid blue line shows OD_{595} values with the red blood cells in the presence of the pneumolysin pre-incubated with each peptide. It is possible to observe that the OD_{595} obtained in presence of each of the thirteen peptides are very close to the OD_{595} of the pneumolysin (full haemolysis) control. Whereas, in the case of inhibition of pneumolysin by a peptide (e.g. peptide P2), OD_{595} values similar to that of the red blood cells alone control are seen. Hence, the analysis of the graphs shows the inability of these peptides to inhibit pneumolysin haemolytic activity *in vitro*.

From the *in vitro* screening stage, four peptides (P1, P2, P5 and P6) were identified as pneumolysin inhibitors and therefore were selected for further *in vivo* testing. Despite not showing inhibitory activity, two other peptides (P3 and P4) were considered for *in vivo* testing because they were found to strongly bind to pneumolysin during the screening stage for selection of pneumolysin-binding peptides (section 3.1.1).

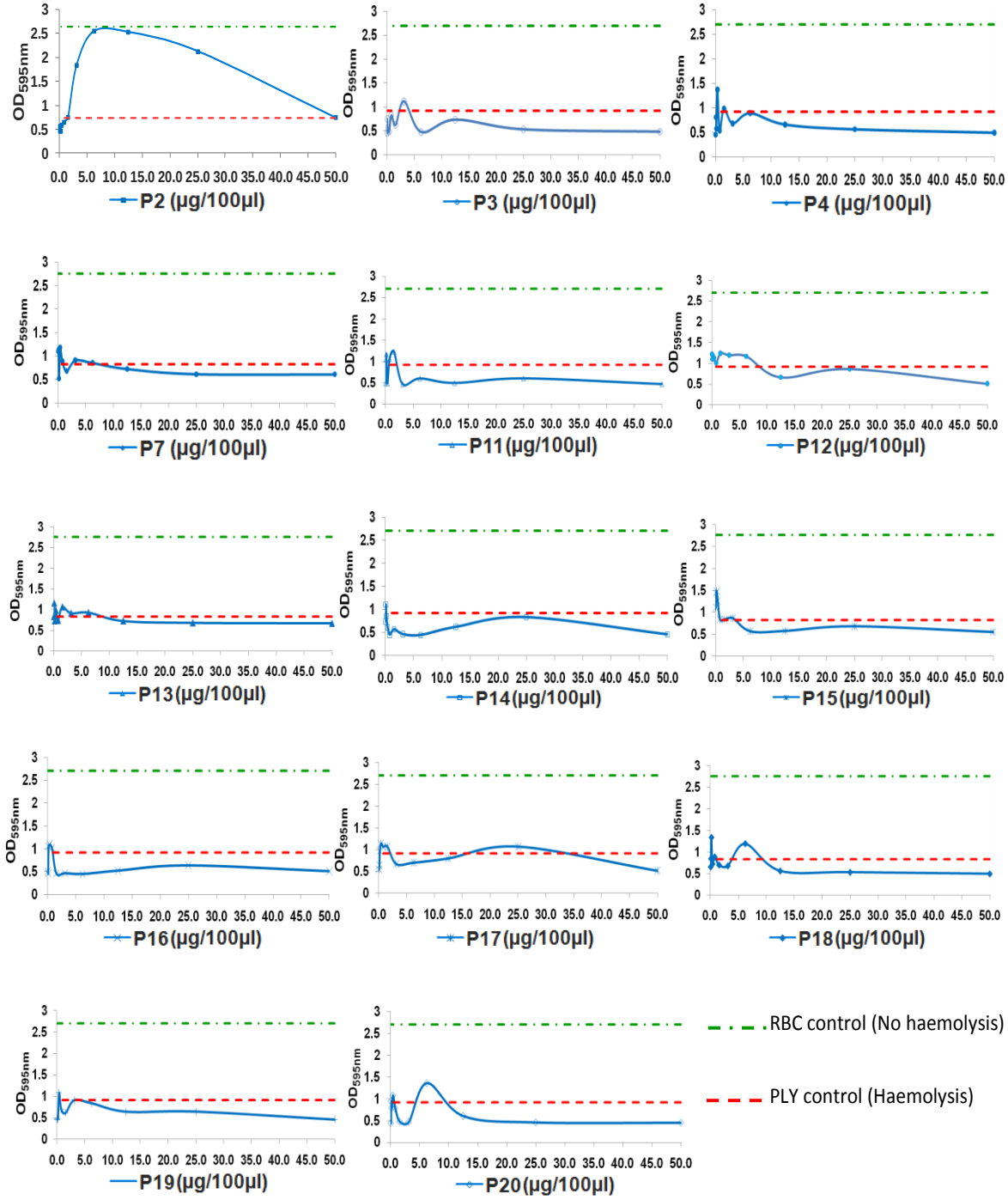

Figure 3.2 – OD_{595} obtained from the *in vitro* inhibition assays with thirteen pneumolysin-binding peptides (P). In each graph there are two control lines corresponding to the OD_{595} of the wells with red blood cells alone (dash dotted green line) and with red blood cells in presence of pneumolysin (dashed red line). Each solid blue line is the OD_{595} for the wells containing red blood cells exposed to pneumolysin pre-incubated with different concentrations of peptide.

3.1.3. *In vivo* studies for evaluation of the efficacy of anti-pneumolysin peptides in a pneumonia model

The initial *in vivo* studies were performed by employing a pneumonia model to test peptides P5 and P6, using the experimental design described previously (section 2.10.4.12). The control group received wild-type *S. pneumoniae* strain D39 in PBS, and the test group had D39 with peptide (50 μg/50 μl/ mouse) in PBS. Thereafter, each animal was administered PBS or peptide in PBS intranasally thrice daily, as appropriate. The survival curves of the control (dashed blue lines) and treatment (solid green lines) groups obtained with peptides P5 and P6 are presented in Figure 3.3 A and B, respectively. Although differences in the survival of the control and P5 group are suggested by Figure 3.3 A, at no time was the percentage of survival in the two groups significantly different ($p > 0.05$). A similar picture was seen with peptide P6. At no time in the experiment did the percentage of survival of the control and test groups differ significantly ($p>0.05$).

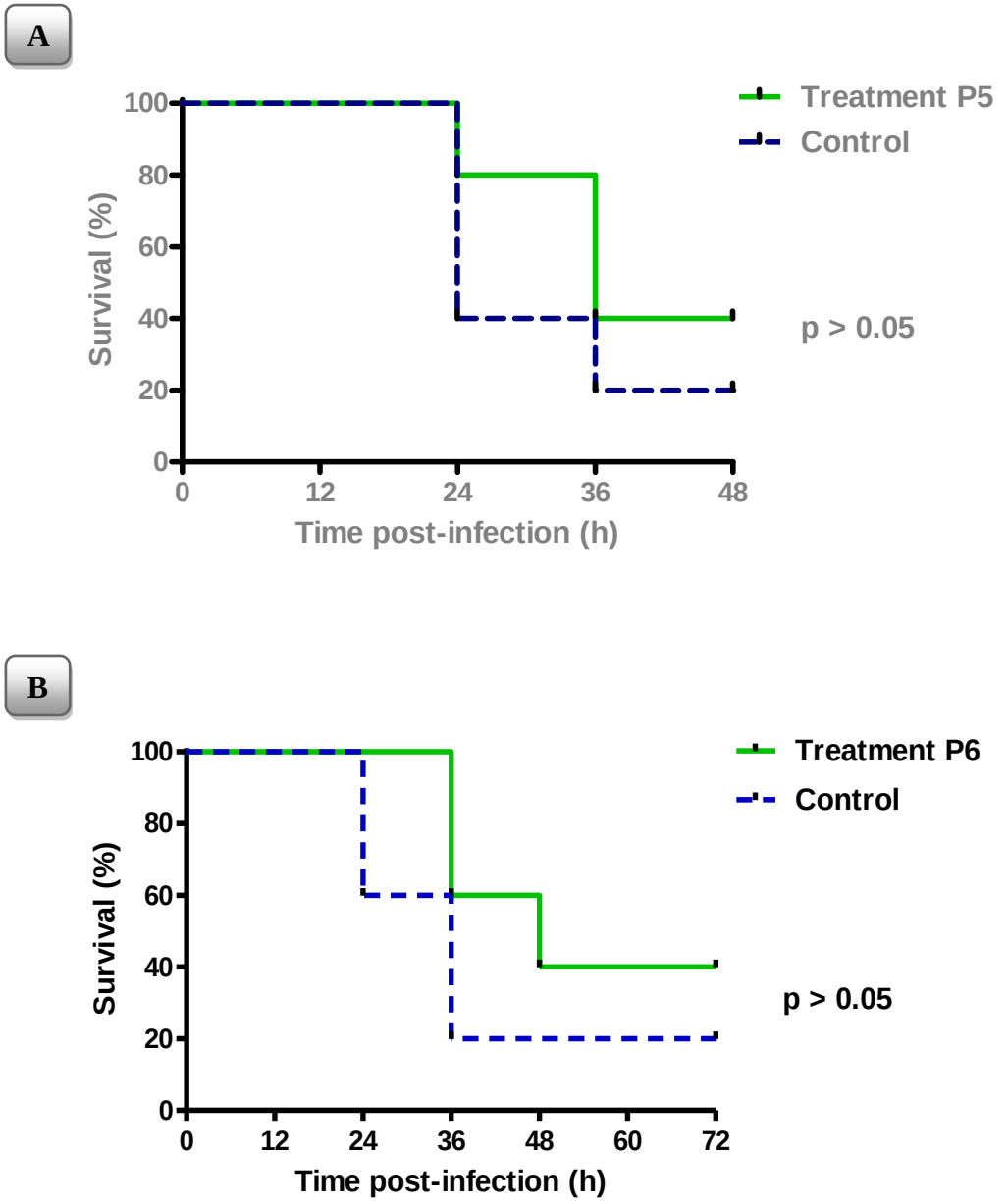

Figure 3.3 – Survival of mice intranasally infected with *S. pneumoniae* D39. Peptide (A) P5 and (B) P6 in PBS or PBS were administered intranasally with the infectious dose and every 6 hours thereafter. The p-values were calculated by means of the log-rank (Mantel-Cox) test (n = 5/group).

Despite the statistical analysis of the survival curves showing no significant differences between the groups, the median of survival times were slightly prolonged in the case of the treatment groups (36 hours for the P5 group against 24 hours for the control; 48 hours in the case of the P6 group as opposed to 36 hours for the control group), suggesting that these peptides may have some degree of protection effect *in vivo*. This may not have been significant due to the relatively small size of the groups. Consequently, the decision was made to increase the group size (10 mice per group) in subsequent experiments.

The introduction of a larger number of mice in the *in vivo* studies meant that more time would be spent during the handling of animals and the experimental procedures. Therefore, anti-pneumococcal tests were undertaken to evaluate the effect of the six selected peptides (P1, P2, P3, P4, P5 and P6) on D39 viability (section 2.10.4.11), after an exposure period of 2 hours. The results for these tests can be seen in Figure 3.4. There were no significant differences between the controls and test groups with peptides P1, P2, P3 and P4 ($p>0.05$). However, in the case of the peptides P5 and P6, there was a significant decrease ($p < 0.001$ for both) in the number of pneumococci after 2 hours in contrast to the controls. This demonstrated that premixing of D39 with the peptides P5 and P6 would compromise the viability of the infectious dose.

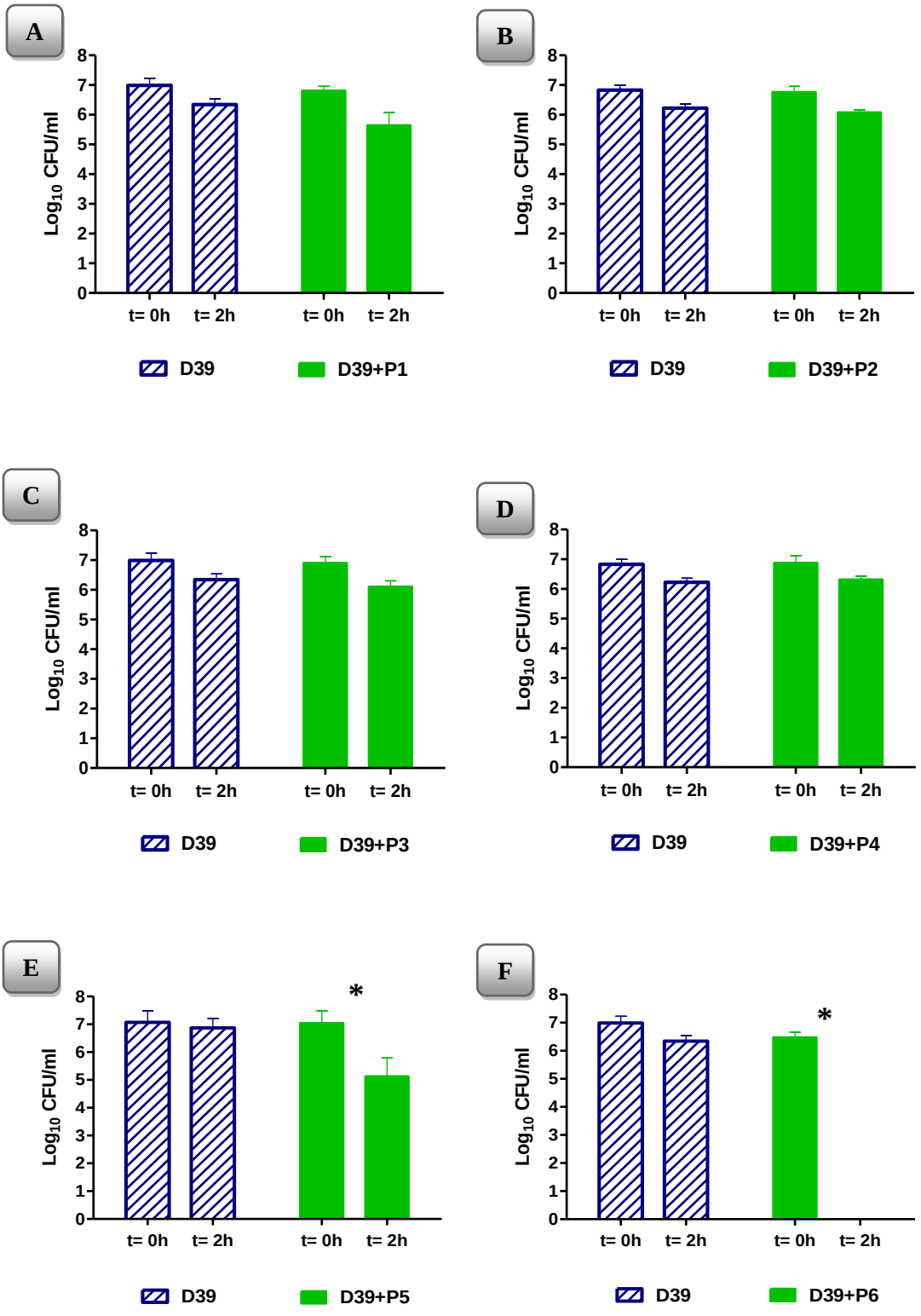

Figure 3.4 – *In vitro* assessment of the antimicrobial effect of peptides P1, P2, P3, P4, P5 and P6 on *S. pneumoniae* strain D39. CFU values obtained for the control group (D39 in PBS) and for the test group (D39 plus peptide in PBS), at 0 hours and 2 hours after incubation at 37ºC, are presented. A-F: CFU values for the peptides P1-P6. Graphs show means ± SD; *****, $p < 0.05$ between groups at 2 hours (n=4).

Another *in vivo* study was performed using the peptide P5 in a pneumonia model but with some adjustments in the experimental design. These consisted of increasing the group size to ten mice; challenging mice intranasally with D39 in PBS, in the absence of peptide; administration of peptide in PBS or only PBS, as appropriate, every 12 hours. The results obtained with this new experimental design are shown in Figure 3.5 A and B. As can be seen in Figure 3.5 A, there is no indication that at any time during the experiment did the percentage of survival of the control and P5 groups differ significantly ($p > 0.05$). In Figure 3.5 B the numbers of pneumococci in the blood of mice 24 hours post-infection with D39 are presented. At this time-point, the CFUs in the blood of the mice in the treatment group were within the same range of those of the control group ($p > 0.05$). Contrary to the indications in the first set of *in vivo* studies (Figure 3.3 A), this experiment did not provide any evidence that the administration of peptide P5 contributed to an improvement in the outcome of the disease. Given this, the experimental design used in the studies with peptide P5 was reviewed.

Following these experiments, the two peptides found to compromise D39 viability (P5 and P6) were not used in other *in vivo* experiments. The other four (P1, P2, P3 and P4) then were tested *in vivo* using a pneumonia model, as described in section 2.10.4.12. Mice from the test group were intranasally challenged with D39 mixed with peptide in PBS, whereas the control received D39 in PBS. The peptide dosing regime was every 6 hours. Results obtained from the *in vivo* study with peptide P1 can be seen in Figure 3.6 A, B and C.

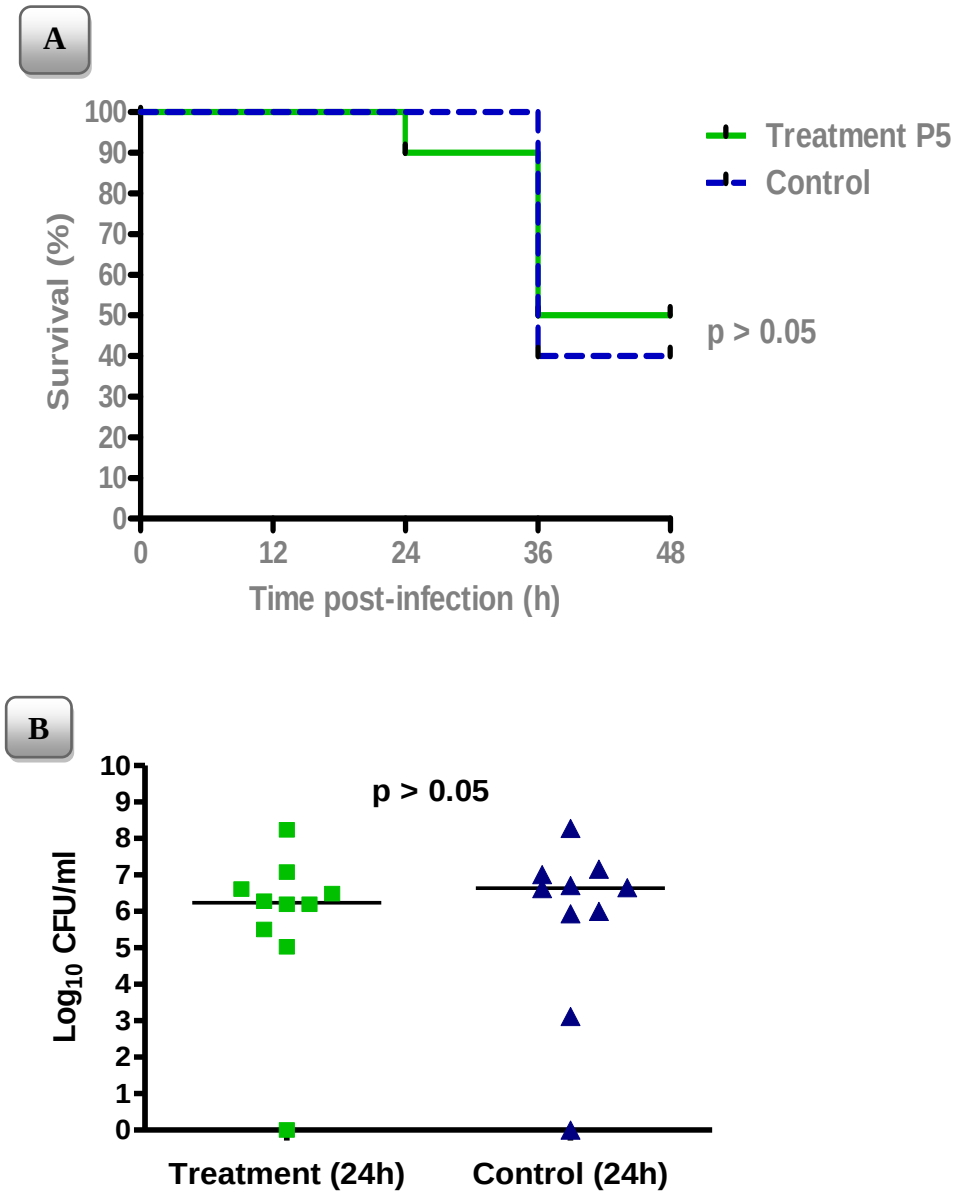

Figure 3.5 - Results obtained from the *in vivo* study with peptide P5. Mice were intranasally infected with *S. pneumoniae* strain D39 in PBS. One hour after infection, animals started being given peptide P5 in PBS or PBS, as appropriate, and every 12 hours thereafter. (A) Kaplan-Meier curves showing the survival rate of mice from control and treatment groups; the p-value was calculated by means of the log-rank (Mantel-Cox) test (n = 10/group). (B) Comparison of the number of pneumococci in blood of mice at 24h post-infection; each symbol (■;▲) represents the CFU count from an individual mouse in the treatment and control group, respectively; horizontal lines represent medians; the p-value was calculated using an Mann-Whitney test.

As can be seen in Figure 3.6 A, the numbers of survivors in the control group declined over time so that by 48 hours only 10 % survived. This single mouse remained alive until the conclusion of the experiment. In contrast, in the group receiving P1 numbers declined more slowly and at 72 hours 50 % were still alive. This was significantly more ($p < 0.05$) than in the control group. The treatment group also had significantly less ($p < 0.05$) pneumococci in the blood at 24 hours post-infection (Figure 3.6 B). In addition, the treatment group had a significantly lower disease score ($p < 0.05$) at 54 hours post-infection (Figure 3.6 C).

Figure 3.7 A, B and C show the results obtained during the *in vivo* study with peptide P2. As can be seen in Figure 3.7 A, there is no indication that at any stage of the experiment was the percentage of survival in the two groups significantly different ($p > 0.05$). The CFU counts in the blood of mice at 12 hours post-infection, suggested a delay of the invasion of pneumococci into the blood stream (Figure 3.7 B), yet when compared with the control group the differences were not statistically significant ($p > 0.05$). In addition, mice from the control exhibited disease signs slightly higher than the treatment group at 18 hours post-infection (Figure 3.7 C). However, there were no significant differences between the groups ($p > 0.05$).

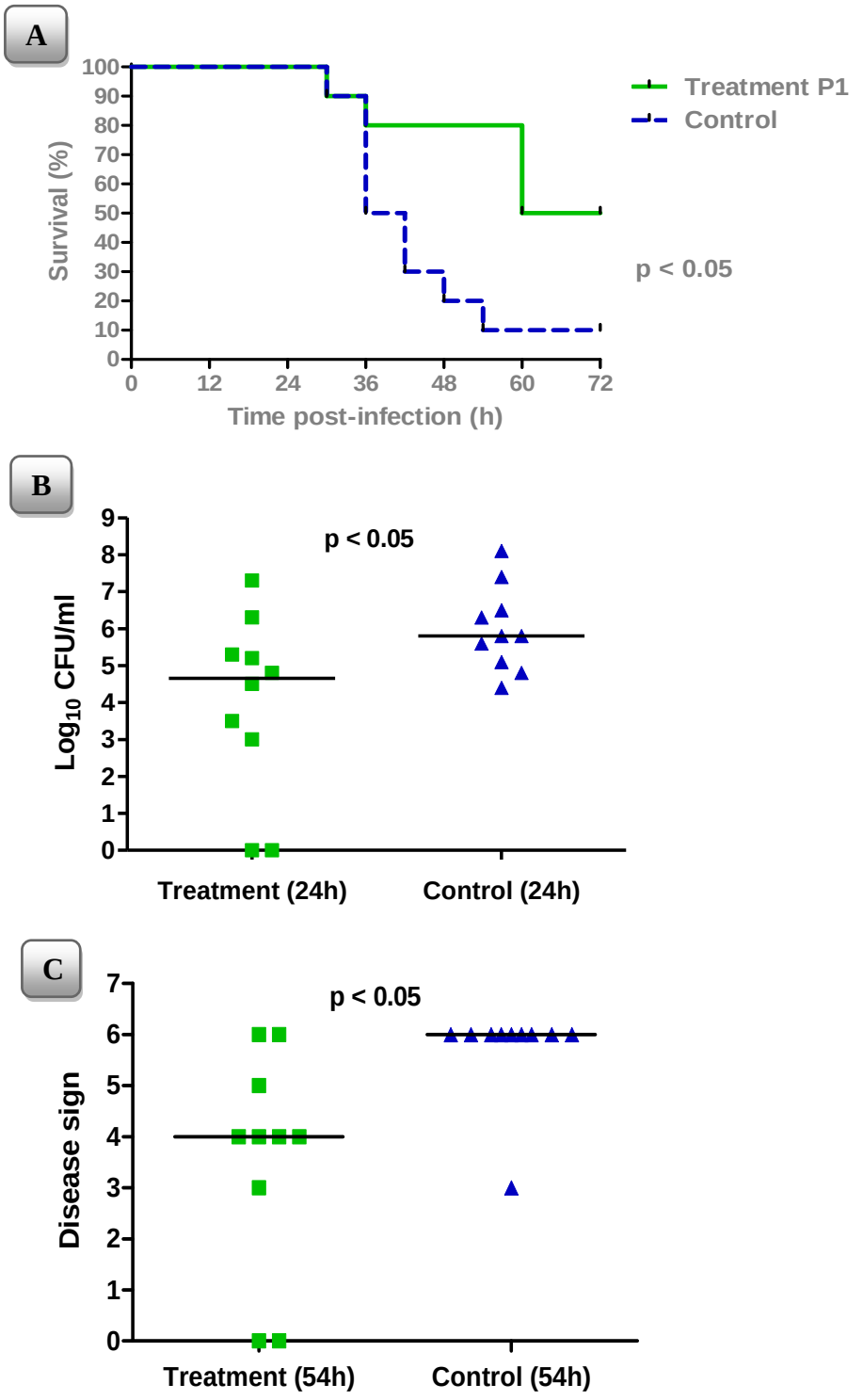

Figure 3.6 - *In vivo* results obtained with peptide P1. Peptide P1 in PBS or PBS was administered intranasally with the infectious dose and every 6 hours thereafter. **(**A) Kaplan-Meier curves showing the survival rate of mice from control and treatment groups; the p-value was calculated by means of the log-rank (Mantel-Cox) test (n = 10/group). (B) Comparison of the number of pneumococci in blood of mice at 24h post-infection. (C) Comparison of the signs of disease 54h post-infection. In B and C, each symbol (■;▲) represents an individual mouse in the treatment and control group, respectively; horizontal lines represent medians; p-values were calculated by a Mann-Whitney test.

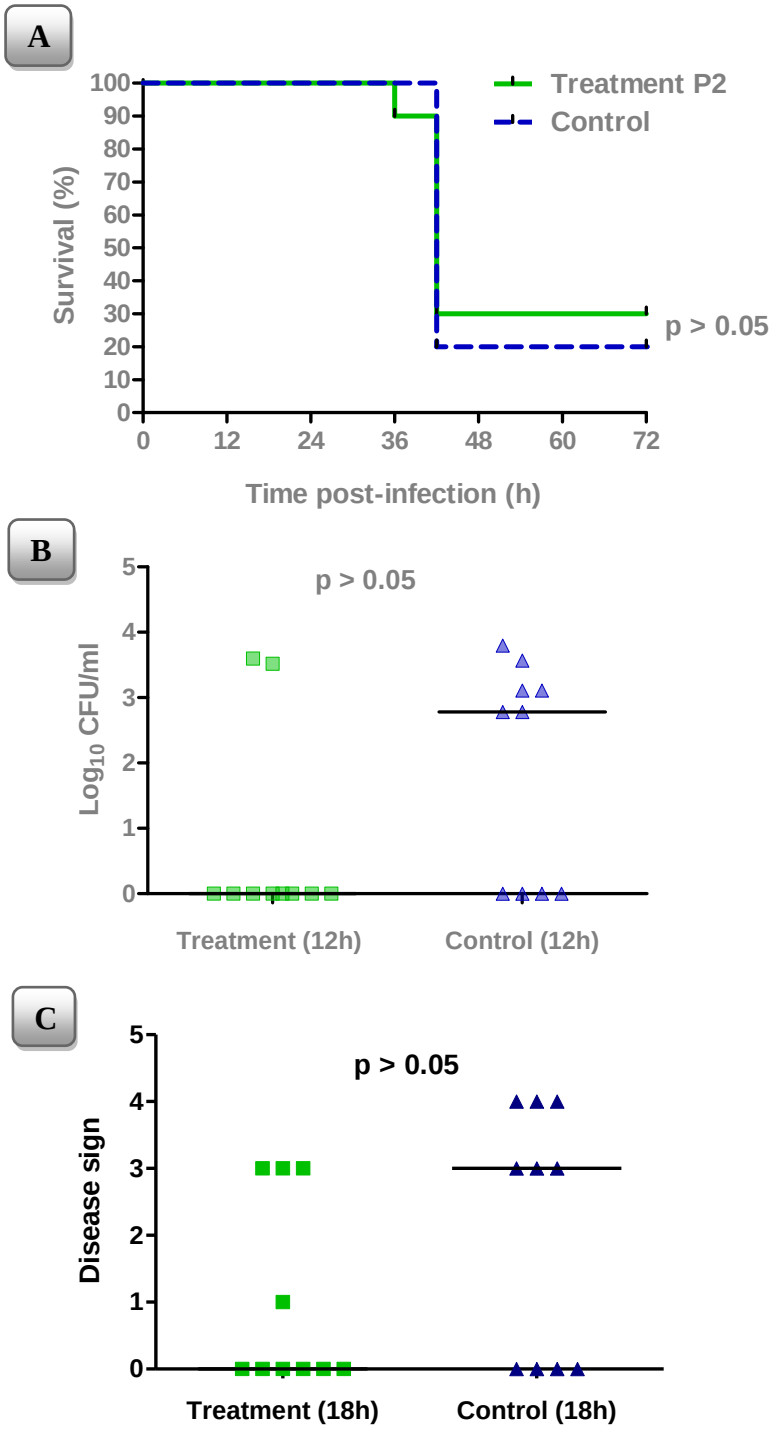

Figure 3.7 - *In vivo* results obtained with peptide P2. Peptide P2 in PBS or PBS was administered intranasally with the infectious dose and every 6 hours thereafter. (A) Kaplan-Meier curves showing the survival rate of mice from control and treatment groups; the p-value was calculated by means of the log-rank (Mantel-Cox) test (n = 10/group). (B) Comparison of the number of pneumococci in blood of mice at 12h post-infection. (C) Comparison of the signs of disease 18h post-infection. In B and C, each symbol (■;▲) represents an individual mouse in the treatment and control group, respectively; horizontal lines represent medians; p-values were calculated using a Mann-Whitney test.

Results for the *in vivo* experiments with peptides P3 and P4 are shown in Figure 3.8 and Figure 3.9. The survival curves resultant from the experiments with the peptides P3 (Figure 3.8 A) and P4 (Figure 3.9 A), demonstrated that there were no significant differences in survival of the test and control groups ($p > 0.05$). There was also no evidence of decrease of the invasion of pneumococci into the blood stream (Figures 3.8 B and 3.9 B; $p > 0.05$) or in the progress of the signs of the disease (Figures 3.8 C and 3.9 C; $p > 0.05$).

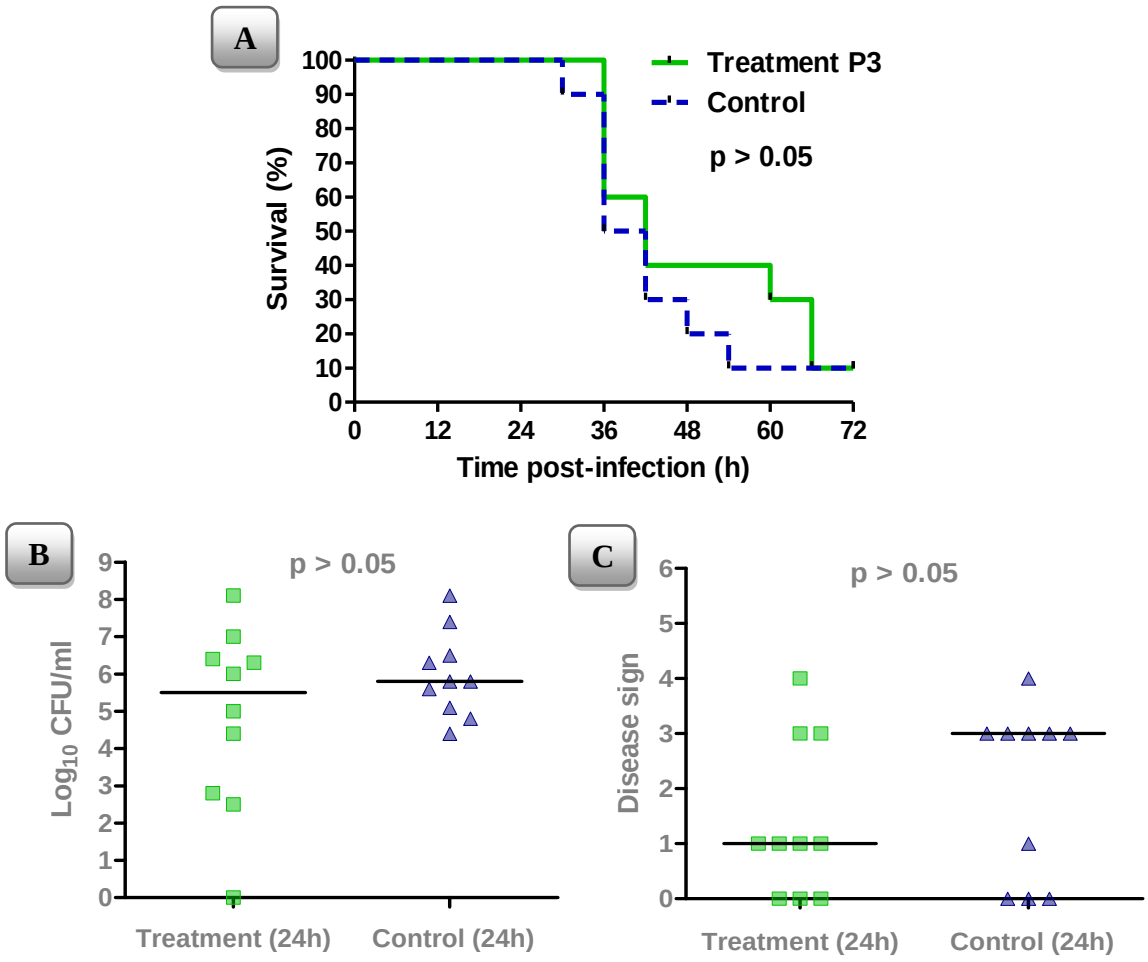

Figure 3.8 – Results obtained *in vivo* with peptide P3. Peptide P3 in PBS or PBS was administered intranasally with the infectious dose and every 6 hours thereafter. (A) Kaplan-Meier curves showing the survival rate of mice from control and treatment groups; the p-value was calculated by means of the log-rank test (n = 10/group). (B) Comparison of the number of pneumococci in blood of mice at 24h post-infection. (C) Comparison of the signs of disease 24h post-infection. In B and C, each symbol (■;▲) represents an individual mouse in the treatment and control group, respectively; horizontal lines represent medians; p-values were calculated by using a Mann-Whitney test.

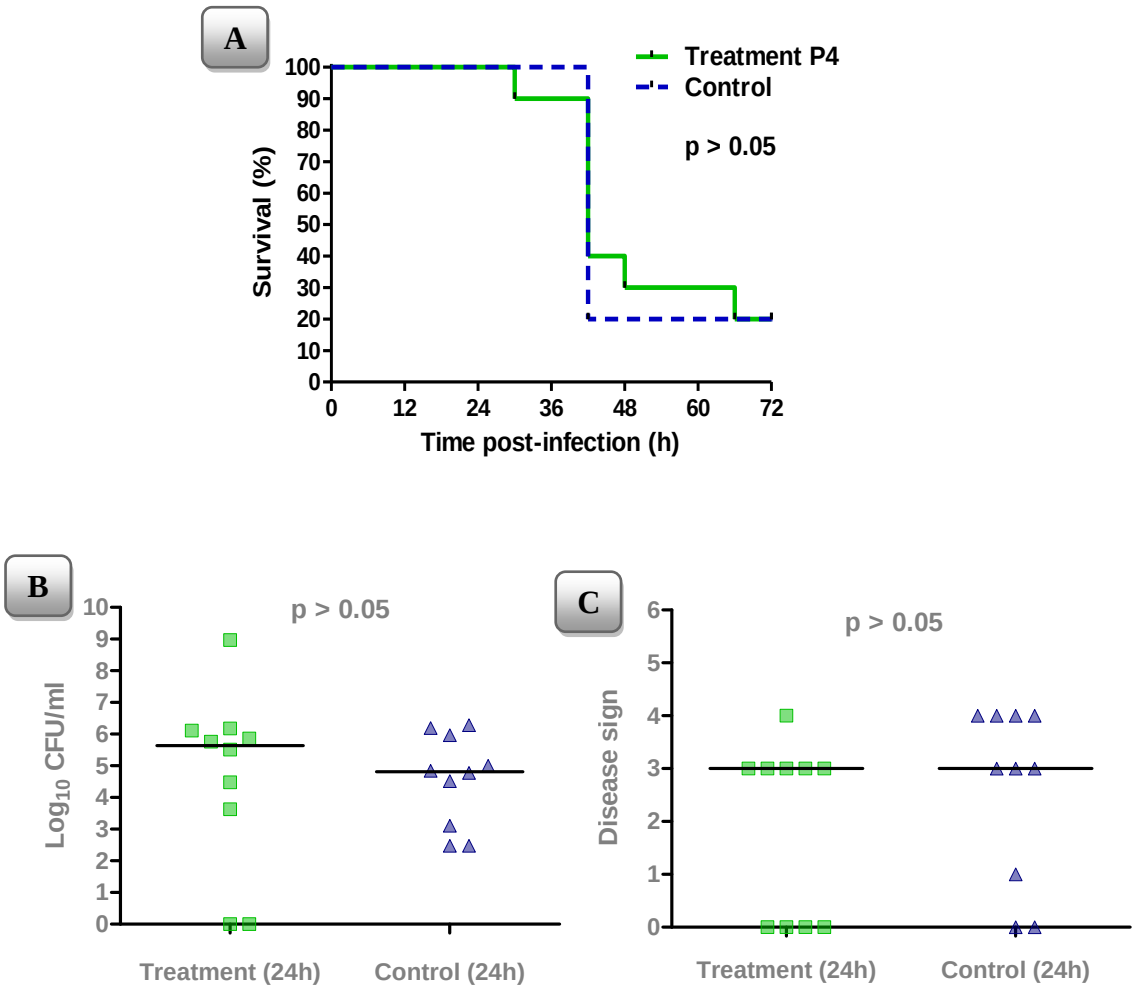

Figure 3.9 – Results obtained *in vivo* with peptide P4. Peptide P4 in PBS or PBS was administered intranasally with the infectious dose and every 6 hours thereafter. (A) Kaplan-Meier curves showing the survival rate of mice from control and treatment groups; the p-value was calculated by means of the log-rank test (n = 10/group). (B) Comparison of the number of pneumococci in blood of mice at 24h post-infection. (C) Comparison of the signs of disease 24h post-infection. In B and C, each symbol (■;▲) represents an individual mouse in the treatment and control group, respectively; horizontal lines represent medians; p-values were calculated by using a Mann-Whitney test.

In summary, peptide P1 passed the *in vivo* screen by significantly improving outcome of the treatment group over the control group, when considering the CFU values in the blood, disease sign score and survival. These results suggested P1 as a potential candidate for further testing in drug discovery.

With the peptides P2, P3 and P4, no evidence of significant enhanced protection *in vivo* was observed. The results obtained with the selected peptides are summarised in Table 3.3.

Table 3.3- Summary of the results obtained with the peptides in the *in vivo* and *in vitro* assays.

Peptides ID	***in vitro* inhibition(Ψ)**	***in vivo* inhibition (Ψ) (pneumonia model)**			**Anti-pneumococcal Toxicity (∗)**
	Haemolysis	Signs of disease	Survival	CFU in blood	
P1	**+**	**+**	**+**	**+**	**-**
P2	**+**	**-**	**-**	**-**	**-**
P3	**-**	**-**	**-**	**-**	**-**
P4	**-**	**-**	**-**	**-**	**-**
P5	**+**	**N.D.**	**N.D.**	**N.D.**	**+**
P6	**+**	**N.D.**	**N.D.**	**N.D.**	**+**

(Ψ) '**+**' – Passed by showing statistically significant protective effect; '**-**' – Failed to show statistically significant protective effect; 'N.D.' - Not Done.

(∗) '**+**' – Viability of wild-type *S. pneumoniae* strain D39 significantly compromised by the peptide;

'**-**' – Viability of wild-type *S. pneumoniae* strain D39 not compromised by the peptide.

3.2. Pneumolysin inhibitory small molecules

3.2.1. Identification and selection of small molecules by high throughput screening (HTS)

Before the beginning of the high throughput screening it was necessary to determine the minimum concentration of pneumolysin required to produce complete lysis of the red blood cells. If excess pneumolysin was used in the screening, the inhibitory effect of the small molecules may have been missed, whereas too low a concentration could result in incomplete lysis and thus in a raised baseline. Pneumolysin activity was assayed in the HTS by lysis of red blood cells.

The results obtained from the experiments to determine the optimal pneumolysin concentration are presented in Figure 3.10. In Figure 3.10 A, the formation of a red pellet along with a clear a supernatant in the control wells, containing only red blood cells (RBCs) in PBS, showed the absence of haemolysis, confirming the integrity of the cells. Pneumolysin was two-fold serially diluted across twelve wells. Occurrence of full haemolysis can been seen up to well 9, demonstrated by the presence of a red transparent supernatant. Partial haemolysis started to appear in wells 10 with full haemolysis in well 12. Hence, the minimum lytic concentration of pneumolysin able to cause complete lysis of red blood cells was 0.8 µg/ml at well 9. To confirm the lytic activity of the chosen concentration, pneumolysin was retested at 0.8 µg/ml and below. For this, 25 µl of pneumolysin were added to wells containing 25 µl of PBS as a proxy for the small molecule in the HTS. After 45 minutes incubation, 50 µl 4% (v/v) sheep red blood cells suspension were added to the wells, followed by further 30 minutes incubation at 37ºC. The result can be seen in Figure 3.10 B. As expected, the concentration of pneumolysin was confirmed to generate full lysis whereas

concentrations below caused incomplete lysis (0.4 to 0.025 µg/ml) or no lysis at all (0.0125 µg/ml). Therefore, 0.8 µg/ml was selected for use in the HTS.

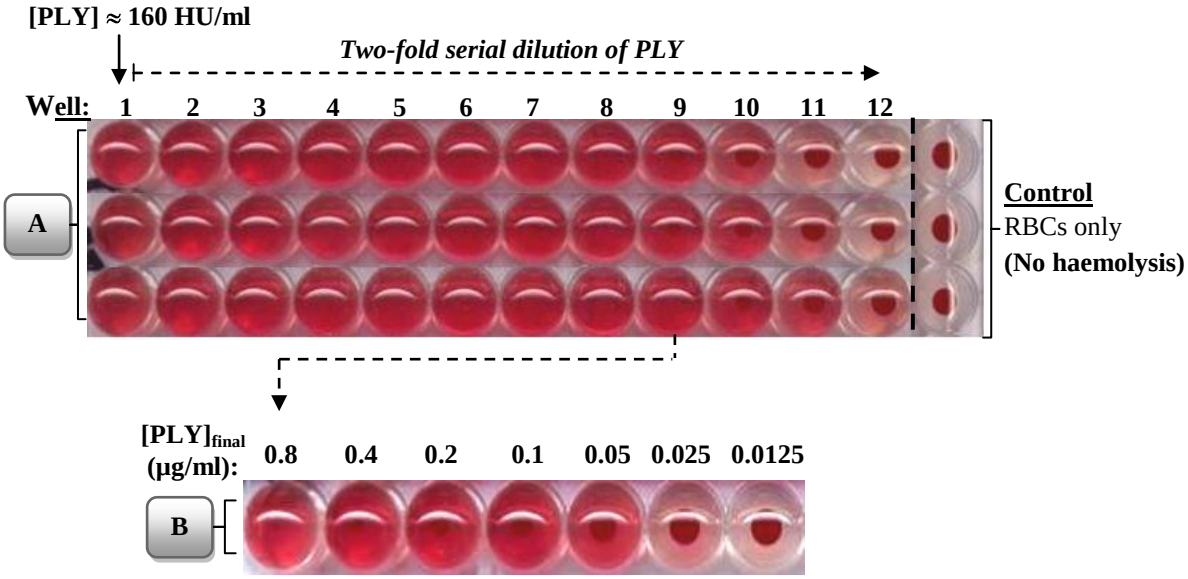

Figure 3.10- Determination of the minimum concentration of pneumolysin required for haemolysis. (A) Assessment of the haemolytic activity of the toxin; 'RBCs' – red blood cells. (B) Testing of the lytic activity at the chosen concentration, at the conditions of the inhibition assay.

3.2.1.1. Validation of the inhibition assay

Once the optimal concentration of toxin was determined, it was necessary to validate the assay. This task was undertaken by a team of scientists at the University of St. Andrews, responsible for the high throughput screening (HTS) of a commercial library of small molecules.

The initial validation of the inhibition assay was done manually, on a round-bottom 96-well plate. During this stage, a positive control for inhibition of pneumolysin haemolytic activity was tested. This control was meant to be introduced in phase of HTS, in order to facilitate the identification of pneumolysin-inhibitory small molecules. The testing for the positive control consisted of pre-incubating pneumolysin with different concentrations of the inhibitory anti-pneumolysin monoclonal antibody, PLY4 (De Los Toyos *et al.*, 1996). At 100 ng per well, PLY4 efficiently blocked pneumolysin activity (data not shown).

The assay then was adapted to a robotic platform of a liquid handling system at the University of St. Andrews (Minitrak^{TM}; Perkin Elmer). In Figure 3.11 the layout of the plate used at this stage is shown. According to the layout, PBS was dispensed into the wells of the columns 1-11, while anti-pneumolysin monoclonal antibody PLY4 (100 ng/well) was added in column 12. Pneumolysin was then dispensed into columns 2-12. This was followed by incubation of the plate at 37ºC for 45 minutes. Finally, the red blood cell suspension was dispensed into all wells and the plate was incubated for further 30 minutes at 37ºC. As expected, the analysis of the plate showed that no haemolysis had occurred in columns 1 and 12 and that there was lysis of the red blood cells in columns 2-11 (data not shown). These results confirmed that the assay could be reproduced using the screening robotics.

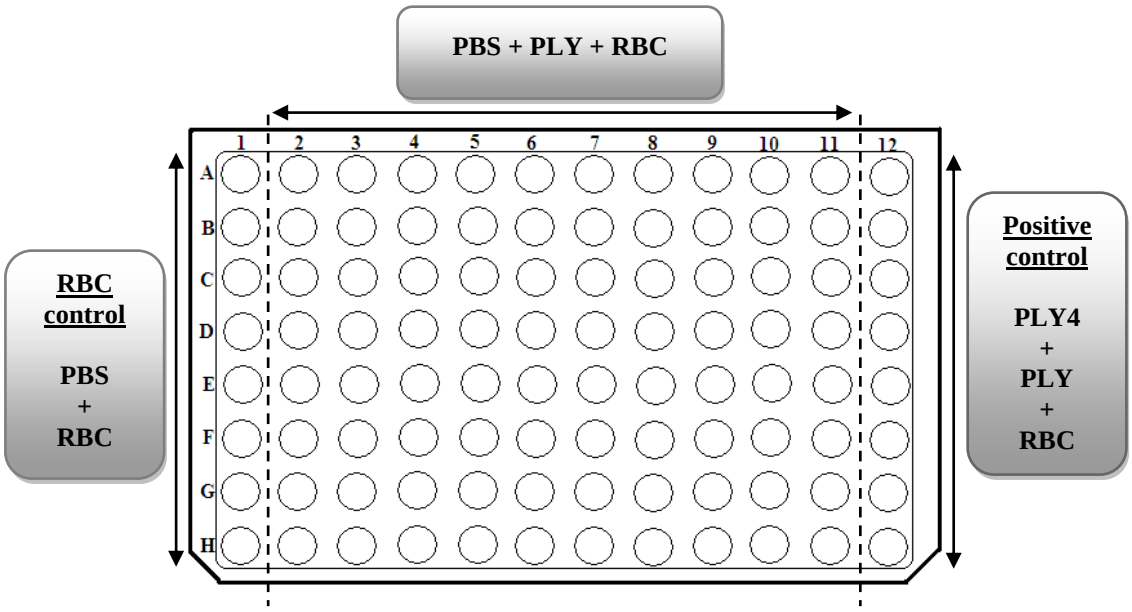

Figure 3.11 – Layout of the plate used on the robotic platform of a liquid handling system (Minitrak™; Perkin Elmer), during the inhibition assay validation at the University of St. Andrews. Column 1 - control with only red blood cells in PBS (RBC control); columns 2-11 - red blood cells exposed to pneumolysin in PBS (as a proxy for the small molecule); column 12 - control with red blood cells exposed to pneumolysin pre-incubated with the inhibitory anti-pneumolysin monoclonal antibody PLY4 (positive control); the term 'positive' refers to positive inhibition of pneumolysin haemolytic activity.

3.2.1.2. Hit identification in the high throughput screening (HTS)

The screening of a commercial library of 16000 small molecules was carried out at the University of St. Andrews, using a robotic liquid handling system (MinitrakTM; Perkin Elmer). The ability of molecules to inhibit pneumolysin haemolytic activity was assayed by employing an adjusted plate layout based on the one previously presented in Figure 3.11. The adjustment consisted of dispensing small molecules, at 10 µM, into the wells of columns 2-11, instead of PBS.

55 hits were identified in this early screening stage. These primary hits were then cherry picked and retested for their ability to inhibit pneumolysin haemolytic activity in the HTS. From this, 10 small molecules were classified as false positives (as when retested they did not inhibit haemolysis by pneumolysin), leaving a hit set of 45.

3.2.1.3. Preliminary assessment of the chemical structures of confirmed hits

Preliminary assessment of the chemical structures of the 45 confirmed hits was carried out by Dr. Nick Westwood at the University of St. Andrews. This assessment led to the classification of the hits into four categories, with a fifth category being used to include all small molecules with miscellaneous structures.

Category 1 included all molecules that contained a maleimide unit, the structure of which is shown in Figure 3.12 A. Maleimides are known to covalently modify thiol side chains in proteins (Haquette *et al.*, 2007). In categories 2 and 3 were included the structures containing thioester and quinone units, respectively. The general structures for thioesters and quinones can be seen in Figure 3.12 B and Figure 3.12 C, correspondingly. These groups also are known for their ability to react with thiol groups, either in thioesterification reactions (thioesters) or in analogous manner to maleimides (quinones) (Wilken & Kent, 1998; Li *et al.*, 2005).

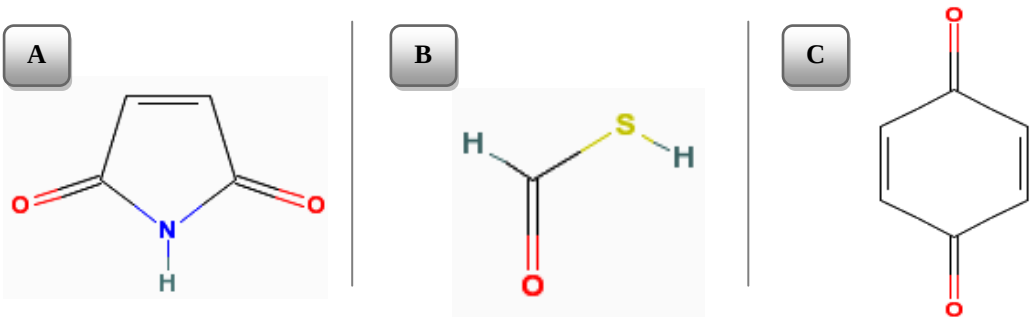

Figure 3.12 – General chemical structure for a (A) maleimide, (B) thioester and (C) quinone. Structures obtained from (NCBI - National Centre for Biotechnology Information, 2010); SID: 57390622; 56464366 and 498546, respectively.

This provided an excellent validation of the assay since the molecules in these categories likely behave as cysteine inhibitors, and pneumolysin has a single cysteine residue (Cys_{428}). However, cysteine residues are found in many other proteins, some of them playing important biological functions in humans. Given to the possibility that structures in categories 1, 2 and 3 could disrupt biological functions of other proteins in

humans, these small molecules did not constitute a real interest in a drug discovery context.

The small molecules placed in category 4 were considered a priority group, as they did not contain unfavourable moieties from the medicinal chemistry point of view. Therefore, they were viewed as the mostly likely to be of interest in terms of drug development.

In category 5, four of the ten small molecules were considered of little relevance in drug discovery, due to their structural proximity to dithio(bis)nitrobenzoic acid (a known pneumolysin Cys_{428} labelling compound). The remaining six small molecules did not have structural characteristics that ruled them out of the study and therefore they were considered for further testing.

The small molecules that passed the assessment were retested in the University of Leicester for their potency in inhibiting pneumolysin, with the exception of one that was no longer commercially available. A summary of preliminary assessment of the chemical structures for the 45 hits is presented as a fluxogram in Figure 3.13.

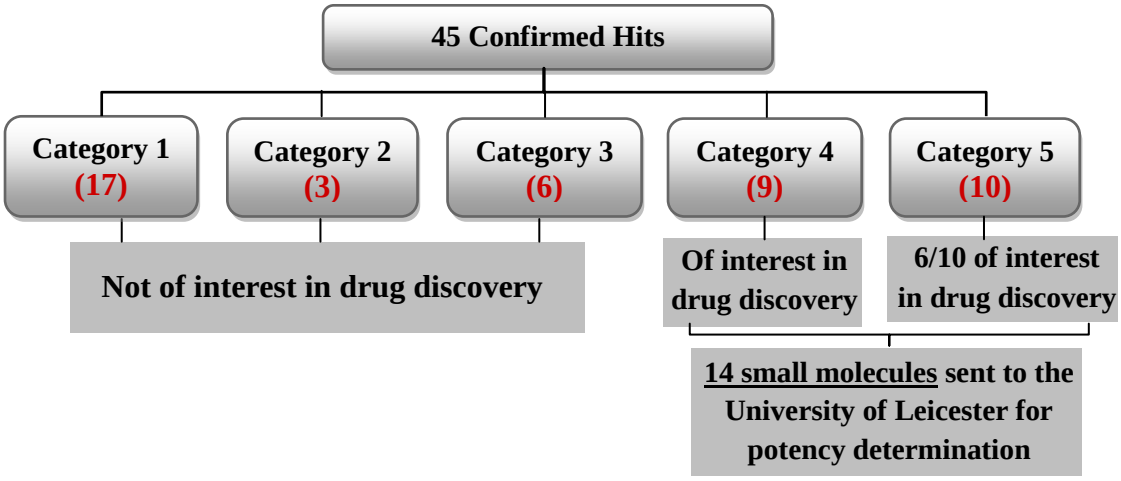

Figure 3.13 – Summary fluxogram of preliminary assessment of the chemical structures for the 45 hits with ability to inhibit pneumolysin activity. Made by Dr. Nick Westwood at the University of St. Andrews.

3.2.2. *In vitro* inhibition of pneumolysin-induced haemolysis by small molecules

The 14 small molecules selected from the HTS done at the University of St. Andrews, were retested *in vitro*, employing the inhibition assay previously described (section 2.10.3). The results obtained with these compounds are shown in Figure 3.14. The fourteen compounds (SM) were two-fold serial diluted across eleven wells (Figure 3.14 A, B, C and D). Pneumolysin (PLY) was added to each dilution of the compounds, at 80 ng per well. Control 1 (PLY + RBC), 2 (RBC only) and 3 (SM + RBC) were included on each plate.

As expected, full lysis of the red blood cells was registered in the wells of control 1, confirming the use of fully active toxin and ensuring that the observation of any positive result was due to the action of the small molecule. In the control wells with red blood cells only, there was no occurrence of haemolysis, indicating that there were no problem with the red blood cells used in the assay and that any observation of lysis was due to pneumolysin's activity.

All small molecules were able to inhibit, to different extents, the haemolytic activity of pneumolysin. For example, in Figure 3.14 A, SM13 showed complete inhibition of the toxin up to well 9 (0.5 µM), whereas SM1 was only able to produce partial inhibition at the highest concentration (125 µM). Additionally, in control 3, no lysis of the red blood cells occurred at any of the tested concentrations, confirming that at these concentrations the compounds did not compromise the integrity of the red blood cells.

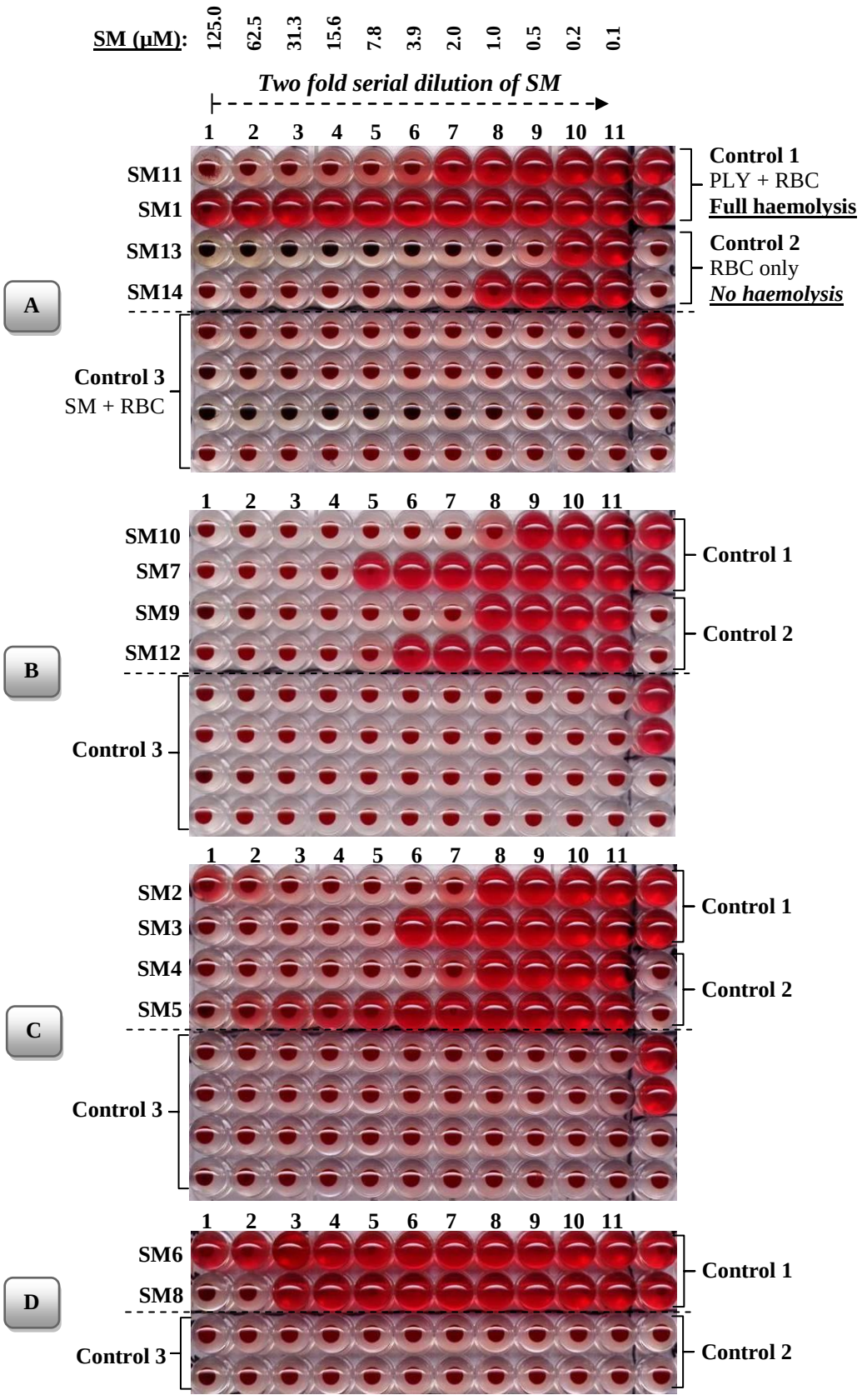

Figure 3.14 – *In vitro* inhibition of pneumolysin-induced lysis of red blood cells obtained with the 14 small molecules selected from the HTS done at the University of St. Andrews.

3.2.2.1. Potency determination (IC50)

The OD_{595} of the microtitrer plates were measured in order to determine half maximal inhibitory concentration (IC50) for each small molecule.

The IC50 values were determined using statistical software GraphPad Prism v.5.00, using a non-linear regression curve fitting, applying the log [inhibitor] vs. response – variable slope model. For that, the log of the tested concentrations for each small molecule (log [inhibitor]) were plotted against the percentage inhibition (response), estimated on basis of the OD_{595} values obtained, not assuming a standard slope but rather fitting the Hill Slope from the data (variable slope). This way, the identification of the IC50 values provided a measure of the effectiveness of the small molecules to inhibit pneumolysin haemolytic activity.

The dose-response curves and the parameters involved in the calculation of the IC50 values of each small molecule are presented in Figures 3.15-3.19. In general, all dose-response curves obtained for each small molecule presented a typical sigmoidal shape.

From the analysis of the remaining curves it was possible to localize the 50% inhibition and then, to determine the logarithm of the inhibitory concentration of small molecule (Log_{10} IC50). A summary of the results obtained *in vitro* with the fourteen small molecules can be found in Table 3.4

Table 3.4 – Summary of the inhibition results and IC50 values obtained *in vitro* for the fourteen small molecules.

Small Molecule ID	*In vitro* inhibition of PLY (assessed by eye)	IC50 (µM)
SM1	**+/-**	**> 20**
SM2	**+**	**1.1**
SM3	**+**	**5.0**
SM4	**+**	**1.1**
SM5	**+**	**6.0**
SM6	**+/-**	**> 20**
SM7	**+**	**7.6**
SM8	**+**	**> 20**
SM9	**+**	**1.1**
SM10	**+**	**0.6**
SM11	**+**	**1.2**
SM12	**+**	**4.3**
SM13	**+**	**0.2**
SM14	**+**	**0.6**

Note: **+** represents inhibition of haemolytic activity; **+/-** represents partial inhibition of haemolytic activity

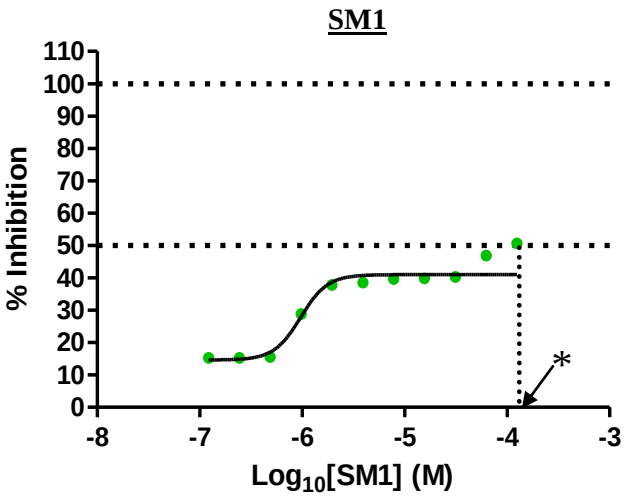

Log(inhibitor) vs. response: Variable slope - SM1	
*Log_{10} IC50	-3.90
IC50	**>20 µM**
R^2	0.9643

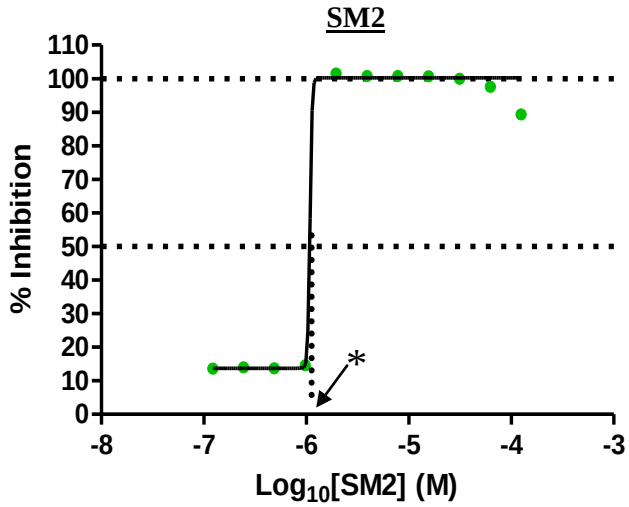

Log(inhibitor) vs. response: Variable slope – SM2	
*Log_{10} IC50	-5.97
IC50	1.07×10^{-6}M (**1.1 µM**)
R^2	0.9995

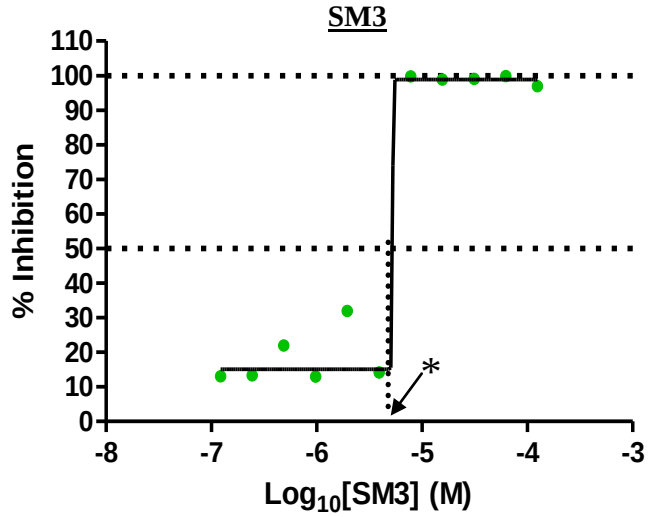

Log(inhibitor) vs. response: Variable slope – SM3	
*Log_{10} IC50	-5.30
IC50	5.01×10^{-6}M (**5.0 µM**)
R^2	0.9963

Figure 3.15 – Dose-response curves and IC50 parameters calculated for the anti-pneumolysin small molecules SM1, SM2 and SM3.

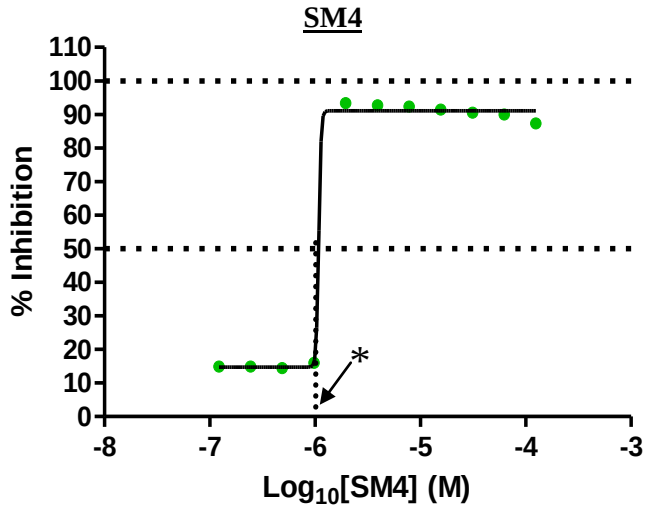

Log(inhibitor) vs. response: Variable slope – SM4	
*Log_{10} IC50	-5.97
IC50	1.07×10^{6}M (**1.1 µM**)
R^2	0.9983

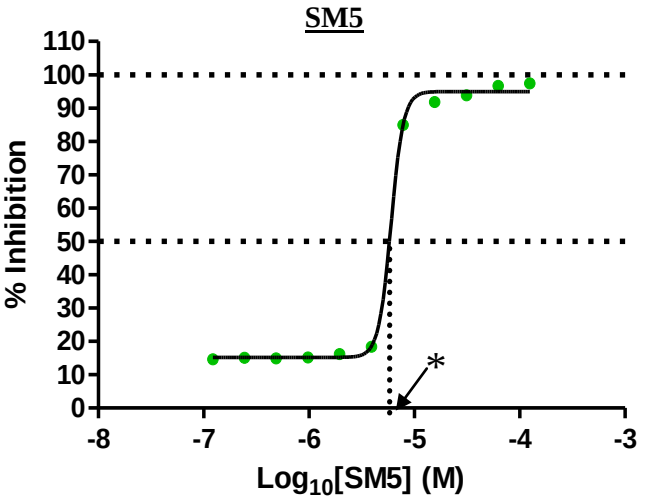

Log(inhibitor) vs. response: Variable slope – SM5	
*Log_{10}IC50	-5.22
IC50	6.03×10^{-6}M (**6.0 µM**)
R^2	0.9987

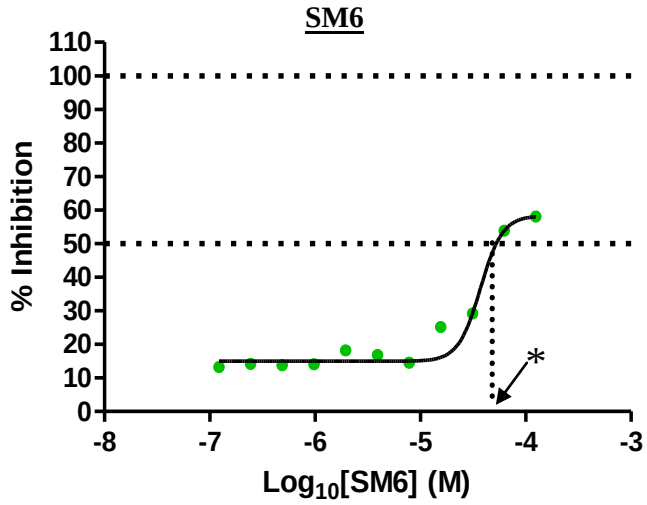

Log(inhibitor) vs. response: Variable slope – SM6	
*Log_{10}IC50	-4.28
IC50	**>20 µM**
R^2	0.9925

3.16 – Dose-response curves and IC50 parameters determined for pneumolysin inhibitors SM4, SM5 and SM6.

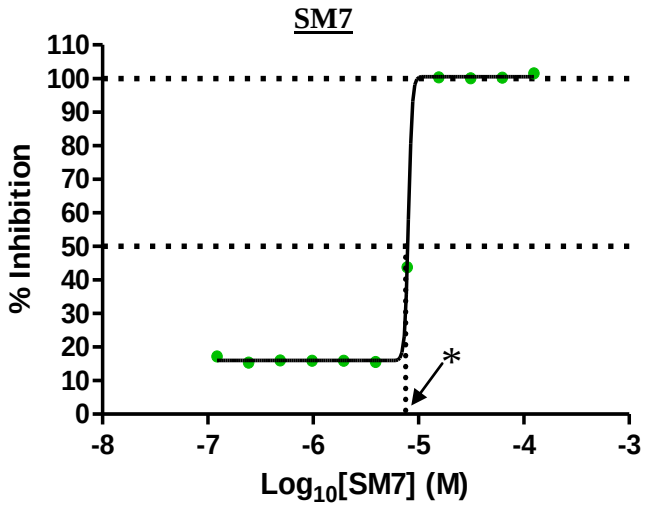

Log(inhibitor) vs. response: Variable slope – SM7	
*Log_{10} IC50	-5.12
IC50	7.59×10^{-6}M (**7.6 µM**)
R^2	0.9998

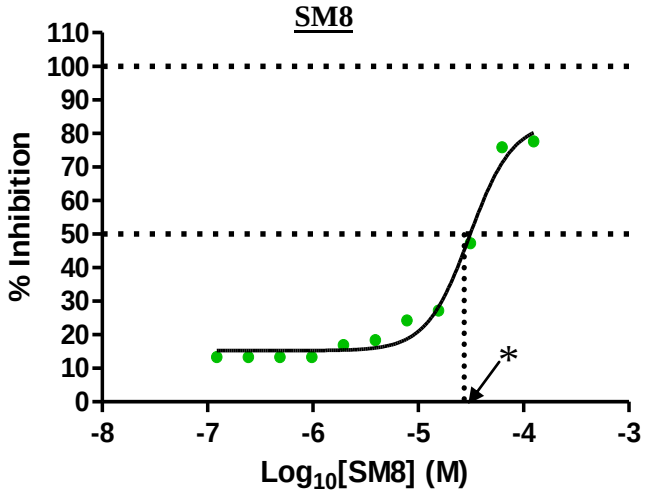

Log(inhibitor) vs. response: Variable slope – SM8	
*Log_{10} IC50	-4.52
IC50	**>20 µM**
R^2	0.9858

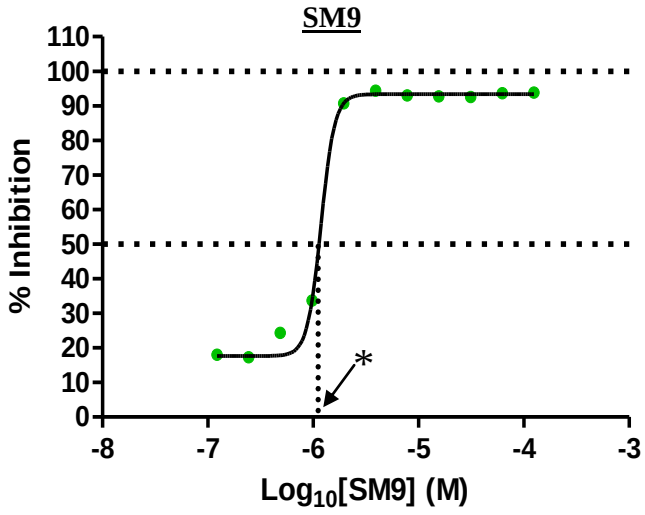

Log(inhibitor) vs. response: Variable slope – SM9	
*Log_{10} IC50	-5.97
IC50	1.07×10^{-6}M (**1.1 µM**)
R^2	0.9997

Figure 3.17- Dose-response curves and IC50 parameters calculated for the anti-pneumolysin small molecules SM7, SM8 and SM9.

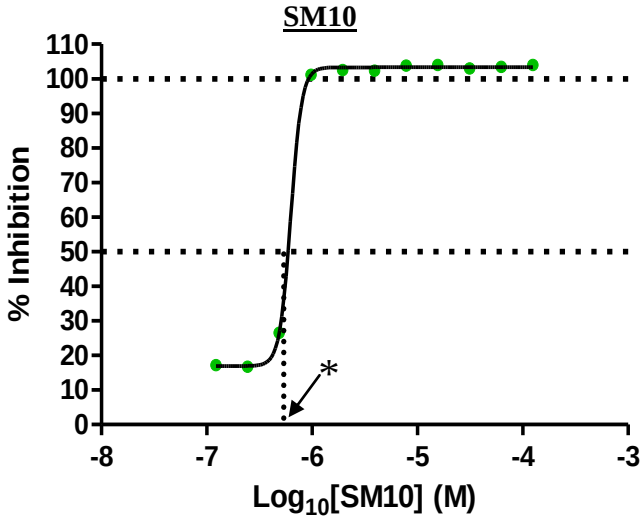

Log(inhibitor) vs. response: Variable slope – SM10	
***Log_{10} IC50**	-6.23
IC50	5.89×10^{-7}M (**0.6 µM**)
R^2	0.9998

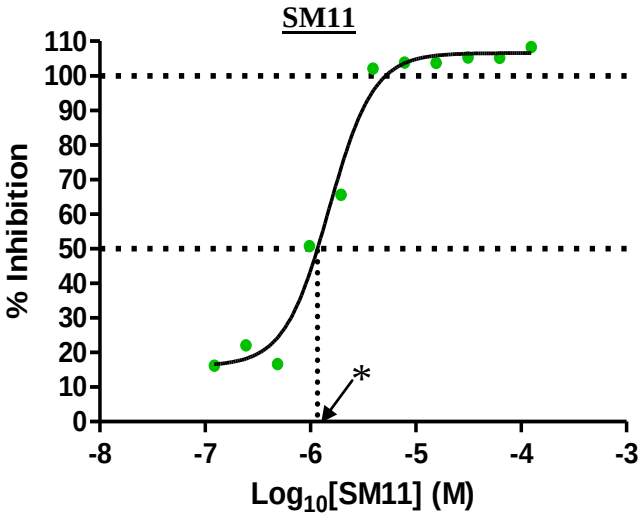

Log(inhibitor) vs. response: Variable slope – SM11	
***Log_{10} IC50**	-5.92
IC50	1.20×10^{-6}M (**1.2 µM**)
R^2	0.9837

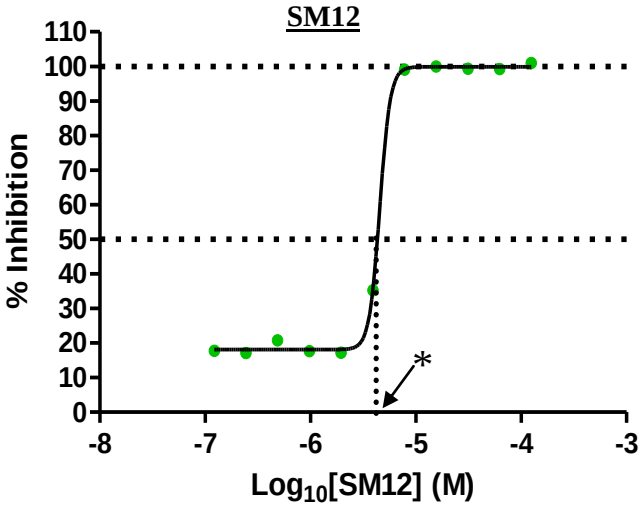

Log(inhibitor) vs. response: Variable slope – SM12	
***Log_{10}IC50**	-5.37
IC50	4.25×10^{-6}M (**4.3 µM**)
R^2	0.9993

Figure 3.18 - Dose-response curves and IC50 parameters determined for pneumolysin inhibitors SM10, SM11 and SM12.

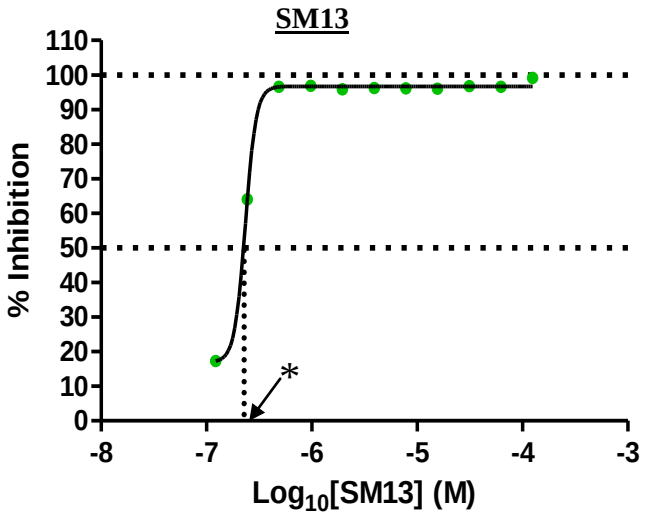

Log(inhibitor) vs. response: Variable slope – SM13	
***Log_{10} IC50**	-6.65
IC50	2.20×10^{-7}M (**0.2 µM**)
R^2	0.9987

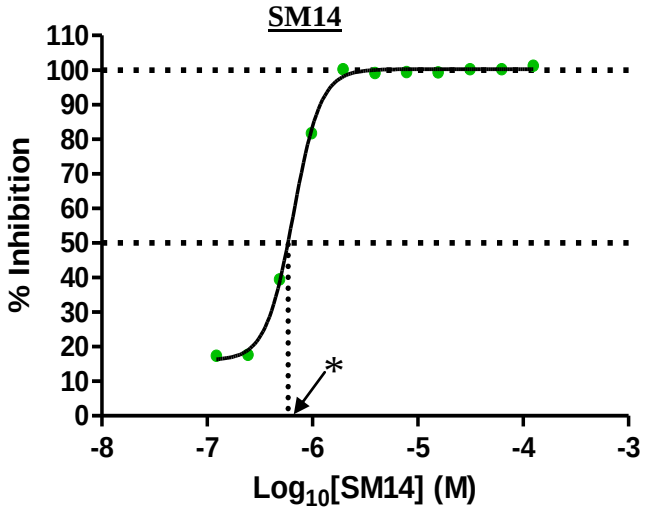

Log(inhibitor) vs. response: Variable slope – SM14	
***Log_{10} IC50**	-6.23
IC50	5.80×10^{-7}M (**0.6 µM**)
R^2	0.9990

Figure 3.19- Dose-response curves and IC50 parameters determined for pneumolysin inhibitors SM13 and SM114.

3.2.3. *In vivo* studies for evaluation of the anti-pneumolysin small molecules efficacy in a pneumonia model

For *in vivo* studies, a pneumococcal pneumonia model was employed (section 2.10.4.13), to study six small molecules selected from the previous *in vitro* screening. SM4, SM9, SM10, SM13 and SM14 were chosen because of their high inhibitory effect on pneumolysin, while SM6, which exhibited a low potential to inhibit the toxin, was chosen for comparison.

In Figure 3.20 the results obtained with the small molecule SM6 are presented. 24 hours after the challenge with the wild-type pneumococcal strain D39, all animals in the control group (dashed blue line) had reached the endpoint (0% survival) whereas only 40% of the group treated with SM6 (solid green line) had died at this time ($p < 0.05$). At 36 hours post-infection, the percentage survival of the treatment group had dropped from 60% to 40% ($p < 0.05$), and then remained constant until the end of the experiment, 48 hours post-infection. Comparison by means of the long-rank (Mantel-Cox) test showed significant difference between the survival curves ($p < 0.05$).

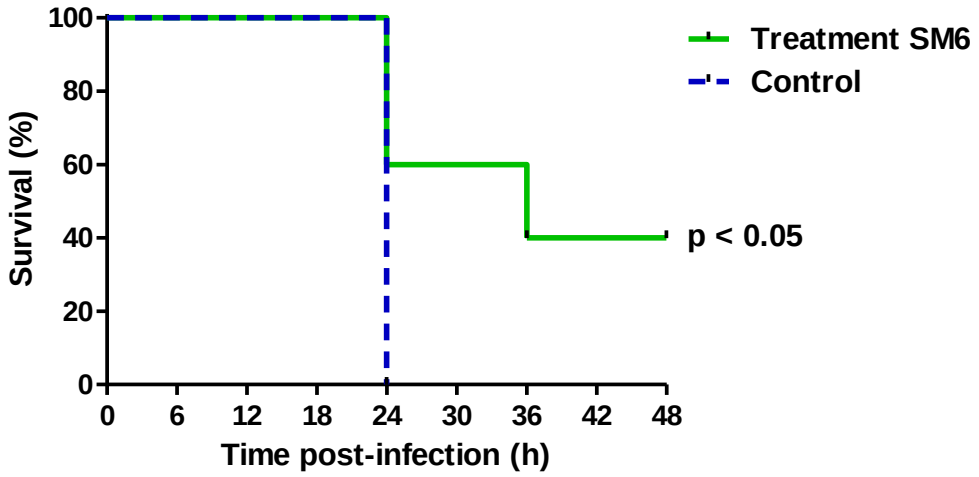

Figure 3.20 - Survival of mice intranasally infected with *S. pneumoniae* D39. One hour after infection, animals received intranasally small molecule SM6 in PBS or PBS, as appropriate, and every 6 hours thereafter. The p-value was calculated by means of the log-rank (Mantel-Cox) test (n = 5/group).

In Figure 3.21 the survival curves obtained from the *in vivo* study with SM10 are shown. 24 hours after infection with D39, the percentage survival of the control group had dropped to 60%, while the group treated with SM10 had not registered any deaths ($p > 0.05$). 36 hours post-infection infection, all mice in the control group had died. At this time-point, the survival rates of the treatment group had dropped to 60% ($p < 0.05$), and then remained constant until the endpoint of the experiment at 60 hours post-infection. Comparison of the survival curves by means of the log-rank (Mantel-Cox) test showed significant differences between control and test groups ($p < 0.05$).

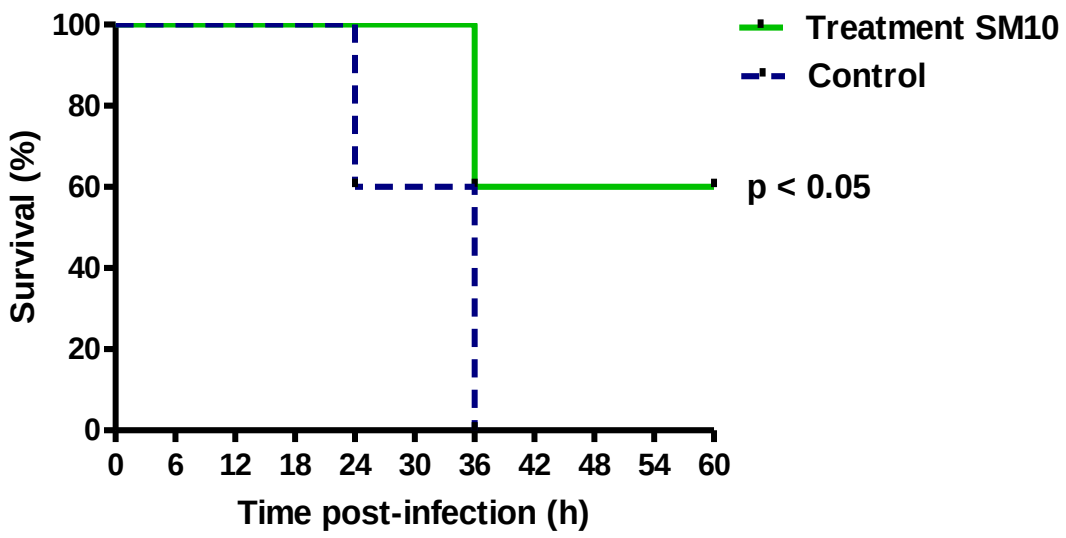

Figure 3.21 – Comparison of survival of the control and treatment groups obtained with SM10, using a pneumonia model. Mice were intranasally infected with *S. pneumoniae* strain D39 in PBS. One hour after infection, animals started being given small molecule SM10 in PBS or PBS, as appropriate, and every 6 hours thereafter. The p-value was calculated by means of the log-rank (Mantel-Cox) test (n = 5/group).

In Figure 3.22 the survival rates obtained from the study with SM14 can be observed. All mice in the control group had reached the endpoint at 24 hours post-infection. In contrast, all mice in the treatment group were alive at this time ($p < 0.05$). At 36 hours post-infection the percentage survival of the treatment group had dropped to 40% ($p < 0.05$), and then remained constant until the endpoint of the experiment at 40 hours post-infection. Again, the statistical comparison of the survival rates demonstrated significant differences between control and test groups ($p < 0.05$).

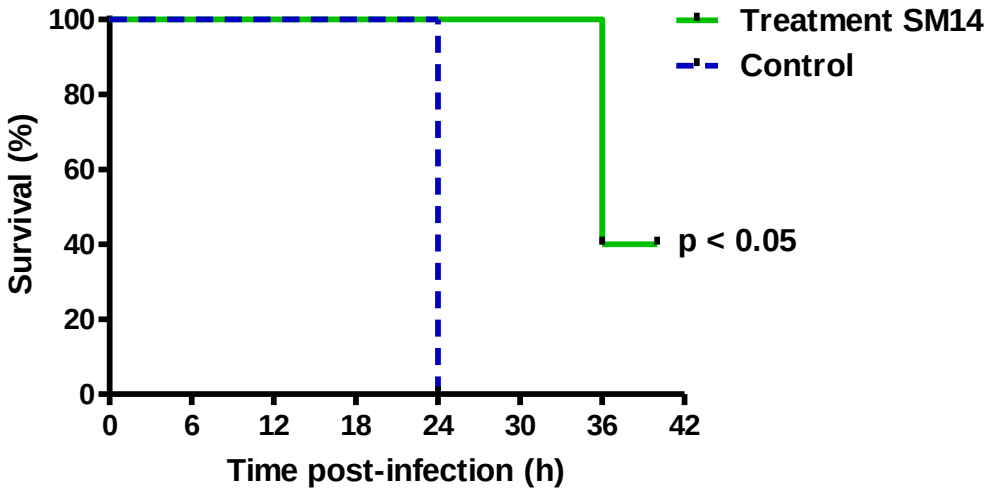

Figure 3.22 - Comparison of survival rates of the control and treatment groups obtained with SM14, using a pneumonia model. Mice were intranasally infected with *S. pneumoniae* strain D39 in PBS. One hour after infection, animals started being given small molecule SM14 in PBS or PBS, as appropriate, and every 6 hours thereafter. The p-value was calculated by means of the log-rank (Mantel-Cox) test (n = 5/group).

The survival curves resultant from the *in vivo* experiments with the small molecule SM4 (Figure 3.23) did not show significant differences between the control and treatment groups ($p > 0.05$). There was also no evidence throughout the experiments that suggested a delay in the progress of the signs of the disease. On the other hand, treatment with SM13 (Figure 3.24) only seemed to aggravate animals' welfare, with all mice dead 12 hours after challenge with D39 ($p < 0.05$).

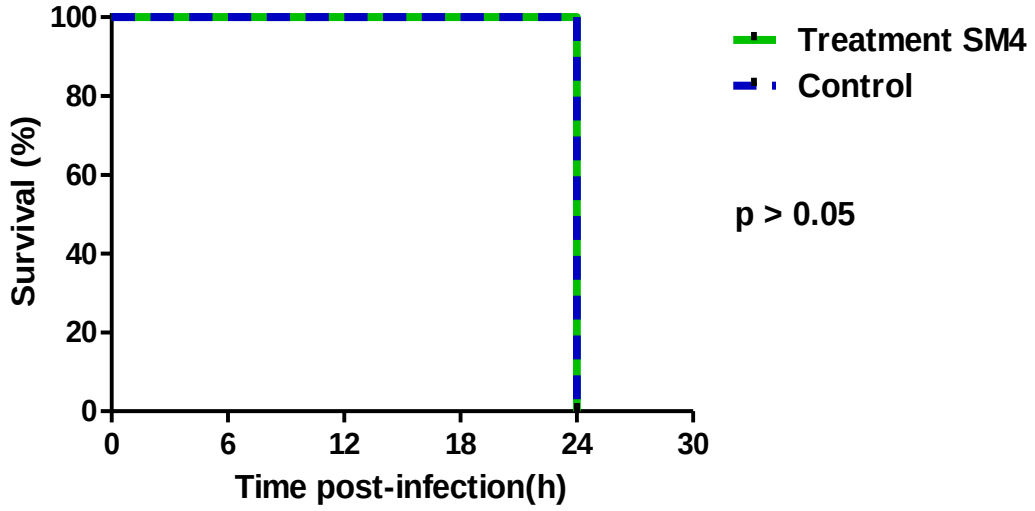

Figure 3.23 - Comparison of survival of the control and treatment groups obtained with SM4, using a pneumonia model. Mice were intranasally infected with *S. pneumoniae* strain D39 in PBS. One hour after infection, animals started being given small molecule SM4 in PBS or PBS, as appropriate, and every 6 hours thereafter. The p-value was calculated by means of the log-rank (Mantel-Cox) test (n = 5/group).

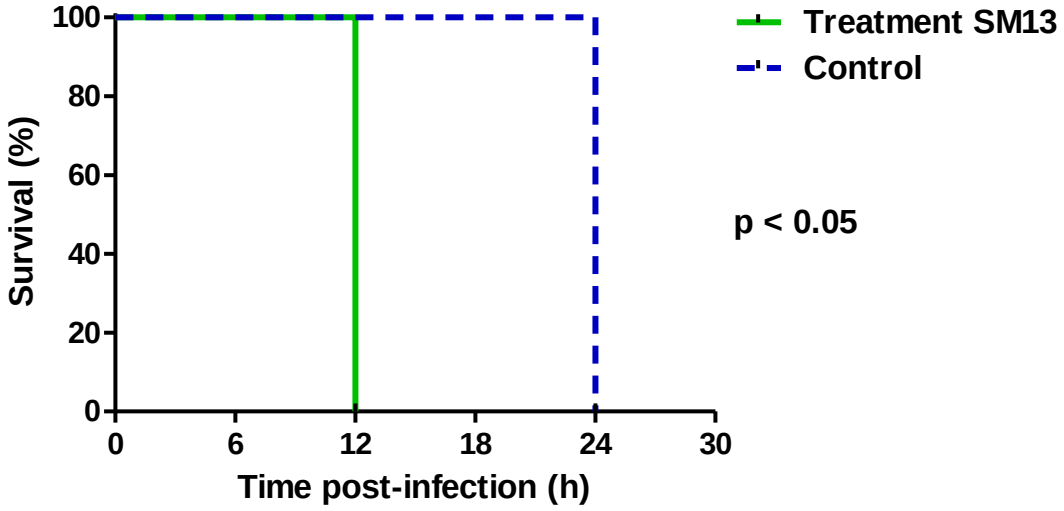

Figure 3.24 - Comparison of survival of the control and treatment groups obtained with SM13, using a pneumonia model. Mice were intranasally infected with *S. pneumoniae* strain D39 in PBS. One hour after infection, animals started being given small molecule SM13 in PBS or PBS, as appropriate, and every 6 hours thereafter. The p-value was calculated by means of the log-rank (Mantel-Cox) test (n = 5/group).

In the case of the small molecule SM9 (Figure 3.25), despite the survival rates being slightly higher for the treatment group by end of the experiment, there was no significant difference ($p > 0.05$).

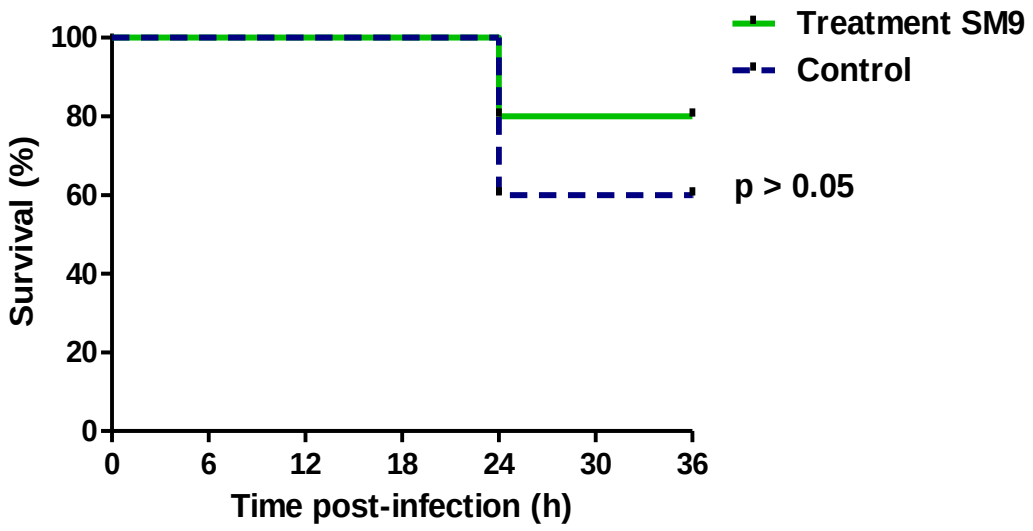

Figure 3.25 - Comparison of survival of the control and treatment groups obtained with SM9, using a pneumonia model. Mice were intranasally infected with *S. pneumoniae* strain D39 in PBS. One hour after infection, animals started being given small molecule SM9 in PBS or PBS, as appropriate, and every 6 hours thereafter. The p-value was calculated by means of the log-rank (Mantel-Cox) test (n = 5/group).

Twelve of the fourteen small molecules (SM7 and SM8 were not commercially available) were tested to evaluate their effect on D39 viability (section 2.10.4.11). The results of these tests can be seen in Figure 3.26. The Figure shows the CFU values of D39 in PBS (patterned blue columns), and D39 in the presence of small molecule in PBS (solid green columns), at 0 hours and 2 hours after incubation at 37ºC. The difference in the CFU values at t_{0h} and t_{2h} was compared between the control and test groups by means of an unpaired t-test. The statistical analysis showed significant differences between the controls and test groups only with SM3, SM5, SM12 and SM13 ($p > 0.05$). The remaining small molecules were not found to compromise the viability of the pneumococcal strain D39.

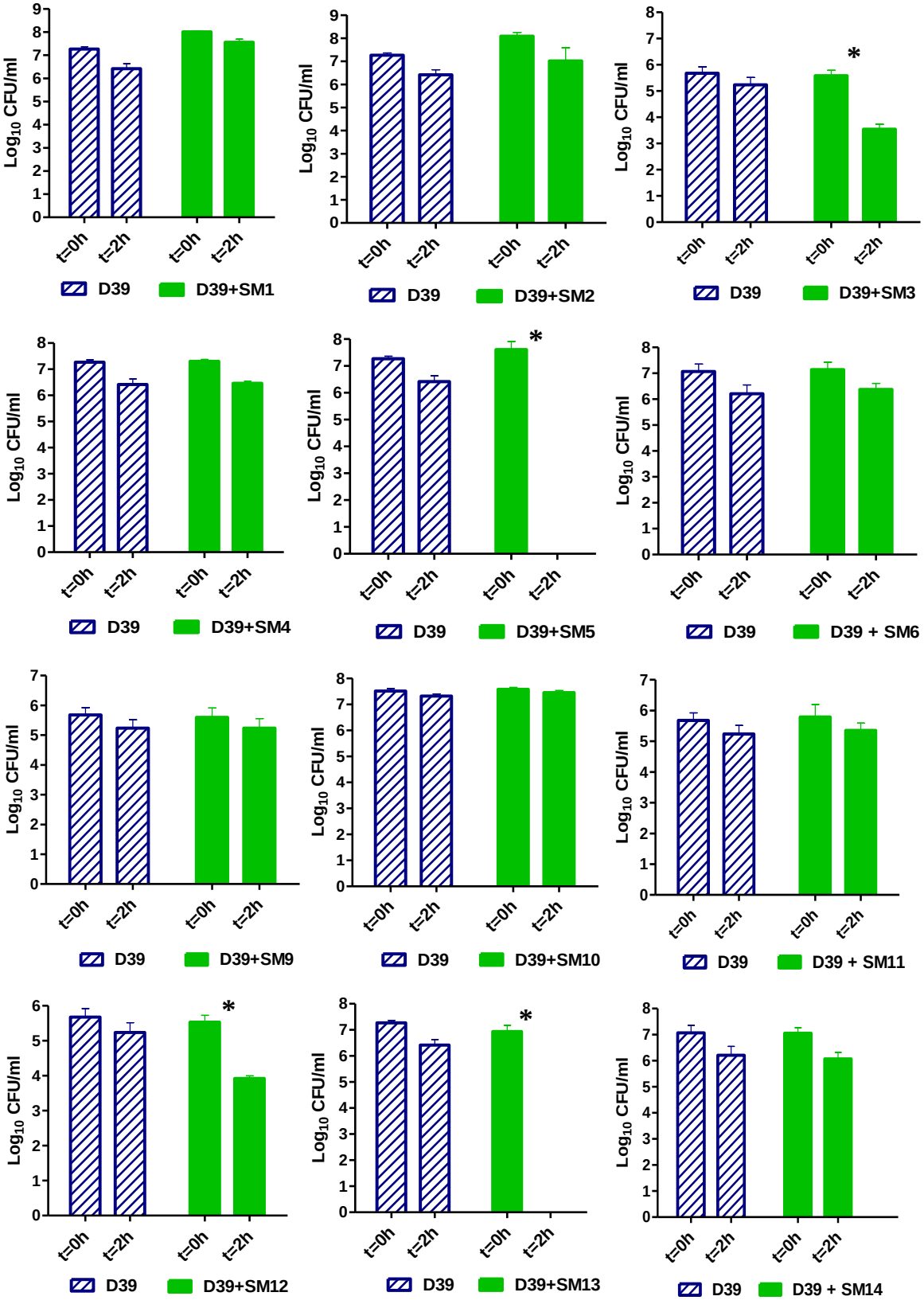

Figure 3.26 - *In vitro* assessment of the antimicrobial effect of small molecules SM1-SM14 on *S. pneumoniae* strain D39. CFU values obtained for the control group (D39 in PBS) and for the test group (D39 plus small molecule in PBS), at 0 hours and 2 hours after incubation at 37ºC, are presented. Graphs show means ± SD; *, $p < 0.05$ between groups at 2 hours (n = 4).

Table 3.5 shows the summary of the results achieved with the small molecules.

Table 3.5- Summary table of the results obtained with the small molecules in the *in vivo* and *in vitro* assays.

SM ID	***in vitro* inhibition (Ψ)**	***in vivo* inhibition (Ψ) (pneumonia model)**			**anti-pneumococcal toxicity (*)**
	Haemolysis	Signs of disease	Survival	CFU in blood	
SM1	**+**	**-**	**-**	**-**	**-**
SM2	**+**	**N.D.**	**N.D.**	**N.D.**	**-**
SM3	**+**	**-**	**-**	**-**	**+**
SM4	**+**	**-**	**-**	**-**	**-**
SM5	**+**	**-**	**-**	**-**	**+**
SM6	**+**	**+**	**+**	**+**	**-**
SM7	**+**	**N.D.**	**N.D.**	**N.D.**	**N.D.**
SM8	**+**	**N.D.**	**N.D.**	**N.D.**	**N.D.**
SM9	**+**	**-**	**-**	**-**	**-**
SM10	**+**	**+**	**+**	**+**	**-**
SM11	**+**	**N.D.**	**N.D.**	**N.D.**	**-**
SM12	**+**	**N.D.**	**N.D.**	**N.D.**	**+**
SM13	**+**	**-**	**-**	**-**	**+**
SM14	**+**	**+**	**+**	**+**	**-**

(Ψ) '**+**' – Passed by showing statistically significant protective effect; '**-**' – Failed to show statistically significant protective effect; 'N.D.' - Not Done.

(*) '**+**' – Viability of wild-type *S. pneumoniae* strain D39 significantly compromised by the small molecule; '**-**' – Viability of wild-type *S. pneumoniae* strain D39 not compromised by the small molecule; 'N.D.' - Not Done.

3.2.4. Assessment of the chemical structures of the anti-pneumolysin small molecules

After the identification of hits in the previous screening stages, it was necessary to verify if they were suitable to be used as starting points in a "MedChem" program. For this reason, an external medicinal chemist, Dr. Fritz Frickel, with internationally recognised expertise in this area, was contacted and asked to analyse the structure of the all fourteen small molecules. His assessment was done purely on the basis of the structures. Based on his assessment, 8 small molecules were discontinued as they potentially contain moieties labile in a biological test system. The remaining seven pneumolysin inhibitors were selected as suitable for a medicinal programme and could represent either a clinical candidate or a lead for a clinical candidate. The result of this assessment is summarized in Table 3.6.

Table 3.6- Summary of the assessment of the structures of the small molecules for use as starting points in a MedChem programme.

Small molecule ID	Assessment's result
SM1	✓
SM2	×
SM3	×
SM4	×
SM5	✓
SM6	×
SM7	✓
SM8	×
SM9	✓
SM10	✓
SM11	✓
SM12	×
SM13	×
SM14	✓

'✓' suitable/ '×' not suitable for a medicinal programme

3.2.5. Assessment of the direct antimicrobial activity of small molecules *in vitro*

As previously mentioned, four of the small molecules showed antimicrobial activity on *S. pneumoniae*. In order to verify if that activity was specific to pneumococcus, SM5 and SM12 were selected to be tested on other bacterial species (section 2.10.5). The small molecules showed an antimicrobial activity against *Streptococcus pyogenes*, *Staphylococcus aureus*, MRSA, *Clostridium perfringens*, *Bacillus cereus* (Table 3.7). The same effect was not observed with *Escherichia coli*, *Pseudomonas aeruginosa* and *E. aerogenes*. In Figure 3.27 some examples of the results obtained are presented. With *Enterobacter aerogenes* (Figure 3.27 A) there are no zones of clearance around the disks containing SM5 and SM12, whereas with *C. perfringens* these zones can be observed (Figure 3.27 B).

Table 3.7 - Direct antimicrobial activity of the small molecules SC5 and SC12 on different bacterial species.

Bacterial species	Zone of clearance	
	SM5	**SM12**
Streptococcus pneumoniae	1.4cm	1.4cm
Streptococcus pyogenes	1.8cm	1.2cm
Escherichia coli	None	None
Staphylococcus aureus	1.4cm	1.5cm
MRSA	1.0cm	0.8cm
Pseudomonas aeruginosa	None	None
Enterobacter aerogenes	None	None
Clostridium perfringens	0.9cm	1.2cm
Bacillus cereus	1.2cm	1.8cm

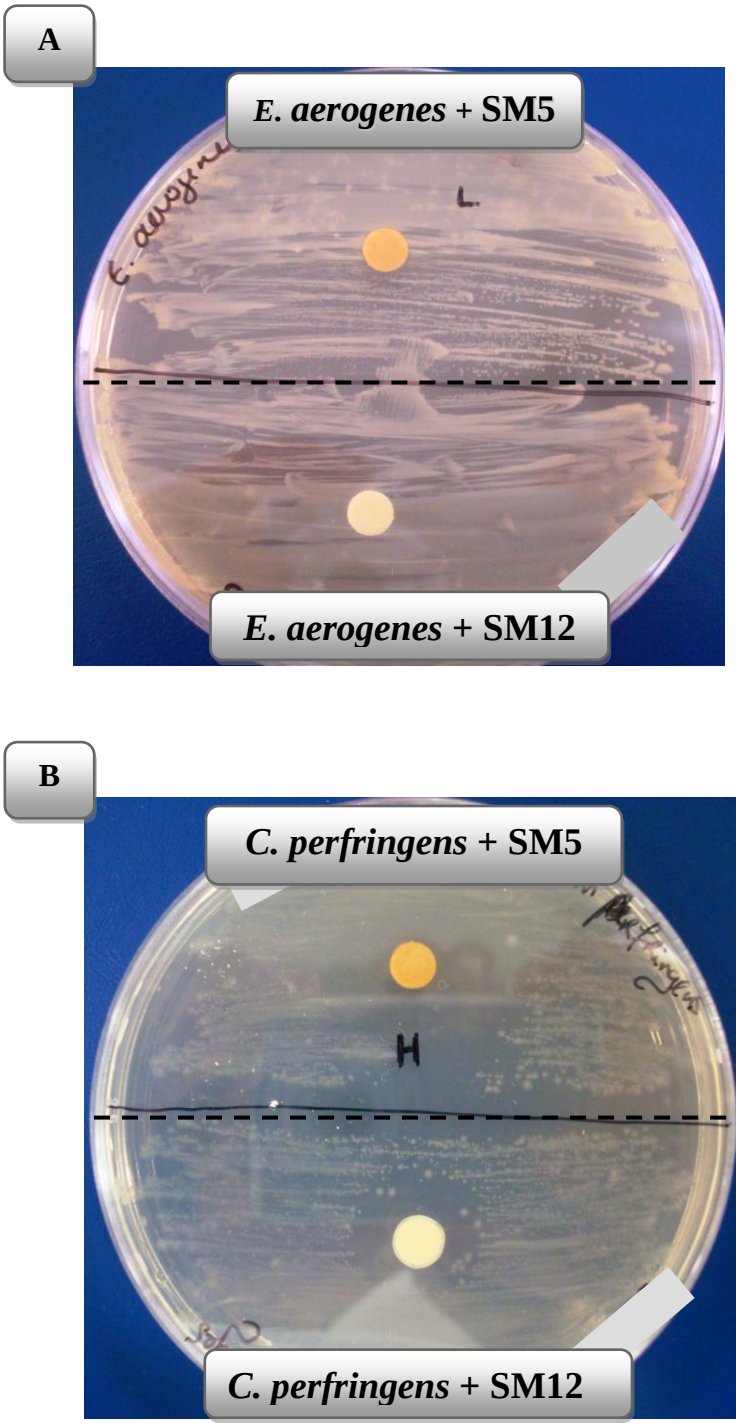

Figure 3.27 - Effect of SM5 and SM12 on A) *Enterobacter aerogenes* and B) *Clostridium perfringens*.

Based on these observations, there seems to be an apparent specificity of the small molecules with antimicrobial activity for Gram-positive bacteria (*S. pneumoniae, S. pyogenes, S. aureus, MRSA, C. perfringens and B. cereus*) but not for Gram-negative.

3.2.6. Pharmacokinetics

Bioanalysis studies on SM10, SM14 and SM9 were outsourced to an UK-based international life sciences company, Tepnel, in order to determine their PK *in vivo*. For this, mice were intravenously (20 μg/100 μl/mouse) or orally (200 μg/100 μl/mouse) administered with small molecule in PBS. Then at pre-selected times, pre-selected groups of three mice were exsanguinated by cardiac puncture (section 2.10.4.9). The serum samples were then sent to Tepnel for analysis.

The results of the experiment with SM10 and SM14 showed that these small molecules were not detected in the blood even shortly (5 minutes) after either i.v. or oral administration of the small molecules (data not available).

In Figure 3.28 the PK profile obtained for SM9 following oral and i.v. administration is presented. Pharmacokinetic parameters were calculated from the "Plasma concentration vs. Time" curves (Table 3.8). In contrast to SM10 and SM14, SM9 was detected in the blood samples collected from mice, shortly after intravenous and oral administrations. It took 0.44 hours (oral route) and 0.08 hours (i.v. route) for the detectable concentration of SM9 in the plasma reach its maximum. Approximately six hours after i.v. administration, and twelve hours after oral administration, SM9 had been completely cleared from the blood stream.

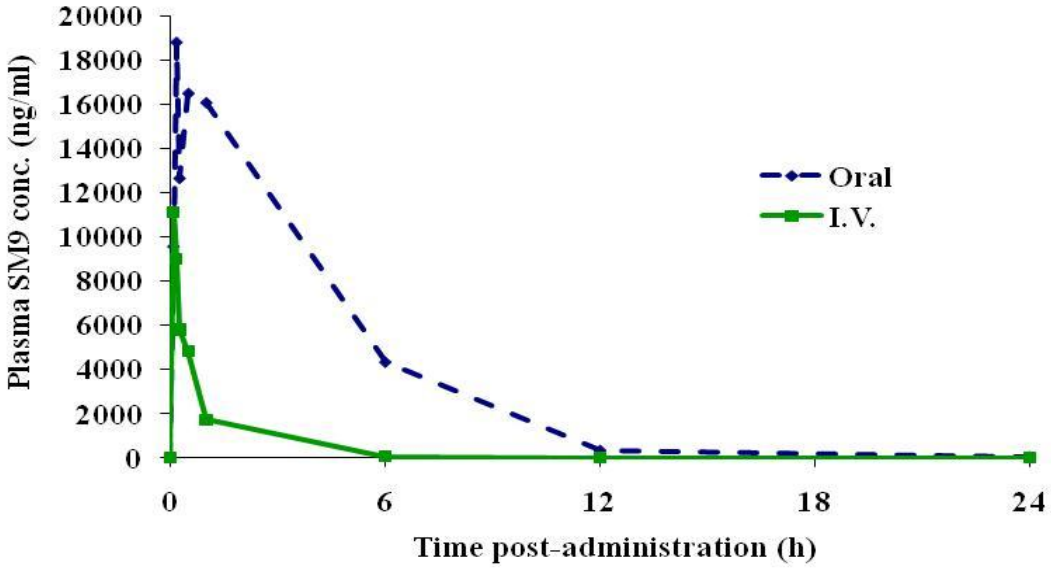

Figure 3.28 – SM9 profile following oral and I.V. administration (n=3).

Table 3.8 – PK parameters calculated for SM9 following the oral and i.v. administration.

Pharmacokinetic parameter	Oral	I.V.
T_{max} (h)	0.44	0.08
C_{max} (ng/ml)	22600	11123
AUC (ng/ml.min)	81503	9524
Relative bioavailability (%)	84	—

C_{max} - highest plasma drug concentration observed.

T_{max} - time at which the C_{max} occurs following administration.

AUC (area under the curve) - measure of total plasma exposure of a drug over a given time period.

Relative bioavailability- bioavailability of the small molecule administered orally in comparison with the availability of the same small molecule given via intravenous route.

3.2.7. *Ex vivo* studies

3.2.7.1. Inhibition of pneumolysin-induced effect on the ciliary function of ependymal cells by SM10 and SM14

The ependymal cells constitute the layer lining the cerebral ventricles and the central canal of the spinal cord, acting as a selective brain barrier. Their surface is covered by cilia which are responsible for the circulation of the cerebrospinal fluid (CFS). The exposure of the cilia to pneumolysin causes a complete or partial reduction of their ciliary beat frequency (CBF). Therefore, the small molecules SM10 and SM14, which passed the previous screening stages, were tested for ability to inhibit pneumolysin's effect on the ciliary function of ependymal cells, using an *ex vivo* model (section 2.10.6.1).

In Figure 3.29 the results obtained in the course of the experiment with the small molecule SM10 are shown. The CBF values registered for the control wells with the ependymal cells and assay medium (control 1; black solid line) were used as a reference of a normal ciliary beat frequency. The CBF measurements remained constant (approximately 48 Hz) throughout the experiment. In the wells where pneumolysin was added to the cells (Figure 3.29; control 2; red solid line) it is possible to observe a rapid drop in the CBF, with complete inhibition by 1 minute. However, when pneumolysin was pre-incubated with SM10 before adding to cells, there was complete abolition of the toxic effect (Figure 3.29; green dotted line). The concentration of small molecule used in this experiment did not affect the CBF, as it can be seen in the control 3 (Figure 3.29; blue dashed line). In addition, the statistical analysis of the CBF measurements showed significant differences ($p<0.05$) between the wells of control 2 and the wells to which the toxin pre-incubated with SM10 was added.

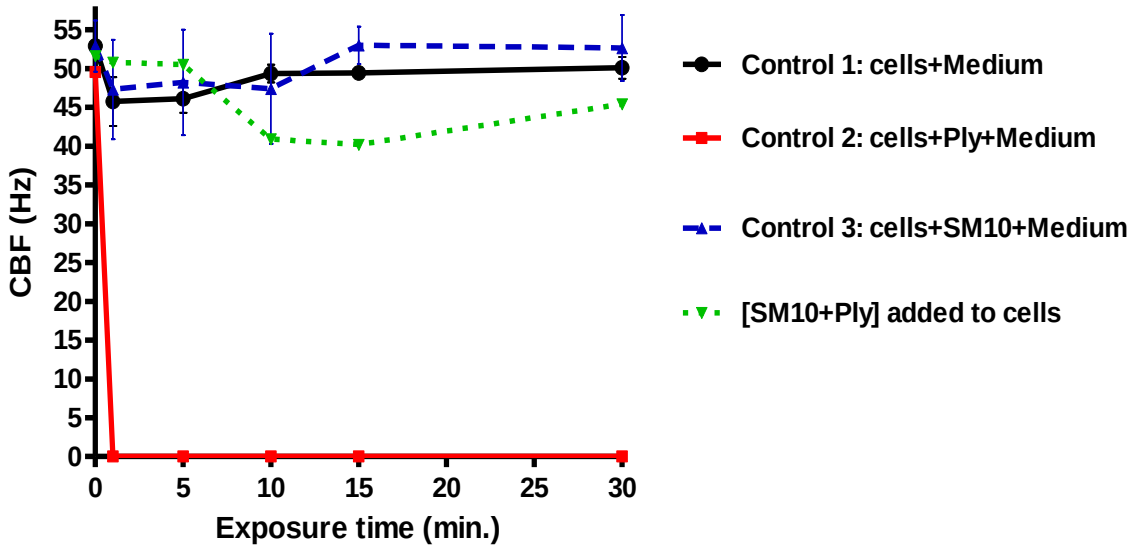

Figure 3.29- Suppression of the pneumolysin inhibitory effect on the ciliary function of the ependymal cells by the small molecule SM10. Each time point represents the mean ± SD of CBF measurement of four individual cilia from each well, for three independent experiments.

A similar scenario was observed in a study involving SM 14 (Figure 3.30). The CBF values registered for control 1 (black solid line) remained constant (approximately 46 Hz) throughout the experiment. It was again possible to observe a rapid drop of the CBF, in the wells where pneumolysin was added to the cells (Figure 3.30; control 2; red solid line). As with SM10, it was possible to completely inhibit pneumolysin's effect by pre-incubating it with SM14 (Figure 3.30; green dotted line). The concentration of SM14 used in this experiment did not affect the CBF (Figure 3.30; control 3; blue dashed line). In addition, the statistical analysis of the CBF measurements showed significant differences ($p<0.05$) between the wells of control 2 and the wells to which the toxin pre-incubated with SM14 was added.

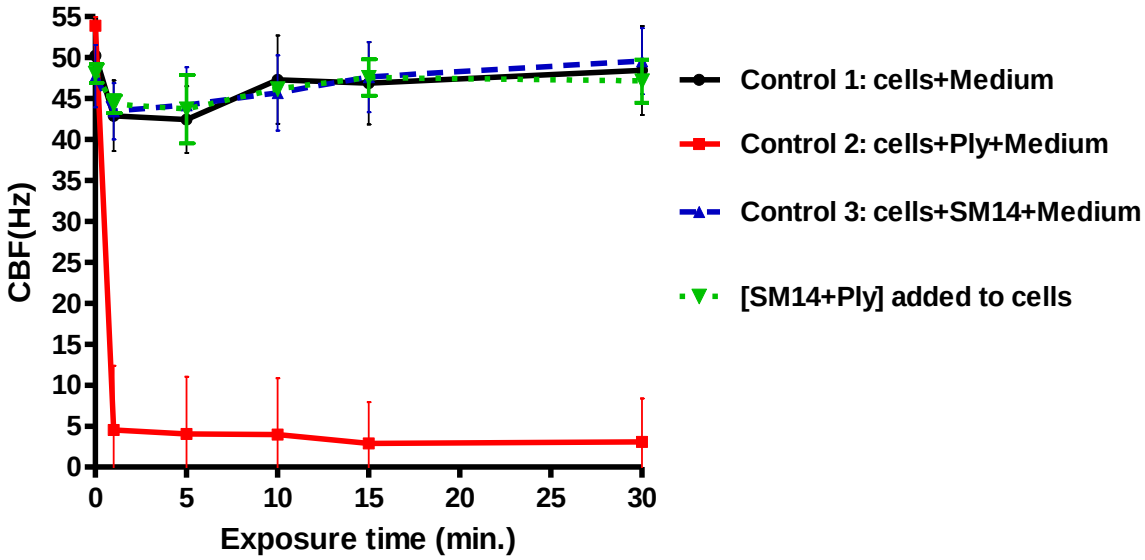

Figure 3.30 - Suppression of the pneumolysin inhibitory effect on the ciliary function of the ependymal cells by the small molecule SM14. Each time point represents the mean ± SD of CBF measurement of four individual cilia from each well, for three independent experiments.

3.2.7.2. Inhibition of the pneumolysin-induced effect on the ciliary function of rat brain slices

Two videos were produced in order to visualise the protection effect exhibited by the small molecules against pneumolysin. For this, rat brain slices were used as previously described in section 2.10.6.2. The videos can be watched in the attached CD, using a common video player software, such as Windows Media Player (Microsoft).

Figure 3.31 shows the structures visible in the videos, to which only pneumolysin (video A) or pneumolysin pre-incubated with SM14 (video B) were added.

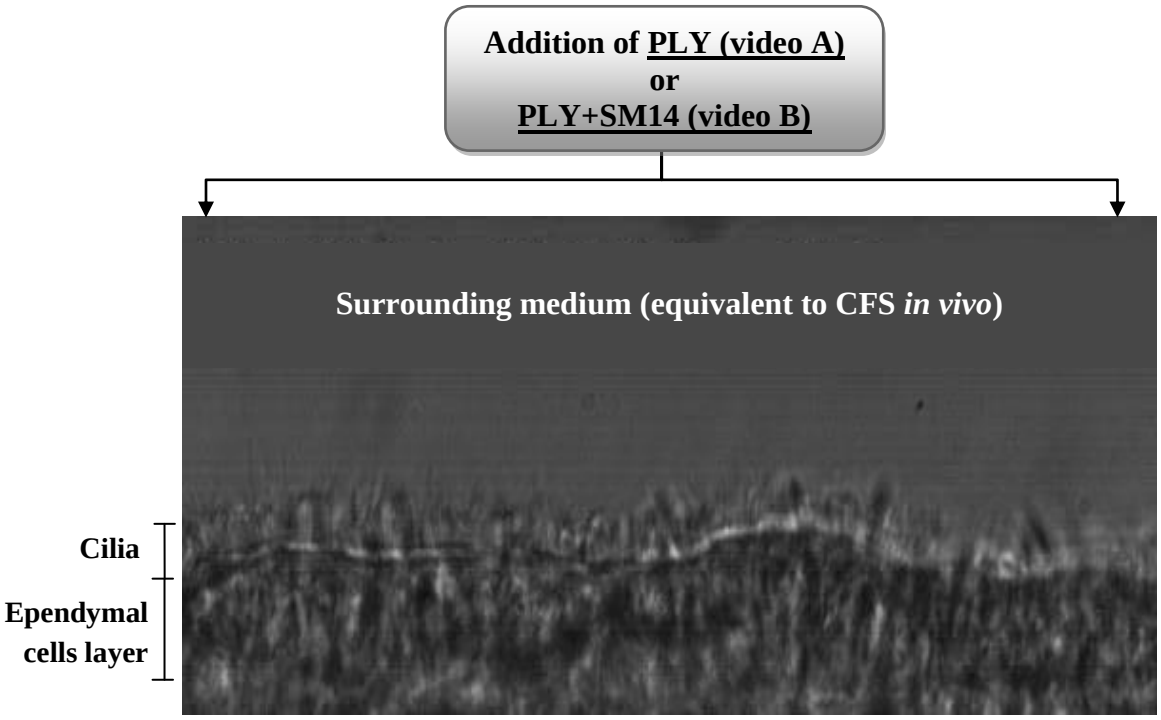

Figure 3.31 – The structures observed in the videos captured during the time course of the *ex vivo* experiments with rat brain slices.

In video A, pneumolysin was added to the cells approximately 2 seconds after the start of recording. The cilia beat normally at first but soon started to slow down eventually becoming completely static. This event was followed by disruption of the ependymal cells layer, demonstrated by the cytoplasmic extrusion that occurred on the top of the cells.

A different scenario was observed in video B. Here the same concentration of pneumolysin was pre-incubated with SM14. This was added to the cells, around the same time as in video A. However, no changes on the CBF can be observed. The cilia beat normally, generating a flow of medium and debris in the adjacent areas.

3.3. Preliminary studies for the understanding of the mode of action of the small molecules

3.3.1. Preliminary studies involving calcein-containing liposomes

In this study liposomes containing the fluorescent dye calcein were used, as earlier described in section 2.11.2. Pneumolysin on its own or pre-incubated with two different concentrations of small molecule SM9 were added to liposome suspensions, and the fluorescence was measured over time. The fluorometric measurements obtained with SM9 are shown in Figure 3.32.

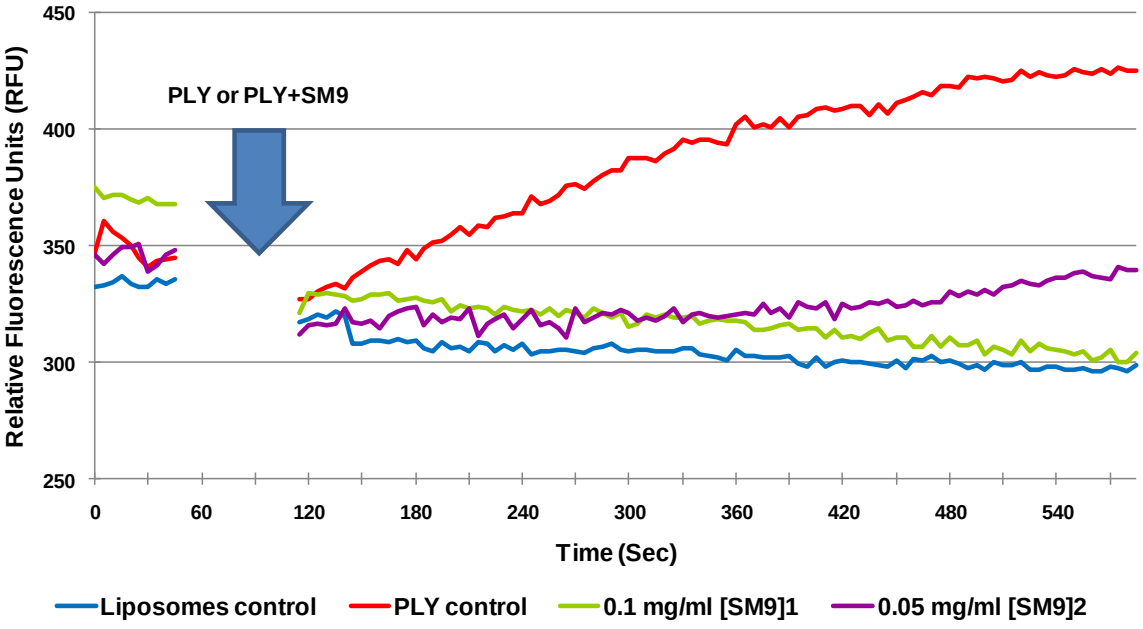

Figure 3.32 – Detection of calcein release from liposomes exposed to pneumolysin (PLY) pre-incubated or not with small molecule SM9. Graph representative of two experiments.

As expected, there was an increase in the fluorescence in to the presence of the toxin (Figure 3.32; PLY control; red line), whereas in the control containing only liposomes (Figure 3.32; blue line) the fluorescence remained constant. Most importantly, the release of calcein in the presence of PLY was prevented by incubation of the toxin with SM9 (Figure 3.32; green and purple lines). It was also possible to observe a dose response to SM9, because when the concentration of compound was decreased by half, the release of calcein increased.

When the readings were completed, the contents of each well were centrifuged. The resultant pellets and supernatants were used in immunoblotting assays. The results for this procedure are shown in Figure 3.33.

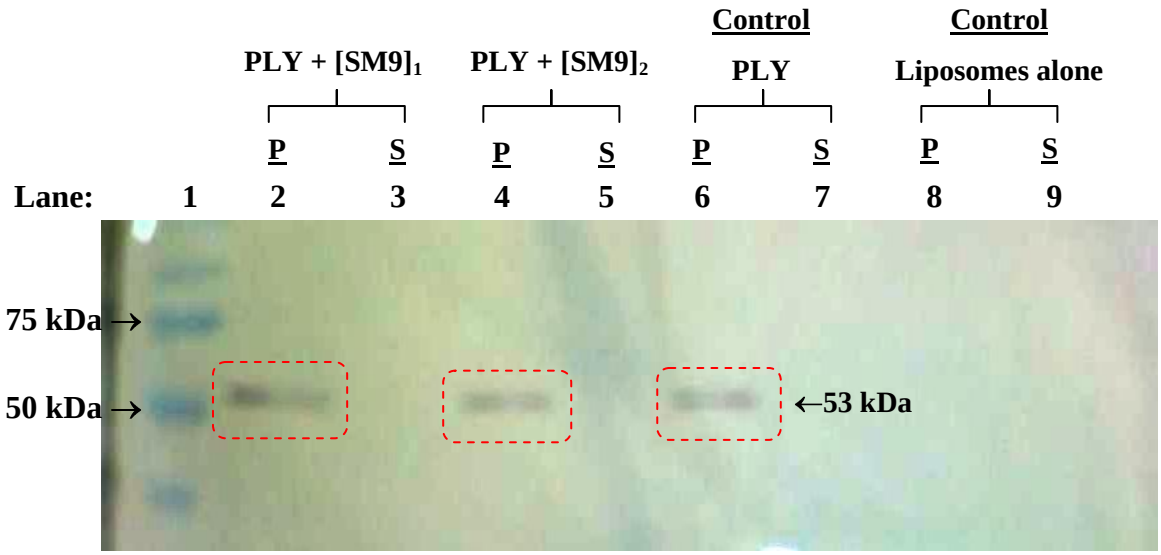

Figure 3.33- Immunoblot analysis of the liposomes samples collected from the previous stage (Figure 3.32), using the mouse anti-pneumolysin monoclonal antibody PLY4 followed by alkaline conjugated secondary antibody. Lane 1: Molecular size marker; Lanes 2 and 3: pellet (P) and supernatant (S) obtained from exposure to PLY plus 0.1 mg/ml SM9; Lanes 4 and 5: pellet (P) and supernatant (S) obtained with 0.05 mg/ml SM9; Lanes 6 and 7: pellet (P) and supernatant (S) obtained with the pneumolysin control; Lanes 8 and 9: pellet (P) and supernatant (S) obtained with the liposome control.

From analysis of the immunoblot, it is possible to detect the presence of bands with an approximate size of 53 kDa, in the pellets of the control with pneumolysin and of the groups that included SM9. Similar observations were found during the analysis of another immunoblot, containing the same type of samples but using the small molecule SM14 (Figure 3.34 and Figure 3.35).

Given that the size of the bands present in the pellets corresponds to the size of the toxin, the observations suggest that these small molecules (SM9 and SM10) in particular, do not affect the binding of pneumolysin to the membranes. It is possible then, that they may be acting at the level of the process of oligomerisation or insertion of the toxin oligomers into the membranes.

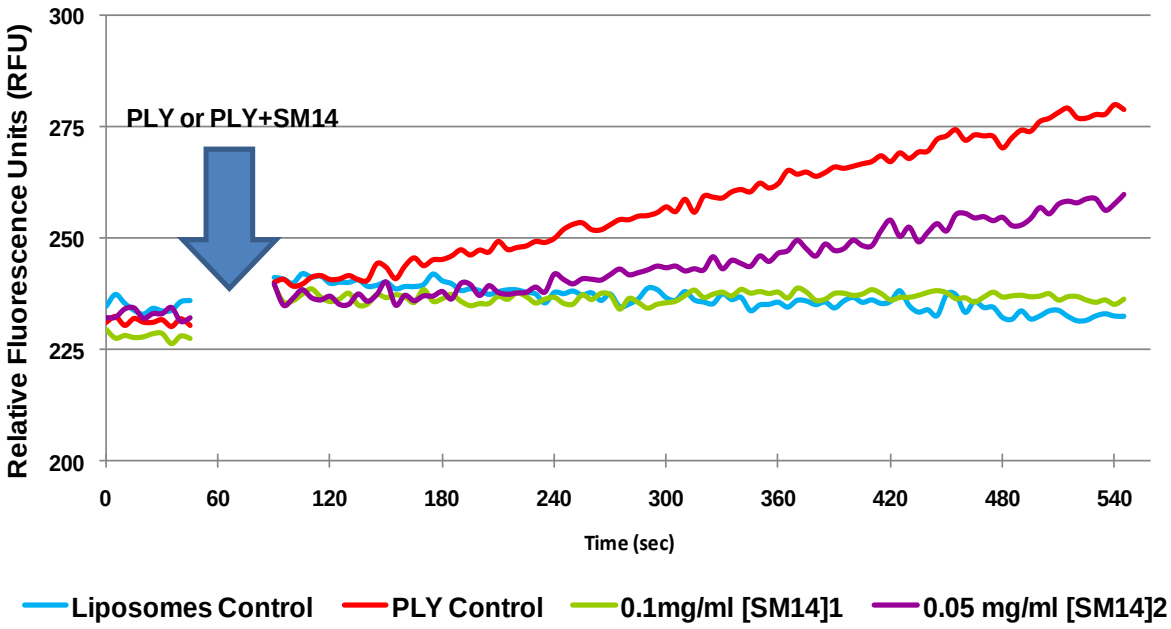

Figure 3.34 - Detection of calcein release from liposomes exposed to pneumolysin (PLY) pre-incubated or not with small molecule SM14. Graph representative of two experiments.

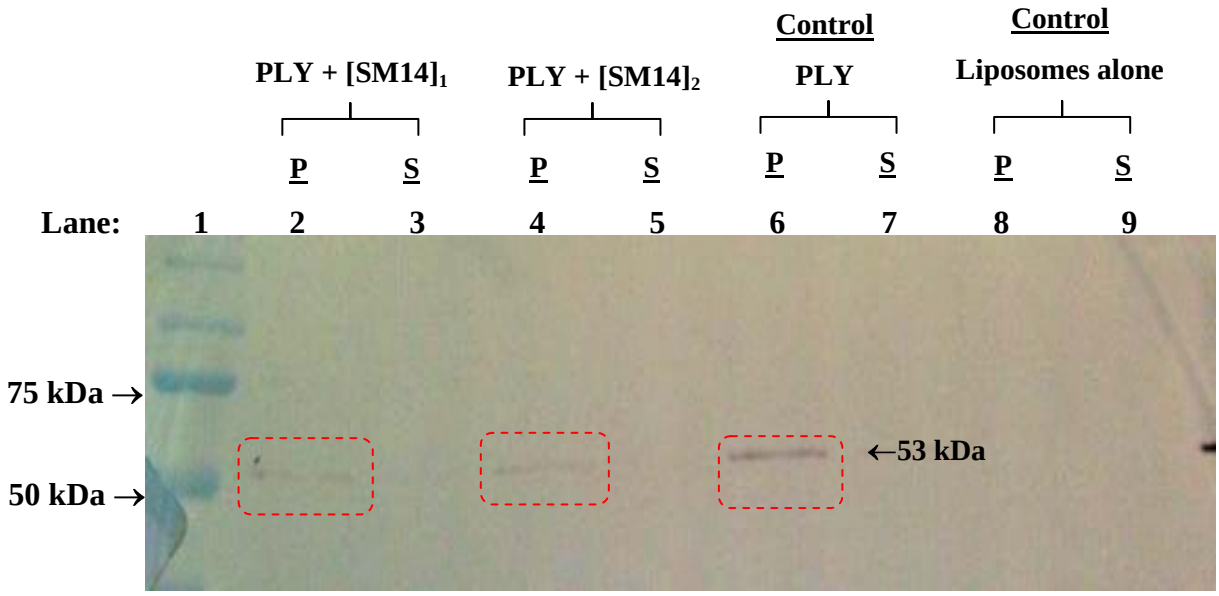

Figure 3.35 - Immunoblot analysis of the liposomes samples collected from the previsous stage (Figure 3.34), using the mouse anti-pneumolysin monoclonal antibody PLY4 followed by alkaline conjugated secondary antibody. Lane 1: Molecular size marker; Lanes 2 and 3: pellet (P) and supernatant (S) obtained from exposure to PLY plus 0.1 mg/ml SM14; Lanes 4 and 5: pellet (P) and supernatant (S) obtained with 0.05 mg/ml SM14; Lanes 6 and 7: pellet (P) and supernatant (S) obtained with the pneumolysin control; Lanes 8 and 9: pellet (P) and supernatant (S) obtained with the liposome control.

3.3.2. Fusion of *pneumolysin* gene with a gene for an enhanced green fluorescent protein (GFP) from *Aequorea coerulescens*

The fusion of pneumolysin gene with a gene for an enhanced green fluorescent protein was developed with the ultimate aim of transferring of the resulting DNA construct into *Streptococcus pneumoniae*. This attempt would, at least in theory, allow following in real time the involvement of pneumolysin on the progress pneumococcal infection during *in vivo* experiments.

3.3.2.1. Summary of the strategies applied

In this work the ply gene was cloned from the plasmid pKK-ply into a vector harbouring a gene for an enhanced GFP, the pAcGFP1-C In-Fusion Ready (Table 2.3) to give plasmid pMD1. The recombinant vector was then transformed into provided Fusion-BlueTM competent cells (Table 2.4), by heat-pulse transformation. The cells were plated on Luria-Agar plates with kanamycin, to select transformants. After an overnight incubation at 37ºC, colonies were picked and the success of the cloning step was determined by colony PCR screening. The plasmid pMD1 was isolated, by miniprep method, using available commercial kits. Afterwards, the resultant fused product gfp-ply was subcloned into a highly inducible bacterial expression plasmid, the In-fusion Ready pEcoli-Nterm 6xHN (Table 2.3). The plasmid obtained was named pMD2. Transformants were selected on Luria-Agar plates with ampicillin. Plasmid pMD2 was isolated from one transformant and transformed into *E. coli* BL21-Gold (DE3)pLysS chemically competent cells (Table 2.4). The selection of transformants was done on Luria-Agar plates with Ampicillin. The transformed cells were induced with IPTG and then lysed to produce a crude cell extract. An overview of this work is shown on Figure 3.36.

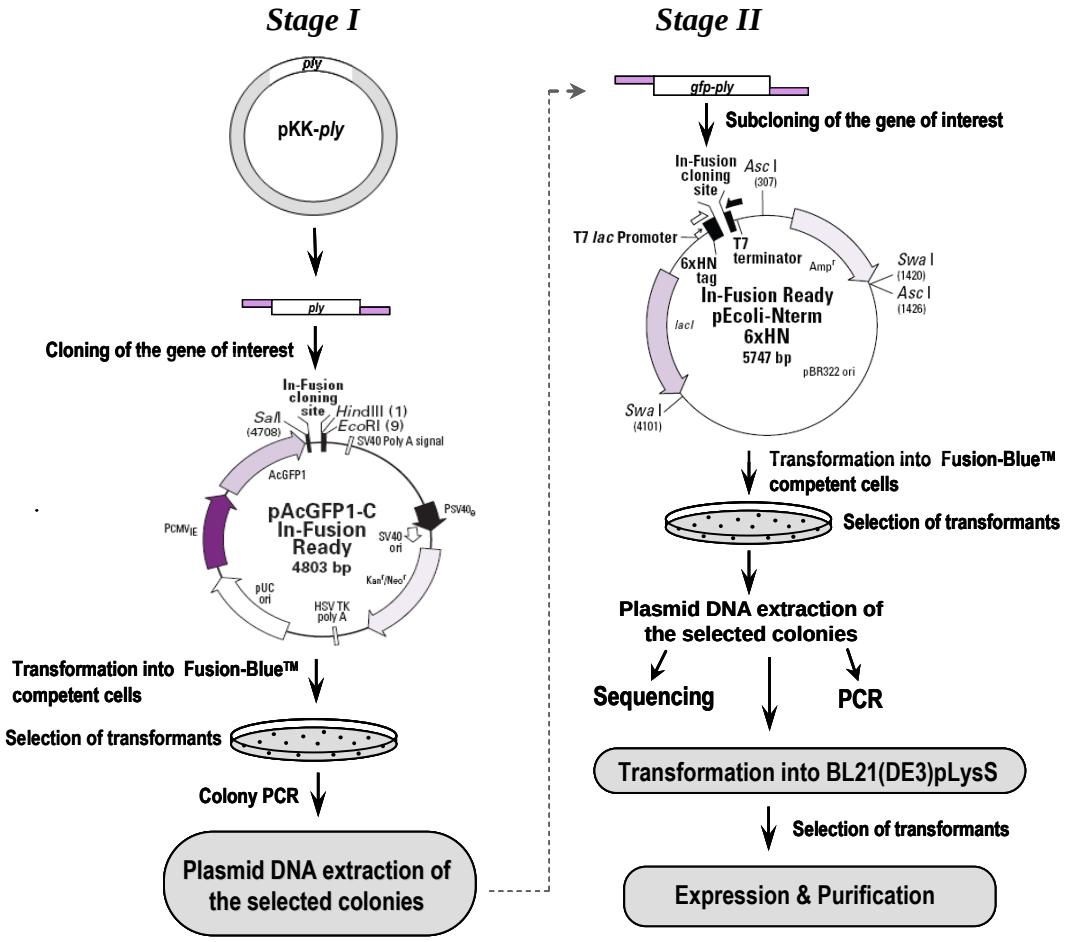

Figure 3.36 - Overview of the strategy applied in the fusion of the *ply* gene with the *gfp* gene.

3.3.2.2. Primer design

The cloning vectors pAcGFP1-C In-Fusion Ready and In-fusion Ready pEcoli-Nterm 6xHN were supplied pre-digested with *Sal I* and *Hind III*. This allowed the direct cloning of the PCR products in frame with the vector, with no need for extra restriction digestion. For the PCR, specific primers (Table 2.5) were designed according to the manufacturer's recommendation, comprising of 5' overhangs sharing 15 bases of sequence homology with the cloning vector on either site of insertion, and a 24-base sequence corresponding to the gene of interest.

3.3.2.3. Cloning of the *ply* gene into pAcGFP1-C In-Fusion Ready

The amplified *ply* gene (≈1.5 kb) with 5' overhangs was cloned into pAcGFP1-C In-Fusion Ready and transformed into Fusion-Blue™ competent cells, as described in sections 2.6.6 and 2.6.7.1, respectively. Six randomly selected colonies were screened by colony PCR (section 2.6.3), using specific primers to *ply* (Table 2.5), and analysed on a 0.9% (w/v) agarose gel. As shown in Figure 3.37, in four of the colonies the size of the single DNA fragments obtained was approximately 1.5 Kb, which corresponds to the size of *ply* gene.

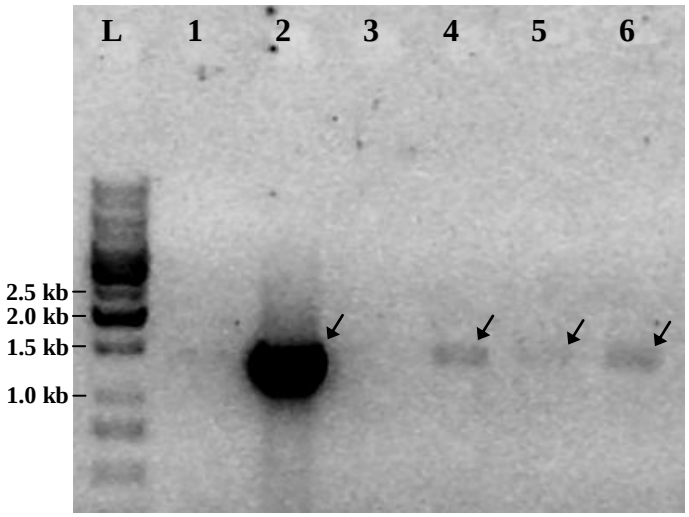

Figure 3.37 – Confirmation of the transformantion of *E. coli* competent cells with pAcGFP1-C vector harbouring *ply*, by colony PCR ($T_{annealing}$= 65ºC). The amplified bands (indicated by arrows) are approximately 1.5 kb. L: 1kb DNA ladder; Lane 1-6: PCR products from colonies 1-6.

The plasmid pMD1 extracted from colonies 2, 4 and 6 was amplified using the specific primers for *gfp-ply* (Table 2.5) and analysed on an 0.9% (w/v) agarose gel (Figure 3.38). As expected, the amplified bands were approximately 2.2 kb, corresponding to the size of the fusion product *gfp-ply* (700 bp_{gfp} + 1500 bp_{ply}). One plasmid was selected and named pMD1.

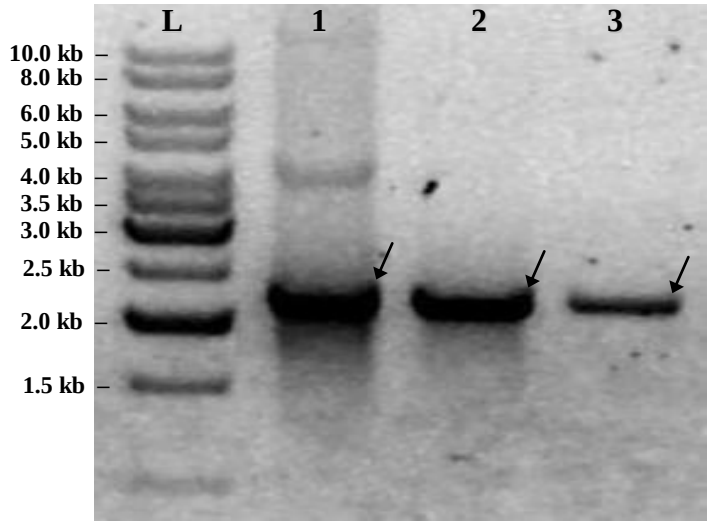

Figure 3.38 - Purified PCR products from selected *E. coli* transformants ($T_{annealing}$= 68ºC). The amplified bands (indicated by arrows) are at approximately 2.2 kb. L: 1kb DNA ladder; Lane 1-3: purified PCR products of plasmid DNA extracted from colonies 2, 4 and 6.

3.3.2.4. Subcloning of *gfp-ply* gene into the vector In-fusion Ready pEcoli-Nterm 6xHN

As the vector pAcGFP1-C In-Fusion Ready is only suitable for protein expression in mammalian cells, the amplified DNA products from colonies 4 and 6 (Figure 3.38), containing 5' overhangs, were subcloned into a vector suitable for protein expression in bacterial cells, the In-fusion Ready pEcoli-Nterm 6xHN, and transformed into Fusion-Blue™ competent cells. The plasmid DNA isolated from twelve randomly selected transformants was screened for the presence of *gfp-ply* insert by PCR (section 2.6.2). Nine clones were positive for *gfp-ply* fusion gene, as they contained a 2.2 kb insert (Figure 3.39). The plasmid DNA isolated from colony 12 was sent for sequencing by MWG. The sequence obtained was compared with the wild-type *gfp-ply* gene, using the BLASTN 2.2.21+ algorithm (NCBI - National Centre for Biotechnology Information).

The cloned sequence shared 100% identity with the published sequence (Figure A. 1 in Appendix).

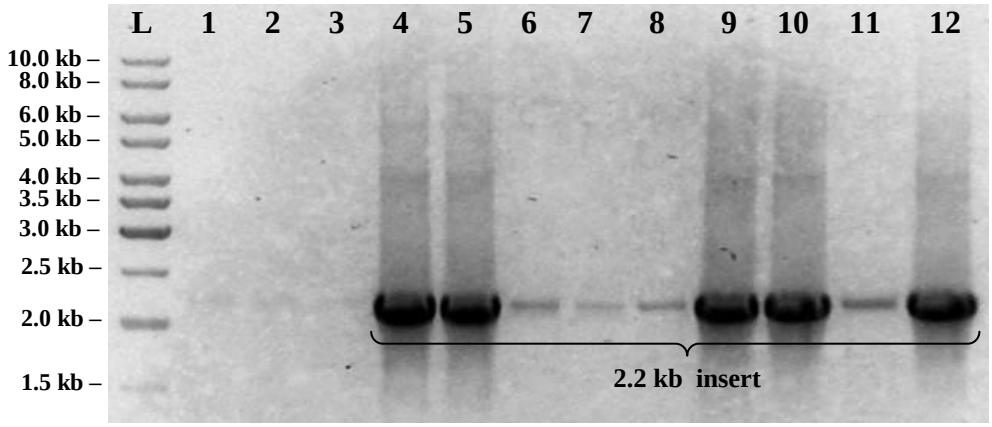

Figure 3.39 - PCR confirmation ($T_{annealing}$= 68ºC) of the transformation of *E. coli* competent cells with the pEcoli-Nterm 6xHN vector carrying the fusion product *gfp-ply*. The amplified DNA fragments are at approximately 2.2 kb. L: 1kb DNA ladder; Lane 1-12: purified PCR products of plasmid DNA extracted from colonies 1-12 selected from LA + ampicillin plates.

The DNA construct isolated from colony 12 and with confirmed *gfp-ply* insert was transformed into *E. coli* BL21-Gold (DE3)pLysS chemically competent cells (Table 2.4) for further protein expression and purification. The plasmid was named pMD2.

3.3.2.5. Expression and activity studies of the purified recombinant fusion protein GFP-PLY

The expression of the His-tagged GFP-PLY by the BL21-Gold (DE3)pLysS transformants was induced as described in section 2.8.2. The crude extract obtained from the bacterial sonicates was confirmed as being haemolytic (data not shown), indicating the expression of the fusion protein. The crude extract was used for purification using Ni^{2+} affinity chromatography (section 2.8.4). The collected fractions

were analysed by Western blotting using the anti-pneumolysin monoclonal antibody PLY4 (section 2.9.3). The immunoblot (Figure 3.40) revealed the presence of a band in each of the purified fractions (Lane 1-4) with an approximate molecular size of 80 kDa, corresponding to the expected size of the His-tagged fusion protein. In addition, the detection of other bands with higher molecular size suggests the formation of protein aggregates.

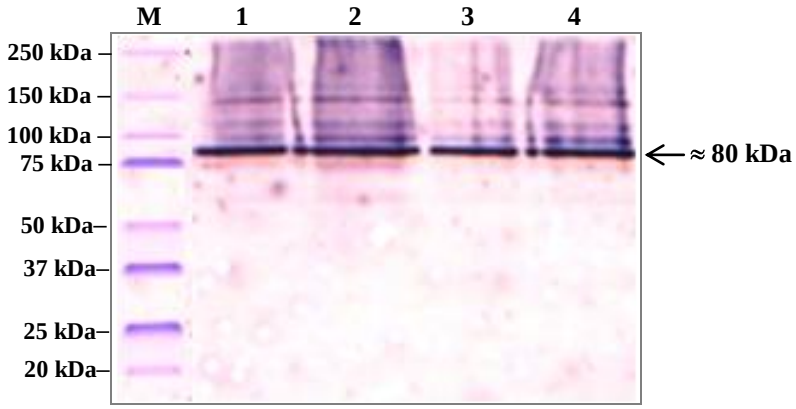

Figure 3.40 – Immunoblot analysis of the purified fractions of GFP_PLY with the mouse anti-pneumolysin monoclonal antibody PLY4 followed by alkaline conjugated secondary antibody. M: Molecular size marker; Lane 1-4: purification fractions 1-4.

The activity of the GFP_PLY present in the purified fractions was assessed by means of a haemolytic assay and fluorometric measurements. In Figure 3.41 it is possible to observe haemolysis pattern in the four fractions (rows F1-F4), with most activity in fraction 2 corresponding to 20480 HU/ml (22022 HU/mg).

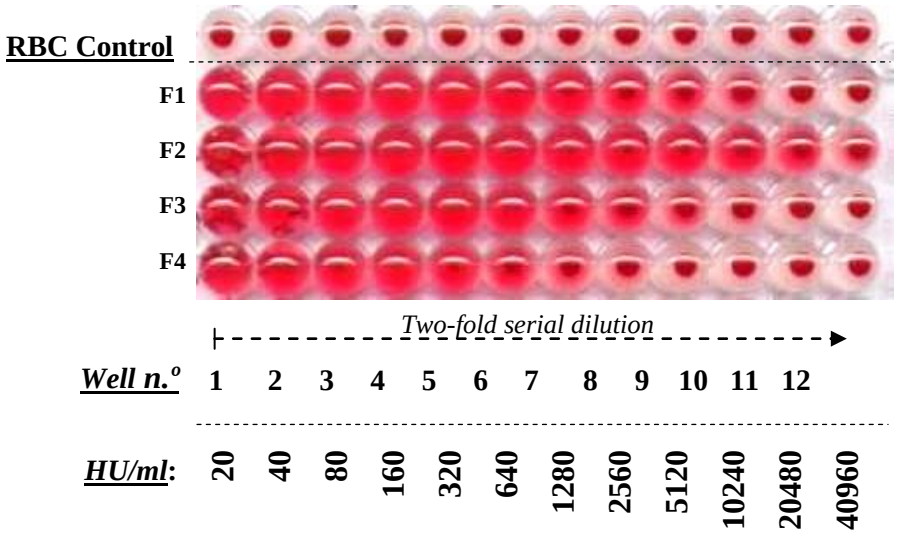

Figure 3.41 – Haemolytic assay of the purification fractions for the fusion protein GFP-PLY. F1-F4: fractions 1-4; RBC control: Sheep red blood cells in PBS (no haemolysis).

Fraction 2 was used in comparative fluorometric measurements of the recombinant fusion protein with recombinant wild-type pneumolysin. For this, solutions of both proteins, at 0.02 mg/ml, were prepared in triplicate and their fluorescence measured in a spectral scanning multimode reader (Varioskan Flash; Thermo Electron Corporation) with an excitation wavelength of 475 nm and emission wavelength of 505 nm. In Figure 3.42 it can be seen that the fluorescence intensity of the samples containing the fusion protein GFP-PLY is significantly higher ($p < 0.05$) than the fluorescence intensity of the samples containing wild-type pneumolysin, confirming the expression of an active GFP domain.

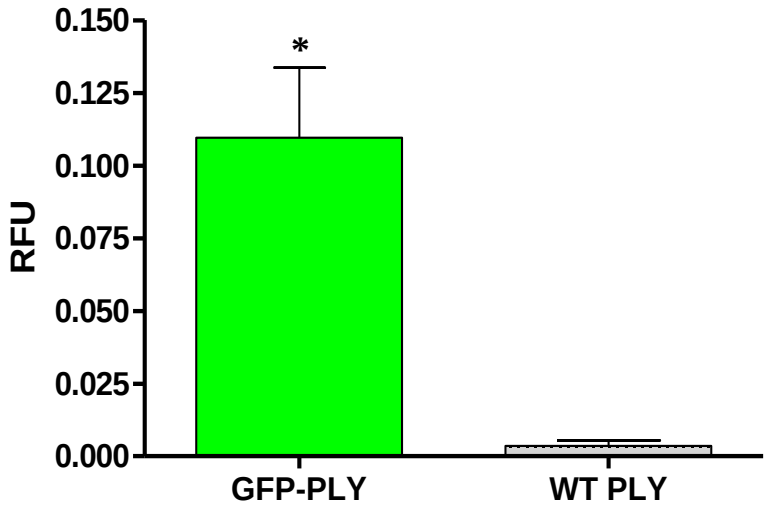

Figure 3.42 - Fluorometric intensity ($\lambda_{Excitation}$= 475 nm/ $\lambda_{Emission}$=505nm) of a purified fraction containing the recombinant fusion product GFP-PLY and recombinant wild-type PLY. Graphs show means ± SD; *, $p < 0.05$ between GFP-PLY and PLY (n = 3). RFU: relative fluorescence units.

Chapter 4 - Discussion

4.1. Target validation

Evidence obtained from different animal infection studies (Berry *et al.*, 1989; Benton *et al.*, 1995; Canvin *et al.*, 1995; Hirst *et al.*, 2008), demonstrating that pneumolysin plays a vital role in the pathogenesis of invasive pneumococcal diseases, have contributed to the recognition of its potential as a target for new adjunctive therapy for delivery with antibiotics (Hirst *et al.*, 2004b; Cockeran *et al.*, 2005).

Using pneumolysin as a target has two potential advantages. The immunosuppressive properties of dexamethasone have been associated with impairment of the ability of the body to fight infection, which may be even more aggravated if an appropriate antibiotic is not chosen (Feldman, 1992; Manson *et al.*, 2009). Therefore, anti-pneumolysin therapy may prove to be safer and more effective than corticosteroids because of its high specificity, which means if administered to patients suffering from non-pneumococcal disease, there is likely to be no adverse effects. Second, efficacy of the treatment is likely to be enhanced because anti-pneumolysin therapy will not only decrease the host inflammatory response induced by toxin, but it also will neutralise the direct toxicity of pneumolysin.

In this work, peptides and small molecules able to inhibit pneumolysin activity have been identified. The future development of these peptides and small molecules and their use as adjunctive therapies, would potentially lead to a considerable reduction in mortality and long term disabilities in severe cases of pneumococcal diseases.

4.2. Anti-pneumolysin peptides

Data presented in section 3.1.1 indicate that, by using random peptide libraries of different lengths and levels of constraint, it is possible to obtain peptides specifically binding to pneumolysin. Interestingly, the amino acid sequences of the isolated peptides differed from each other, with apparent even representation of all the twenty amino acids (with the exception of the invariant cysteine residues introduced in order to create a collection of disulphide constrained loops of different size), and no discernible consensus amino acid sequence. Such result likely reflects the ability of random peptide libraries to provide structural diversity for binding of ligands to different parts of pneumolysin.

When tested *in vitro*, only four (P1, P2, P5 and P6) out of the twenty binding-peptides demonstrated the ability to inhibit the haemolytic activity of the pneumolysin. Curiously, all four peptides inhibited haemolysis at the exact same low micromolar concentrations. The results obtained somewhat suggested that these peptides may share some sort of similarity, which would promote their binding to a common motif in pneumolysin structure, causing inhibition to the same extent. However, when a multiple alignment of the sequences was made using ClustalW program (Thompson *et al.*, 1994), only a maximum of 25% identity was displayed (sequence alignments of P1 with P2, and P1 with P6). Since it is rare for two aligned sequences to share 100% identity, many researchers use a 30-40% score as a significant level of identity (Smith, 2005). This threshold is usually relevant to proteins, but had been previously applied in the case of small peptide mimics (Smith, 2005). Based on this threshold, the level of similarity shared by the amino acid sequences of the inhibitory peptides from this study is not significant. It is possible, then, that these peptides inhibit pneumolysin via a small binding motif. It would be interesting to run the same experiments performed with the

inhibitory small molecules (section 2.11), in order to learn a little bit more about the mode of action of these peptides.

Two of the inhibitory peptides (P5 and P6) demonstrated antimicrobial activity against the wild-type *S. pneumoniae* strain D39. Over the last fifty years there have been several publications describing a variety of peptide antibiotics (Perlman & Bodanszky, 1971; Rodriguez-Tudela *et al.*, 1992; Hancock & Chapple, 1999; Zhang *et al.*, 2000b; Cherkasov *et al.*, 2009). In general, antimicrobial peptides have two to nine positively charged amino acids (arginine or lysine), which are thought to promote interaction between antimicrobial peptides and bacterial outer and cytoplasmic membranes (Hancock & Chapple, 1999). Looking at the primary amino acid sequence of the peptides P5 and P6, it is possible to notice the presence of two or more positively charged amino acids (i.e. arginine or lysine), conferring net charges (at neutral pH) of +2.0 and +3.0. These observations suggest that the peptides are cationic in nature, which could be a possible explanation for their antimicrobial properties. On the other hand, all the other peptides tested *in vitro* have inferior net charges, with the exception of peptide P3 whose net charge is +2.0. Despite P5 and P3 having equal net charges, P3 did not exerted *in vitro* antimicrobial activity, which may be associated with the fact that P3 primary amino acid sequence has a different level of constraint (presence of more than two cysteine residues). This confers peptide P3 a different conformational arrangement, which is a characteristic known to influence the antimicrobial activity of peptides (Brogden, 2005). Rodriguez-Tudela et al. had previously described four peptides antibiotics with *in vitro* activity against penicillin-resistant *S. pneumoniae* isolated from cerebrospinal fluid (Rodriguez-Tudela *et al.*, 1992). Although those peptides were effective as antimicrobial agents, there was no additional information that they could also target pneumolysin. Therefore, it seems interesting to further investigate the

potential of peptides P5 and P6 as both antimicrobial agents against the pneumococcus and as adjunctive therapies to address the cytoxicity induced by the release of pneumolysin.

Only one of the four peptides (P1) tested in a mouse pneumonia model, gave protection against the pneumococcal infection. Similar outcome had been previously reported in other study, where the treatment of mice with anti-pneumolysin monoclonal antibodies (PLY-4, PLY-5 and PLY-7 on their own or combined), prior to infection with *S. pneumoniae*, provided protection against pneumococcal pneumonia, which was shown by the significant increase in the survival times and survival rates of the treated mice with respect to those in the control group (Del Mar Garcia-Suarez *et al.*, 2004). Similarly to the data obtained with peptide P1, the combined administration of these monoclonal antibodies was also associated with a decrease of the invasion of pneumococci into the blood. Therefore, P1 could be a candidate to further testing in drug discovery. Although the remaining peptides may have not passed the *in vivo* screening with this particular model and design, it may be worth testing them in other infectious disease models (i.e. bacteraemia and/or meningitis model) or with other experimental designs, to further explore their potential therapeutic effect in a different set-up.

The pros and cons of selecting peptides as lead candidates for drug discovery will be further discussed in section 4.4.

4.3. Anti-pneumolysin small molecules

4.3.1. Identification and testing of inhibitory small molecules

The evolution in the medicinal chemistry approaches observed in the last decade, mostly driven by automation of processes, has allowed rapid high-throughput screens of large number of compounds against defined targets (Cho & Juliano, 1996; Abou-Gharbia, 2009). The application of this automated process in the screening of 16000 library compounds, gave a rapid identification of forty five small molecules with inhibitory properties against the cytolytic activity of pneumolysin. Thirty of these small molecules were, however, provisionally excluded from the study as they were likely to be inhibitors of cysteine. A possible way to investigate if these thirty molecules had acted exclusively as cysteine inhibitors would have been to assess their ability to neutralise the haemolytic activity of pneumolysin Cys428Ala, a mutant generated by the replacement of cysteine by alanine but with unaltered haemolytic activity (Saunders *et al.*, 1989). The compounds that showed activity to neutralise the modified toxin, would have proved that the initial assumption was wrong and, therefore, could have been re-introduced into the study. However, due to the considerable number of other compounds available to test and to the limited time-schedule of the project, this assessment was never performed.

The fourteen small molecules considered of interest for drug discovery were tested *in vitro* for determination of potency. Most of the compounds were highly potent, exhibiting IC_{50} values in the low micromolar range. Interestingly, the same range of values has been reported in other studies involving the screening and identification of potent inhibitory small molecules against other protein toxins, such as the lethal toxin from *Bacillus anthracis* (Schepetkin *et al.*, 2006; Chen *et al.*, 2008; Johnson *et al.*, 1980) and the exoenzyme S from *Pseudomonas aeruginosa* (Arnoldo *et al.*, 2008).

Three out of six small molecules (SM6, SM10 and SM14) tested in a mouse pneumococcal pneumonia model, demonstrated enhanced protection *in vivo* against the pneumococcal infection. Similar results were found by a collaborator, Dr. Marco Oggioni (University of Siena), when testing the same compounds in a mouse pneumococcal bacteraemia model (unpublished data). This finding provided a line of evidence supporting the efficacy of these small molecules *in vivo*. In a different experiment, Oggioni and colleagues also observed that the survival rates of mice treated with a small molecule (SM10), after intravenous challenge with wild-type pneumococcal strain D39, followed the same pattern of the survival rates of the group infected with the pneumolysin mutant strain PLN-A, in the absence of treatment (unpublished data). This result seems to be consistent with the experimental outcome from an earlier study, where the intranasal and intravenous challenge of mice with PLN-A had shown reduced virulence, accompanied by an significant increase in the survival times and survival rates with respect to the mice infected with the wild-type pneumococcal strain D39 (Berry *et al.*, 1989). This suggests that the therapeutic effect in pneumococcal disease observed *in vivo* during the present study is due to the inhibitory activity of the small molecules against pneumolysin.

The small molecules SM10 and SM14 were later used in an *ex vivo* model, to verify the potential beneficial effect of using these small molecules as an auxiliary therapy in cases of pneumococcal meningitis. Again, SM10 and SM14 demonstrated the ability to inhibit pneumolysin activity, this time on the ciliary function of ependymal cells. Similar outcome was observed in a previous study (Hirst *et al.*, 2004b) where ependymal ciliary stasis caused by pneumolysin was blocked by the use of anti-pneumolysin monoclonal antibodies (De Los Toyos *et al.*, 1996). As in the case of the *ex vivo* work with the small molecules SM10 and SM14, the use of anti-pneumolysin

monoclonal antibodies in the latter study helped to maintain the ependymal ciliary beating frequency unchanged ($p>0.05$) in comparison to the control group (not exposed to pneumolysin), and it also prevented cellular damage induced by the toxin.

4.3.2. Pharmacokinetics

The experiments undertaken to determine the pharmacokinetic profiling of the small molecules SM10 and SM14 revealed it was not possible to detect their presence in the plasma of mice, even shortly after intravenous or oral administrations. Since the small molecules demonstrated *in vitro*, *in vivo* and *ex vivo* efficacy, these findings suggest that they had been converted into pharmacologically active metabolites. In drug discovery these kind of compounds are referred to as bioprecursor prodrugs, inactive chemical entities which upon a metabolic (e.g. enzymatic) or chemical (e.g. oxidation, reduction) transformation by a mammalian system, are converted into active agents (Rautio *et al.*, 2008). An example of these prodrugs is Nabumetone (Relafen), a non-steroid drug used in the management of the pain and inflammation caused by arthritis, which after being absorbed at the gastrointestinal tract undergoes rapid oxidative transformation to the active metabolite and, therefore, is not detectable in the human plasma in its parental form (RxList Inc., 2007). It would be interesting to further investigate the hypothesis that SM10 and SM14 had been converted into active metabolites. The application of biotinylation methods (Gustavson *et al.*, 1994) for the labelling of these small molecules would constitute a possible way for the detection of active substances. Theoretically, if a biotin-labelled active metabolite was formed (provided the biotin was not attached to the cleavage site or to the active site of the small molecule), it would be possible to detect and quantify its presence in the plasma of the animals, using anti-biotin antibodies in ELISA assays. Alternatively, high performance liquid chromatography

coupled to mass spectrometry could represent a faster and, perhaps, a more efficient way for the profiling, identification and quantification of active metabolites in the plasma of mice, following the administration of the small molecules (Nicholson *et al.*, 2001; Castro-Perez, 2007).

Contrary to SM10 and SM14, SM9 was detected in the blood samples collected from mice as shortly as 5 minutes following to its administration either via oral or intravenous route. The difference between the times at which the concentration of SM9 detected in the plasma of mice reached its maximum, following oral and intravenous administrations, is associated with the fact that via i.v. route a drug, enters directly into the systemic circulation becoming immediately available, whereas after oral administration a drug must cross several semipermeable membranes and also survive potential detrimental conditions (e.g. low pH conditions in the stomach, enzymes present in gastrointestinal secretions), therefore taking more time until becoming available in the bloodstream (MERCK, 2007). Nevertheless, the 84% relative bioavailability of the SM9 via the oral route, suggests that the compound must had been well absorbed from the gastrointestinal tract. Approximately six hours after i.v. administration, and twelve hours after oral administration, SM9 was no longer detected in the plasma. These figures provide substantial information, which supports the 6 hours dose regime adopted in the experiments conducted *in vivo*.

4.3.3. *In vitro* antimicrobial activity of the small molecules SM5 and SM12

In the current study, in addition to the capacity to block pneumolysin's haemolytic activity, small molecules SM5 and SM12 showed an antimicrobial activity against Gram-positive bacteria, whereas with the Gram-negative species this activity was not observed. To confirm this was independent of inhibition of pneumolysin,

complementary *in vitro* tests were performed to assess their effect on the pneumolysin-negative mutant, PLN-A. PLN-A viability was also found to be compromised by SM5 and SM12 (data not shown).

As SM5 and SM12 seem to compromise the viability of Gram-positive bacteria rather than Gram-negative bacteria, one can speculate whether if these small molecules may be acting at the level of cell wall, more specifically, if these small molecules inhibit cell wall synthesis of Gram-positive bacteria in a similar way to vancomycin and penicillin (i.e. preventing cross-linking of cell wall peptidoglycan) (Lundstrom & Sobel, 2004). On the other hand, it is possible that SM5 and SM12, like macrolides, interfere with protein biosynthesis in Gram-positive bacteria. SM5 and SM12 have distinct chemical structures and do not share any structural similarities with other antimicrobial agents against Gram-positive bacteria that could have helped to explain the mechanism of action of these small molecules.

It would be interesting to further explore the apparent specificity of the small molecules with antimicrobial activity for Gram-positive bacteria by attempting to use them as an antimicrobial therapy that would at the same time prevent the damages induced by pneumolysin or perhaps, in the case of other species such as *C. Perfringens*, *S. pyogenes* and *S. aureus*, perfringolysin O, streptolysin O and α-toxin.

4.3.4. Preliminary experiments to understand the mode of action of small molecules

Preliminary functional studies were undertaken using calcein-containing liposomes, in order to begin to understand at what level the small molecules interfere with the activity of pneumolysin. The results obtained suggest that SM9 and SM14 do not affect the binding of the toxin to the membranes, as shown by the presence of pneumolysin in the

pellets the liposomes exposed to the toxin pre-incubated with small molecules. A similar result was observed in a previous study of anti-pneumolysin monoclonal antibodies (De Los Toyos *et al.*, 1996), where the monoclonal antibody PLY-4, despite having effectively neutralised the haemolytic activity of the toxin, did not affect the binding of pneumolysin to the erythrocytes. Instead it was found to block the assembly of pore structures in liposomes, indicating that PLY-4 may be interfering with the process of oligomerisation. Similarly, SM9 and SM14 must be acting at a further stage of the mechanism of pore formation, either by interfering with the i) process of oligomerisation, ii) unravelling of the α-helical bundles in domain 3 and/or insertion of the transmembrane β-hairpins into the membrane or iii) functioning of the pores formed (i.e. conductance). Also in the study by De Los Toyos et al., it was found that the pre-incubation of the toxin with two other monoclonal antibodies, PLY-5 and PLY-7, prevented binding of the toxin to the cells. In addition, analysis of the binding of the antibodies to two proteolytic fragments of the toxin (with the molecular sizes of approximately 15 kDa, comprising the N-terminus, and 37 kDa, comprehending the C-terminus) showed that PLY-5 and PLY-7 recognised two distinct regions of the C-terminus of pneumolysin. In contrast, PLY-4 recognised only the intact toxin, not recognising either of the fragments, which suggested that the neutralising eptitope recognised by PLY-4 was located within a region of proteolytic cleavage (between amino acid residues 142 and 143 of pneumolysin), distant of the C-terminus. Given that SM9 and SM14 do not seem to affect binding, and that the recognition of the C-terminal of the toxin by PLY-5 and PLY-7 appeared to affect the binding to the cells, one can speculate whether the small molecules SM9 and SM14 may be acting on a motif distant from the C-terminus of pneumolysin.

The results of these preliminary studies with SM9 and SM14 were interesting but not conclusive. It would be important to further test SM9 and SM14 to determine which further stage of the mechanism of pore assembly (i.e. oligomerisation or membrane insertion) or functioning of pores they inhibit. A possible way to find out if these compounds interfere with the process of oligomerisation would be to repeat the experiments with liposomes (section 2.11.1) but using SDS-agarose gel electrophoresis instead to allow separation and detection of high molecular-weight oligomeric complexes potentially formed. In addition, cryo-EM or atomic force microscopy could be employed to investigate the inhibition of the formation of transmembrane pore structures by these small molecules, in a similar way to that described in Tilley *et al.*, 2005 and Czajkowsky *et al.*, 2004, respectively. The patch clamp technique, as described in El-Rachkidy *et al.*, 2008, could be employed to evaluate the effect of the small molecules on the electrophysiological properties (i.e. conductance) of transmembrane channels formed by pneumolysin. It would also be interesting to learn about the location of the neutralising motifs on pneumolysin, where these small molecules act. A possible way of doing this would be to express isolated versions of pneumolysin's domains (e.g. domain 4), and investigate where do these small molecules bind. Alternatively, proteolytic fragments of pneumolysin (De Los Toyos *et al.*, 1996) could be used. It would be also interesting to extend the study to other small molecules (e.g. SM10).

Moreover, a fusion protein was constructed, consisting of pneumolysin fused to a monomeric green fluorescent protein (AcGFP1). As shown in section 3.3.2, the fusion of this monomeric fluorescent tag at the N-terminus of pneumolysin enabled the toxin to be monitored without compromising its activity. Due to time constrictions it was not possible to take this work into a next stage. Nevertheless, this fusion protein would be

particular useful in the understanding of the effect of the small molecules on the activity of pneumolysin when applied to fluorescent microscopy, using FRAP technique *in vitro* and/or, ultimately, *in vivo* imaging systems (Zacharakis *et al.*, 2005; Beckmann *et al.*, 2007; Mehta *et al.*, 2008) to evaluate, in real time, the therapeutic efficacy of the small molecules administered during infectious studies in animals.

4.4. Potential of small molecules, peptides or monoclonal antibodies as lead candidate for drug discovery

The ability of certain small molecules, peptides and monoclonal antibodies to inhibit pneumolysin activity has been described. Nevertheless, small molecules seem to have a stronger potential as lead candidates in drug discovery in comparison to macromolecular inhibitors such as recombinant peptides and monoclonal antibodies (Cho & Juliano, 1996). Recombinant peptides and monoclonal antibodies may be attractive candidates for drug development due to the specific activity that can, at least theoretically, be attained by their use, leading to lower side effects than conventional small molecule-based drugs (Cho & Juliano, 1996). Macromolecular drugs may be also attractive because of their characteristic short half-lives, meaning that they are more rapidly cleared by the body and, thus, less likely to form toxic metabolic by-products (Hummel *et al.*, 2006; Shire *et al.*, 2010). However, when a macromolecule is the lead candidate the direction of development is often towards small molecule mimics (Hummel *et al.*, 2006). One of the main reasons for this, are the high-costs associated with the synthesis of monoclonal antibody/peptide-based drugs (Cho & Juliano, 1996); Hummel *et al.*, 2006; Imai & Takaoka, 2006; Abcam, 2010). The expensive production costs are in turn reflected in the selling-price of these therapies, which constitutes an obstacle for their use even in Western countries. Another reason is the fact that small molecules, due to their characteristic low molecular weights, are more likely to easily

cross membrane barriers and so to access their targets (Cho & Juliano, 1996; Imai & Takaoka, 2006). Other major disadvantage of macromolecules is their low stability due to proteolytic degradation which reduces their availability in the body to exert therapeutic activity (Cho & Juliano, 1996; Soltero, 2005; Hummel *et al.*, 2006). Another issue regarding the use of macromolecules is that they are likely to elicit an immune response and consequently to attenuate the therapeutic benefit (Cho & Juliano, 1996). Small molecules offer a broad range of delivery routes, such as oral and parental administration, whereas antibodies and peptides, as they are easily degraded by proteases and pH of gastrointestinal secretions, are preferably delivered by injection (Soltero, 2005; Hummel *et al.*, 2006). This delivery route may be viable in the case of hospitalised patients but for out-patients oral delivery is a more practical option. In addition, in "developing countries", given the poor health-infrastructures, the scarce equipment resources (e.g. needles and syringes) and the high incidence of HIV and Hepatitis B cases among patients, oral administration of therapeutic drugs constitutes a more easy and convenient delivery route.

4.5. Prospective work

4.5.1. Welcome Trust's Seeding Drug Discovery Initiative award

The data obtained with the small molecules in this work, contributed to an award of £3.5 million funding, under the Welcome Trust's Seeding Drug Discovery Initiative. The project aims to deliver the preclinical development of small molecule-based drugs for application in clinical trials, as therapies adjunctive to the anti-microbial treatment of acute pneumococcal infections. This process will involve a programme of medicinal chemistry, wherein the identified lead compounds will undergo pharmacokinetic, pharmacodynamic and toxicology testing, either using cell-based systems or animal models.

4.5.2. Summary of proposed experiments to understand the mechanism of action of the identified pneumolysin inhibitors

Throughout this research project peptides and small molecules were identified, with the ability to inhibit pneumolysin activity *in vitro*, *in vivo* and, in the case of the small molecules, *ex vivo*. There are questions that, either due to time constrictions or lack of funding, remain unanswered*: the mechanism of interaction of the inhibitors with pneumolysin, the binding site and which stage of pore-formation do they interfere with. Are they also able to inhibit pneumolysin-induced production of cytokines? In which way do these inhibitors halt the progress of pneumococcal infection when tested in vivo?*

It would be interesting to learn about the location of the binding site of the inhibitors. A possible way to investigate this would have been to produce truncated versions of pneumolysin's domains, for example domain 4, or proteolytic fragments of the toxin and mix them with pneumolysin's inhibitors. The activity of the anti-pneumolysin peptides and small molecules could then have been reassessed by means of an *in vitro* inhibition of haemolysis' assay. In theory, if they had lost activity in the presence of a specific fragment or domain, one could infer that they will be exerting its activity by binding to the same corresponding motif on the whole pneumolysin. Alternatively, two other methods, isothermal titration calorimetry (ITC) or surface plasmon resonance (SPR), could have been used to study the biomolecular interactions of pneumolysin's inhibitors with the fragments or domains of the toxin.

It would also be important to further test these molecules to determine which further stage of the mechanism of pore assembly (i.e. binding, oligomerisation or membrane insertion) or functioning of pores they inhibit. A possible way would have been to repeat the experiments with liposomes (section 2.11.1) and, in the case of binding to

membranes was not affected, use SDS-agarose gel electrophoresis instead to allow separation and detection of high molecular-weight oligomeric complexes potentially formed. In addition, cryo-EM or atomic force microscopy could be employed to investigate the inhibition of the formation of transmembrane pore structures by these molecules, in a similar way to that described in Tilley *et al.*, 2005 and Czajkowsky *et al.*, 2004, respectively. The patch clamp technique, as described in El-Rachkidy *et al.*, 2008, could be employed to evaluate the effect of the pneumolysin's inhibitors on the electrophysiological properties (i.e. conductance) of transmembrane channels formed by pneumolysin.

It has been shown that pneumolysin stimulates the production of inflammatory cytokines, such as tumor necrosis factor alpha (TNF-α) and interleukin-1beta (IL-1β), by human monocytes (Houldsworth *et al.*, 1994). Therefore, it would be interesting to investigate the potential involvement of pneumolysin's inhibitors on the modulation of host immune response. For this, pneumolysin would have been pre-incubated with the peptide or small molecules and its ability to induce the production of TNF-α or IL-1β retested.

There are also *in vivo* studies that could be done in order to understand the mechanisms by which these molecules are able to improve the outcome of pneumococcal diseases. The fusion protein GFP-PLY (section 3.3.2) would be a useful approach in the understanding of the effect of the small molecules on the activity of pneumolysin when applied to fluorescent microscopy, using *in vivo* imaging systems to evaluate, in real time, the therapeutic efficacy of the small molecules administered during infectious studies in animals.

It is has been shown that the identified pneumolysin's inhibitors are capable of inhibiting the toxin's cytolytic activity *in vitro* and *ex vivo*. However, it is still unknown

whether these molecules, when administered *in vivo*, affect pneumolysin's cytolytic activity, complement activity or both. Using the derivative *Streptococcus pneumoniae* D39 mutant strain H+C- (Berry *et al.*, 1995) in an *in vivo* study with the anti-pneumolysin peptides or small molecules, would contribute to answer that. This strain carries a defined point mutation in the pneumolysin coding sequence, Asp385Asn, which results in the loss of the toxin's complement activity (C-), but with cytolytic activity intact (H+). Hence, if the anti-pneumolysin inhibitors had not provided protection against this mutant strain one could then assume that they play a key role in inhibiting the complement activation by pneumolysin.

Appendix

```
 *  126   ATGGTGAGCAAGGGCGCCGAGCTGTTCACCGGCATCGTGCCCATCCTGATCGAGCTGAAT  185
          ||||||||||||||||||||||||||||||||||||||||||||||||||||||||||||
**  1     ATGGTGAGCAAGGGCGCCGAGCTGTTCACCGGCATCGTGCCCATCCTGATCGAGCTGAAT  60

    186   GGCGATGTGAATGGCCACAAGTTCAGCGTGAGCGGCGAGGGCGAGGGCGATGCCACCTAC  245
          ||||||||||||||||||||||||||||||||||||||||||||||||||||||||||||
    61    GGCGATGTGAATGGCCACAAGTTCAGCGTGAGCGGCGAGGGCGAGGGCGATGCCACCTAC  120

    246   GGCAAGCTGACCCTGAAGTTCATCTGCACCACCGGCAAGCTGCCTGTGCCCTGGCCCACC  305
          ||||||||||||||||||||||||||||||||||||||||||||||||||||||||||||
    121   GGCAAGCTGACCCTGAAGTTCATCTGCACCACCGGCAAGCTGCCTGTGCCCTGGCCCACC  180

    306   CTGGTGACCACCCTGAGCTACGGCGTGCAGTGCTTCTCACGCTACCCCGATCACATGAAG  365
          ||||||||||||||||||||||||||||||||||||||||||||||||||||||||||||
    181   CTGGTGACCACCCTGAGCTACGGCGTGCAGTGCTTCTCACGCTACCCCGATCACATGAAG  240

    366   CAGCACGACTTCTTCAAGAGCGCCATGCCTGAGGGCTACATCCAGGAGCGCACCATCTTC  425
          ||||||||||||||||||||||||||||||||||||||||||||||||||||||||||||
    241   CAGCACGACTTCTTCAAGAGCGCCATGCCTGAGGGCTACATCCAGGAGCGCACCATCTTC  300

    426   TTCGAGGATGACGGCAACTACAAGTCGCGCGCCGAGGTGAAGTTCGAGGGCGATACCCTG  485
          ||||||||||||||||||||||||||||||||||||||||||||||||||||||||||||
    301   TTCGAGGATGACGGCAACTACAAGTCGCGCGCCGAGGTGAAGTTCGAGGGCGATACCCTG  360

    486   GTGAATCGCATCGAGCTGACCGGCACCGATTTCAAGGAGGATGGCAACATCCTGGGCAAT  545
          ||||||||||||||||||||||||||||||||||||||||||||||||||||||||||||
    361   GTGAATCGCATCGAGCTGACCGGCACCGATTTCAAGGAGGATGGCAACATCCTGGGCAAT  420

    546   AAGATGGAGTACAACTACAACGCCCACAATGTGTACATCATGACCGACAAGGCCAAGAAT  605
          ||||||||||||||||||||||||||||||||||||||||||||||||||||||||||||
    421   AAGATGGAGTACAACTACAACGCCCACAATGTGTACATCATGACCGACAAGGCCAAGAAT  480

    606   GGCATCAAGGTGAACTTCAAGATCCGCCACAACATCGAGGATGGCAGCGTGCAGCTGGCC  665
          ||||||||||||||||||||||||||||||||||||||||||||||||||||||||||||
    481   GGCATCAAGGTGAACTTCAAGATCCGCCACAACATCGAGGATGGCAGCGTGCAGCTGGCC  540

    666   GACCACTACCAGCAGAATACCCCCATCGGCGATGGCCCTGTGCTGCTGCCCGATAACCAC  725
          ||||||||||||||||||||||||||||||||||||||||||||||||||||||||||||
    541   GACCACTACCAGCAGAATACCCCCATCGGCGATGGCCCTGTGCTGCTGCCCGATAACCAC  600

    726   TACCTGTCCACCCAGAGCGCCCTGTCCAAGGACCCCAACGAGAAGCGCGATCACATGATC  785
          ||||||||||||||||||||||||||||||||||||||||||||||||||||||||||||
    601   TACCTGTCCACCCAGAGCGCCCTGTCCAAGGACCCCAACGAGAAGCGCGATCACATGATC  660

    786   TACTTCGGCTTCGTGACCGCCGCCGCCATCACCCACGGCATGGATGAGCTGTACAAGTCC  845
          ||||||||||||||||||||||||||||||||||||||||||||||||||||||||||||
    661   TACTTCGGCTTCGTGACCGCCGCCGCCATCACCCACGGCATGGATGAGCTGTACAAGTCC  720

    846   GGACTTAAGGCCTCTGTCGACATGGCAAATAAAGCAGTAAATGACTTTATACTAGCTATG  905
          ||||||||||||||||||||||||||||||||||||||||||||||||||||||||||||
    721   GGACTTAAGGCCTCTGTCGACATGGCAAATAAAGCAGTAAATGACTTTATACTAGCTATG  780

    906   AATTACGATAAAAAGAAACTCTTGACCCATCAGGGAGAAAGTATTGAAAATCGTTTCATC  965
          ||||||||||||||||||||||||||||||||||||||||||||||||||||||||||||
    781   AATTACGATAAAAAGAAACTCTTGACCCATCAGGGAGAAAGTATTGAAAATCGTTTCATC  840

    966   AAAGAGGGTAATCAGCTACCCGATGAGTTTGTTGTTATCGAAAGAAAGAAGCGGAGCTTG  1025
          ||||||||||||||||||||||||||||||||||||||||||||||||||||||||||||
    841   AAAGAGGGTAATCAGCTACCCGATGAGTTTGTTGTTATCGAAAGAAAGAAGCGGAGCTTG  900

    1026  TCGA  1029
          ||||
    901   TCGA  904
```

Figure A. 2 - BLAST alignment of the cloned nucleotide sequence from colony 12 with the nucleotide sequence of wild-type *gfp-ply*. In red is represented the initial part of *ply* sequence. **gfp-ply* cloned sequence (colony 12); ***gfp-ply* wild-type sequence

Bibliography

Abcam, 2010. *Polyclonal and monoclonal: A comparison | Abcam.* [online]. Available at: http://www.abcam.com/index.html?pageconfig=resource&rid=11269&pid=11287 [2010].

Abou-Gharbia, M., 2009. Discovery of innovative small molecule therapeutics. *Journal of medicinal chemistry.* **52,** 2-9.

Afessa, B., Greaves, W.L., Frederick, W.R., 1995. Pneumococcal bacteremia in adults: A 14-year experience in an inner-city university hospital. *Clinical Infectious Diseases.* **21,** 345-351.

Alexander, J.E., Lock, R.A., Peeters, C.C.A.M., Poolman, J.T., Andrew, P.W., Mitchell, T.J., Hansman, D., Paton, J.C., 1994. Immunization of mice with pneumolysin toxoid confers a significant degree of protection against at least nine serotypes of Streptococcus pneumoniae. *Infection and immunity.* **62,** 5683-5688.

Alonso de Velasco, E., Verheul, A.F.M., Verhoef, J., Snippe, H., 1995. Streptococcus pneumoniae: Virulence factors, pathogenesis, and vaccines. *Microbiological reviews.* **59,** 591-603.

Alouf, J., 2003. Molecular features of the cytolytic pore-forming bacterial protein toxins. *Folia microbiologica.* **48,** 5-16.

Angel, C.S., Ruzek, M., Hostetter, M.K., 1994. Degradation of C3 by Streptococcus pneumoniae. *Journal of Infectious Diseases.* **170,** 600-608.

Arnoldo, A., Curak, J., Kittanakom, S., Chevelev, I., Lee, V.T., Sahebol-Amri, M., Koscik, B., Ljuma, L., Roy, P.J., Bedalov, A., Giaever, G., Nislow, C., Merrill, R.A., Lory, S., Stagljar, I., 2008. Identification of small molecule inhibitors of Pseudomonas aeruginosa exoenzyme S using a yeast phenotypic screen. *PLoS Genetics.* **4,** ate of Pubaton: Feb 2008.

Azzazy, H.M.E. & Highsmith Jr, W.E., 2002. Phage display technology: Clinical applications and recent innovations. *Clinical biochemistry.* **35,** 425-445.

Baba, H., Kawamura, I., Kohda, C., Nomura, T., Ito, Y., Kimoto, T., Watanabe, I., Ichiyama, S., Mitsuyama, M., 2001. Essential role of domain 4 of pneumolysin from streptococcus pneumoniae in cytolytic activity as determined by truncated proteins. *Biochemical and biophysical research communications.* **281,** 37-44.

Bashford, C.L., 2001.
Pore-forming toxins: attack and deffence at the cell surface. **6,** 328-333.

Beckmann, N., Kneuer, R., Gremlich, H.U., Karmouty-Quintana, H., Ble, F.X., Muller, M., 2007. In vivo mouse imaging and spectroscopy in drug discovey. *NMR in biomedicine.* **20,** 154-185.

Beninati, C., Garibaldi, M., Passo, C.L., Mancuso, G., Papasergi, S., Garufi, G., Pernice, I., Teti, G., Felici, F., 2009. Immunogenic mimics of Brucella lipopolysaccharide epitopes. *Peptides.* **30,** 1936-1939.

Benton, K.A., Everson, M.P., Briles, D.E., 1995. A pneumolysin-negative mutant of Streptococcus pneumoniae causes chronic bacteremia rather than acute sepsis in mice. *Infection and immunity.* **63,** 448-455.

Berry, A.M., Alexander, J.E., Mitchell, T.J., Andrew, P.W., Hansman, D., Paton, J.C., 1995. Effect of defined point mutations in the pneumolysin gene on the virulence of Streptococcus pneumoniae. *Infection & Immunity.* **63,** 1969-1974.

Berry, A.M., Ogunniyi, A.D., Miller, D.C., Paton, J.C., 1999. Comparative virulence of Streptococcus pneumoniae strains with insertion-duplication, point, and deletion mutations in the pneumolysin gene. *Infection and immunity.* **67,** 981-985.

Berry, A.M. & Paton, J.C., 2000. Additive attenuation of virulence of Streptococcus pneumoniae by mutation of the genes encoding pneumolysin and other putative pneumococcal virulence proteins. *Infection and immunity.* **68,** 133-140.

Berry, A.M., Yother, J., Briles, D.E., Hansman, D., Paton, J.C., 1989. Reduced virulence of a defined pneumolysin-negative mutant of Streptococcus pneumoniae. *Infection and immunity.* **57,** 2037-2042.

Birnboim, H.C. & Doly, J., 1979. A rapid alkaline extraction procedure for screening recombinant plasmid DNA. **7(6),** 1513-1523.

Block, H., Maertens, B., Spriestersbach, A., Brinker, N., Kubicek, J., Fabis, R., Labahn, J. and Schäfer, F., 2009. Chapter 27 Immobilized-Metal Affinity Chromatography (IMAC): A Review. In Richard R. Burgess and Murray P. Deutscher, ed, *Methods in Enzymology.* 2nd ed. Academic Press. 439-473.

Boulnois, G.J., 1992. Pneumococcal proteins and the pathogenesis of disease caused by *Streptococcus pneumoniae*. **138,** 249-259.

Boulnois, G.J., Paton, J.C., Mitchell, T.J., Andrew, P.W., 1991. Structure and function of pneumolysin, the multifunctional, thiol-activated toxin of Streptococcus pneumoniae. *Molecular microbiology.* **5,** 2611-2616.

Bowers, E.F. & Jeffries, L.R., 1955. Optochin in the identification of S. pneumoniae. **8,** 58-60.

Braun, J.S., Sublett, J.E., Freyer, D., Mitchell, T.J., Cleveland, J.L., Tuomanen, E.I., Weber, J.R., 2002. Pneumococcal pneumolysin and H_2O_2 mediate brain cell apoptosis during meningitis. *Journal of Clinical Investigation.* **109,** 19-27.

Brogden, K.A., 2005. Antimicrobial peptides: pore formers or metabolic inhibitors in bacteria? **3,** 238-250.

Brown, T.A., ed, 1991. *Essential Molecular Biology: A practical approach.* 1st edition ed. New York: Oxford University Press.

Buchwald, U.K., Lees, A., Steinitz, M., Pirofski, L.-., 2005. A peptide mimotope of type 8 pneumococcal capsular polysaccharide induces a protective immune response in mice. *Infection and immunity.* **73,** 325-333.

Butler, J.C., Hofmann, J., Cetron, M.S., Elliott, J.A., Facklam, R.R., Breiman, R.F., 1996. The continued emergence of drug-resistant Streptococcus pneumoniae in the United States: An update from the Centers for Disease Control and prevention's pneumococcal sentinel surveillance system. *Journal of Infectious Diseases.* **174,** 986-993.

Camara, M., Boulnois, G.J., Andrew, P.W., Mitchell, T.J., 1994. A neuraminidase from Streptococcus pneumoniae has the features of a surface protein. *Infection and immunity.* **62,** 3688-3695.

Canvin, J.R., Marvin, A.P., Sivakumaran, M., Paton, J.C., Boulnois, G.J., Andrew, P.W., Mitchell, T.J., 1995. The role of pneumolysin and autolysin in the pathology of pneumonia and septicemia in mice infected with a type 2 pneumococcus. *Journal of Infectious Diseases.* **172,** 119-123.

Carter, D.M., Gagnon, J.-., Damlaj, M., Mandava, S., Makowski, L., Rodi, D.J., Pawelek, P.D., Coulton, J.W., 2006. Phage display reveals multiple contact sites between FhuA, an outer membrane receptor of Escherichia coli, and TonB. *Journal of Molecular Biology.* **357,** 236-251.

Castro-Perez, J.M., 2007. Current and future trends in the application of HPLC-MS to metabolite-identification studies. *Drug discovery today.* **12,** 249-256.

CDC - Centers for Disease Control and Prevention, 2008. *Active Bacterial Core surveillance (ABCs) Report. Emerging Infections Network, Streptococcus pneumoniae, provisional-2008.* [online]. Available at: http://www.cdc.gov/abcs/survreports/spneu08.pdf [2009].

CDC - Centers for Disease Control and Prevention, 1997. *Prevention of Pneumococcal Disease: Recommendations of the Advisory Committee on Immunization Practices (ACIP).* [online]. Available at: http://www.cdc.gov/mmwr/preview/mmwrhtml/00047135.htm [2009].

Chen, D., Misra, M., Sower, L., Peterson, J.W., Kellogg, G.E., Schein, C.H., 2008. Novel inhibitors of anthrax edema factor. *Bioorganic and Medicinal Chemistry.* **16,** 7225-7233.

Cherkasov, A., Hilpert, K., Jenssen, H., Fjell, C.D., Waldbrook, M., Mullaly, S.C., Volkmer, R., Hancock, R.E.W., 2009. Use of artificial intelligence in the design of small peptide antibiotics effective against a broad spectrum of highly antibiotic-resistant superbugs. *ACS Chemical Biology.* **4,** 65-74.

Cho, M.J. & Juliano, R., 1996. Macromolecular versus small-molecule therapeutics: Drug discovery, development and clinical considerations. *Trends in biotechnology.* **14,** 153-158.

Chudwin, D.S., Artrip, S.G., Korenblit, A., 1985. Correlation of serum opsonins with in vitro phagocytosis of Streptococcus pneumoniae. *Infection and immunity.* **50,** 213-217.

Clontech, 2006a. *In-Fusion™ Ready pEcoli-Nterm 6xHN (Linear) Vector Information (Version No. PR621531).* [online]. Available at: http://www.clontech.com/images/pt/PT3871-5.pdf [2006].

Clontech, 2006b. *pAcGFP1-C In-Fusion™ Ready Vector Information (Version No. PR671952).* [online]. Available at: http://www.clontech.com/images/pt/PT3861-5.pdf [2006].

Cockeran, R., Anderson, R., Feldman, C., 2005. Pneumolysin as a vaccine and drug target in the prevention and treatment of invasive pneumococcal disease. *Archivum Immunologiae et Therapiae Experimentalis.* **53,** 189-198.

Cortese, R., Monaci, P., Nicosia, A., Luzzago, A., Felici, F., Galfre, G., Pessi, A., Tramontano, A., Sollazzo, M., 1995. Identification of biologically active peptides using random libraries displayed on phage. *Current opinion in biotechnology.* **6,** 73-80.

Crain, M.J., Waltman II, W.D., Turner, J.S., Yother, J., Talkington, D.F., McDaniel, L.S., Gray, B.M., Briles, D.E., 1990. Pneumococcal surface protein A (PspA) is serologically highly variable and is expressed by all clinically important capsular serotypes of Streptococcus pneumoniae. *Infection and immunity.* **58,** 3293-3299.

Czajkowsky, D.M., Hotze, E.M., Shao, Z., Tweten, R.K., 2004. Vertical collapse of a cytolysin prepore moves its transmembrane beta-hairpins to the membrane. *EMBO Journal.* **23,** 3206-3215.

Dave, S., Carmicle, S., Hammerschmidt, S., Pangburn, M.K., McDaniel, L.S., 2004. Dual roles of PspC, a surface protein of Streptococcus pneumoniae, in binding human secretory IgA and factor H. *Journal of Immunology.* **173,** 471-477.

De Los Toyos, J.R., Mendez, F.J., Aparicio, J.F., Vazquez, F., Suarez, M.D.M.G., Fleites, A., Hardisson, C., Morgan, P.J., Andrew, P.W., Mitchell, T.J., 1996. Functional analysis of pneumolysin by use of monoclonal antibodies. *Infection and immunity.* **64,** 480-484.

Del Mar Garcia-Suarez, M., Cima-Cabal, M.D., Florez, N., Garcia, P., Cernuda-Cernuda, R., Astudillo, A., Vazquez, F., De Los Toyos, J.R., Mendez, F.J., 2004. Protection against pneumococcal pneumonia in mice by monoclonal antibodies to pneumolysin. *Infection and immunity.* **72,** 4534-4540.

Devlin, J.J., Panganiban, L.C., Devlin, P.E., 1990. Random peptide libraries: A source of specific protein binding molecules. *Science.* **249,** 404-406.

Dowell, S.F., Whitney, C.G., Wright, C., Rose, J., C.E, Schuchatt, A., 2003. Seasonal patterns of invasive pneumococcal disease. *Emerging Infectious Diseases.* **9,** 573-579.

Drug & Market Development, 2001. *High-Throughput Screening in Review.* [online]. Available at: http://pharmalicensing.com/public/articles/view/1005568086_3befc0562a952 [2010].

El-Rachkidy, R.G., 2003. *Relationship of structure to function in the pore-forming toxin pneumolysin from Streptococcus pneumoniae.* Ph. D. Department of Microbiology and Immunology; University of Leicester.

El-Rachkidy, R.G., Davies, N.W., Andrew, P.W., 2008. Pneumolysin generates multiple conductance pores in the membrane of nucleated cells. *Biochemical and biophysical research communications.* **368,** 786-792.

Eskola, J., Kilpi, T., Palmu, A., Jokinen, J., Haapakoski, J., Herva, E., Takala, A., Kayhty, H., Karma, P., Kohberger, R., Siber, G., Makela, P.H., 2001. Efficacy of a pneumococcal conjugate vaccine against acute otitis media. *New England Journal of Medicine.* **344,** 403-409.

Feldman, C., *et al*, 2007. Hyaluronidase augments pneumolysin-mediated injury to human ciliated epithelium. *International journal of infectious diseases : IJID : official publication of the International Society for Infectious Diseases,* [online] **11**(1), pp.11-15.

Feldman, C., Mitchell, T.J., Andrew, P.W., Boulnois, G.J., Read, R.C., Todd, H.C., Cole, P.J., Wilson, R., 1990. The effect of Streptococcus pneumoniae pneumolysin on human respiratory epithelium in vitro. *Microbial pathogenesis.* **9,** 275-284.

Feldman, S.R., 1992. The biology and clinical application of systemic glucocorticoids. *Current problems in dermatology.* **4,** 211-235.

Ferrante, A., Rowan-Kelly, B., Paton, J.C., 1984. Inhibition of in vitro human lymphocyte response by the pneumococcal toxin pneumolysin. *Infection and immunity.* **46,** 585-589.

Folgori, A., Tafi, R., Meola, A., Felici, F., Galfre, G., Cortese, R., Monaci, P., Nicosia, A., 1994. A general strategy to identify mimotopes of pathological antigens using only random peptide libraries and human sera. *EMBO Journal.* **13,** 2236-2243.

French, N., Nakiyingi, J., Carpenter, L.M., Lugada, E., Watera, C., Moi, K., Moore, M., Antvelink, D., Mulder, D., Janoff, E.N., Whitworth, J., Gilks, C.F., 2000. 23-Valent pneumococcal polysaccharide vaccine in HIV-1-infected Ugandan adults: Double-blind, randomised and placebo controlled trial. *Lancet.* **355,** 2106-2111.

Geelen, S., Bhattacharyya, C., Tuomanen, E., 1993. The cell wall mediates pneumococcal attachment to and cytopathology in human endothelial cells. *Infection and immunity.* **61,** 1538-1543.

Giddings, K.S., Johnson, A.E., Tweten, R.K., 2003. Redefining cholesterol's role in the mechanism of the cholesterol-dependent cytolysins. *Proceedings of the National Academy of Sciences of the United States of America.* **100,** 11315-11320.

Gilbert, R.J.C., 2002. Pore-forming toxins. *Cellular and Molecular Life Sciences.* **59,** 832-844.

Gilbert, R.J.C., Rossjohn, J., Parker, M.W., Tweten, R.K., Morgan, P.J., Mitchell, T.J., Errington, N., Rowe, A.J., Andrew, P.W., Byron, O., 1998. Self-interaction of pneumolysin, the pore-forming protein toxin of Streptococcus pneumoniae. *Journal of Molecular Biology.* **284,** 1223-1237.

Gilks, C.F., Ojoo, S.A., Ojoo, J.C., Brindle, R.J., Paul, J., Batchelor, B.I.F., Kimari, J.N., Newnham, R., Bwayo, J., Plummer, F.A., Warrell, D.A., 1996. Invasive pneumococcal disease in a cohort of predominantly HIV-1 infected female sex-workers in Nairobi, Kenya. *Lancet.* **347,** 718-723.

Gillespie, S.H., 1989. Aspects of pneumococcal infection including bacterial virulence, host response and vaccination. *Journal of medical microbiology.* **28,** 237-248.

Gillespie, S.H. & Balakrishnan, I., 2000. Pathogenesis of pneumococcal infection. *Journal of medical microbiology.* **49,** 1057-1067.

Girgis, N.I., Farid, Z., Mikhail, I.A., Farrag, I., Sultan, Y., Kilpatrick, M.E., 1989. Dexamethasone treatment for bacterial meningitis in children and adults. *Pediatric Infectious Disease Journal.* **8,** 848-851.

Giudicelli, S. & Tomasz, A., 1984. Attachment of pneumococcal autolysin to wall teichoic acids, an essential step in enzymatic wall degradation. *Journal of Bacteriology.* **158,** 1188-1190.

Goonetilleke, U.R., Ward, S.A., Gordon, S.B., 2009.
Could Proteomic Research Deliver the Next Generation of Treatments for Pneumococcal Meningitis? **2009,** .

Gray, M.G., 2000. Streptococcus pneumoniae infections. In Stevens, D. L. & Kaplan, E. L., eds, *Streptococcal Infections: Clinical Aspects, Microbiology, and Molecular Pathogenesis.* New York: Oxford University Press. 302-325.

Greenwood, B.M., 2007. Corticosteroids for acute bacterial meningitis. *New England Journal of Medicine.* **357,** 2507-2509.

Gustavson, L.M., *et al*, 1994. Biotinylated small molecules. 548/304.1 ed. Seattle, WA/United States: A61K47/48.

Hancock, R.E.W. & Chapple, D.S., 1999. Peptide antibiotics. *Antimicrobial Agents and Chemotherapy.* **43,** 1317-1323.

Haquette, P., Salmain, M., Svedlunq, K., Martel, A., Rudolf, B., Zakrzewski, J., Cordier, S., Roisnel, T., Fosse, C., Jaouen, G., 2007. Cysteine-specific, covalent anchoring of transition organometallic complexes to the protein papain from Carica papaya. *ChemBioChem.* **8,** 224-231.

Hava, D.L. & Camilli, A., 2002. Large-scale identification of serotype 4 Streptococcus pneumoniae virulence factors. *Molecular microbiology.* **45,** 1389-1405.

Henrichsen, J., 1999. Typing of Streptococcus pneumoniae: Past, present, and future. *American Journal of Medicine.* **107,** 50S-54S.

Henriques, B., Kalin, M., Ortqvist, A., Liljequist, B.O., Almela, M., Marrie, T.J., Mufson, M.A., Torres, A., Woodhead, M.A., Svenson, S.B., Kallenius, G., 2000. Molecular epidemiology of Streptococcus pneumoniae causing invasive disease in 5 countries. *Journal of Infectious Diseases.* **182,** 833-839.

Heuck, A.P., Tweten, R.K., Johnson, A.E., 2003. Assembly and topography of the prepore complex in cholesterol-dependent cytolysins. *Journal of Biological Chemistry.* **278,** 31218-31225.

Hill, J., Andrew, P.W., Mitchell, T.J., 1994. Amino acids in pneumolysin important for hemolytic activity identified by random mutagenesis. *Infection and immunity.* **62,** 757-758.

Hirst, R.A., Gosai, B., Rutman, A., Guerin, C.J., Nicotera, P., Andrew, P.W., O'Callaghan, C., 2008. Streptococcus pneumoniae deficient in pneumolysin or autolysin has reduced virulence in meningitis. *Journal of Infectious Diseases.* **197,** 744-751.

Hirst, R.A., Kadioglu, A., O'Callaghan, C., Andrew, P.W., 2004a. The role of pneumolysin in pneumococcal pneumonia and meningitis. *Clinical and experimental immunology.* **138,** 195-201.

Hirst, R.A., Mohammed, B.J., Mitchell, T.J., Andrew, P.W., O'Callaghan, C., 2004b. Streptococcus pneumoniae-induced inhibition of rat ependymal cilia is attenuated by antipneumolysin antibody. *Infection & Immunity.* **72,** 6694-6698.

Hirst, R.A., Sikand, K.S., Rutman, A., Mitchell, T.J., Andrew, P.W., O'Callaghan, C., 2000. Relative roles of pneumolysin and hydrogen peroxide from Streptococcus pneumoniae in inhibition of ependymal ciliary beat frequency. *Infection and immunity.* **68,** 1557-1562.

Horne, D. & Tomasz, A., 1985. Pneumococcal Forssman antigen: Enrichment in mesosomal membranes and specific binding to the autolytic enzyme of Streptococcus pneumoniae. *Journal of Bacteriology.* **161,** 18-24.

Hostetter, M.K., 1986. Serotypic variations among virulent pneumococci in deposition and degradation of covalently bound C3b: Implications for phagocytosis and antibody production. *Journal of Infectious Diseases.* **153,** 682-693.

Houldsworth, S., Andrew, P.W., Mitchell, T.J., 1994. Pneumolysin stimulates production of tumor necrosis factor alpha and interleukin-1beta by human mononuclear phagocytes. *Infection and immunity.* **62,** 1501-1503.

HTS Research, 2010. *What is high-throughput screening?.* [online]. Available at: http://www.htscreening.org/ [2010].

Hu, T. and Seeley, K., 2010. *IMAC Purification of Polyhistidine-tagged Protein Using the AcroPrep™ 96 Filter Plate, Pall Life Sciences PN33354.* [online]. Available at: http://www.pall.com/pdf/04.0943_IMAC_AcroPrepSTR.pdf [2010].

Hummel, G., Reineke, U., Reimer, U., 2006. Translating peptides into small molecules. *Molecular BioSystems.* **2,** 499-508.

Humphrey, J.H., 1948. Hyaluronidase production by pneumococci. **55,** 273-275.

Huss, A., Scott, P., Stuck, A.E., Trotter, C., Egger, M., 2009. Efficacy of pneumococcal vaccination in adults: A meta-analysis. *Canadian Medical Association journal.* **180,** 48-58.

Imai, K. & Takaoka, A., 2006. Comparing antibody and small-molecule therapies for cancer. **6,** 714-727.

Jedrzejas, M.J., 2001. Pneumococcal virulence factors: Structure and function. *Microbiology and Molecular Biology Reviews.* **65,** 187-207.

Jennings, H.J., Lugowski, C., Young, N.M., 1980. Structure of the complex polysaccharide C-substance from *Streptococcus pneumoniae* type 1. **19,** 4712-4719.

Johnson, M.K., Geoffroy, C., Alouf, J.E., 1980. Binding of cholesterol by sulfhydryl-activated cytolysins. *Infection and immunity.* **27,** 97-101.

Jonhson, M.K., 1977. Cellular locaction of pneumolysin. **2,** 243-245.

Kadioglu, A., Gingles, N.A., Grattan, K., Kerr, A., Mitchell, T.J., Andrew, P.W., 2000. Host cellular immune response to pneumococcal lung infection in mice. *Infection and immunity.* **68,** 492-501.

Kadioglu, A., Weiser, J.N., Paton, J.C., Andrew, P.W., 2008. The role of Streptococcus pneumoniae virulence factors in host respiratory colonization and disease. *Nature Reviews.Microbiology.* **6,** 288-301.

Klugman, K.P., 1994. Activity of teicoplanin and vancomycin against penicillin-resistant pneumococci. *European Journal of Clinical Microbiology and Infectious Diseases.* **13,** 1-2.

Korchev, Y.E., Bashford, C.L., Pasternak, C.A., 1992. Differential sensitivity of pneumolysin-induced channels to gating by divalent cations. *Journal of Membrane Biology.* **127,** 195-203.

Korchev, Y.E., Bashford, C.L., Pederzolli, C., Pasternak, C.A., Morgan, P.J., Andrew, P.W., Mitchell, T.J., 1998. A conserved tryptophan in pneumolysin is a determinant of the characteristics of channels formed by pneumolysin in cells and planar lipid bilayers. *Biochemical Journal.* **329,** 571-577.

Kostyukova, N.N., Volkova, M.O., Ivanova, V.V., Kvetnaya, A.S., 1995. A study of pathogenic factors of Streptococcus pneumoniae strains causing meningitis. *FEMS immunology and medical microbiology.* **10,** 133-137.

Lauterbach, S.B., Lanzillotti, R., Coetzer, T.L., 2003. Construction and use of Plasmodium falciparum phage display libraries to identify host parasite interactions. *Malaria Journal.* **2,** ate of Pubaton: 17 e 2003.

Li, W., Heinze, J., Haehnel, W., 2005. Site-Specific Binding of Quinones to Proteins through Thiol Addition and Additionâˆ’Elimination Reactions. *Journal of the American Chemical Society.* **127,** 6140-6141.

Lopalco, P.L., 2007. Measuring the impact of PCV7 in the European Union: why it is a priority. *Eurosurveillance* [Online] **12,** 2009-3221. Available athttp://www.eurosurveillance.org/ViewArticle.aspx?ArticleId=3221.

Lundstrom, T.S. & Sobel, J.D., 2004. Antibiotics for gram-positive bacterial infections: vancomycin, quinupristin-dalfopristin, linezolid, and daptomycin. *Infectious disease clinics of North America.* **18,** 651-668.

Lyon, D.J., Scheel, O., Fung, K.S.C., Cheng, A.F.B., Henrichsen, J., 1996. Rapid emergence of penicillin-resistant pneumococci in Hong Kong. *Scandinavian journal of infectious diseases.* **28,** 375-376.

Malik, P., Terry, T.D., Bellintani, F., Perham, R.N., 1998. Factors limiting display of foreign peptides on the major coat protein of filamentous bacteriophage capsids and a potential role for leader peptidase. *FEBS letters.* **436,** 263-266.

Malley, R., Henneke, P., Morse, S.C., Cieslewicz, M.J., Lipsitch, M., Thompson, C.M., Kurt-Jones, E., Paton, J.C., Wessels, M.R., Golenbock, D.T., 2003. Recognition of pneumolysin by Toll-like receptor 4 confers resistance to pneumococcal infection. *Proceedings of the National Academy of Sciences of the United States of America.* **100,** 1966-1971.

Manco, S., Hernon, F., Yesilkaya, H., Paton, J.C., Andrew, P.W., Kadioglu, A., 2006. Pneumococcal neuraminidases A and B both have essential roles during infection of the respiratory tract and sepsis. *Infection and immunity.* **74,** 4014-4020.

Manson, S.C., Brown, R.E., Cerulli, A., Vidaurre, C.F., 2009. The cumulative burden of oral corticosteroid side effects and the economic implications of steroid use. *Respiratory medicine.* **103,** 975-994.

Martis, E.A., Radhakrishnan, R., Badve, R.R., 2011. High-Throughput Screening: The Hits andLeads of Drug Discovery- An Overview. *Journal of Applied Pharmaceutical Science.* 1, 2-10.

Matthay, K.K., Mentzer, W.C., Wara, D.W., 1981. Evaluation of the opsonic requirements for phagocytosis of Streptococcus pneumoniae serotypes VII, XIV, and XIX by chemiluminescence assay. *Infection and immunity.* **31,** 228-235.

McDaniel, L.S., Yother, J., Vijayakumar, M., 1987. Use of insertional inactivation to facilitate studies of biological properties of pneumococcal surface protein A (PspA). *Journal of Experimental Medicine.* **165,** 381-394.

Mehta, S.R., Huang, R., Yang, M., Zhang, X.-., Kolli, B., Chang, K.-., Hoffman, R.M., Goto, Y., Badaro, R., Schooley, R.T., 2008. Real-time in vivo green fluorescent protein imaging of a murine leishmaniasis model as a new tool for Leishmania vaccine and drug discovery. *Clinical and Vaccine Immunology.* **15,** 1764-1770.

Menestrina, G., Bashford, C.L., Pasternak, C.A., 1990. Pore-forming toxins: Experiments with S. Aureus alpha-toxin, C. Perfringens theta-toxin and E. Coli haemolysin in lipid bilayers, liposomes and intact cells. *Toxicon.* **28,** 477-491.

MERCK, 2009. *Pneumococcal Infections: Gram-Positive Cocci: Merck Manual Professional.* [online]. Available at: http://www.merck.com/mmpe/sec14/ch171/ch171b.html [2010].

MERCK, 2007. *Absorption: Pharmacokinetics: Merck Manual Professional.* [online]. Available at: http://www.merck.com/mmpe/sec20/ch303/ch303b.html [2010].

Miles, A.A., Misra, S.S., Irwin, J.O., 1938. The estimation of the bactericidal power of the blood. **38,** 732-749.

Mitchell, T.J., 1999. Pneumolysin: structure, function and role in disease. In Alouf, J. E. & Popoff, M. R., eds, *Comprehensive Sourcebook of Bacterial Protein Toxins.* Second edition ed. London: Academic Press. 476-495.

Mitchell, T.J., Andrew, P.W., Saunders, F.K., Smith, A.N., Boulnois, G.J., 1991. Complement activation and antibody binding by pneumolysin via a region of the toxin homologous to a human acute-phase protein. *Molecular microbiology.* **5,** 1883-1888.

Mohammed, B.J., Mitchell, T.J., Andrew, P.W., Hirst, R.A., O'Callaghan, C., 1999. The effect of the pneumococcal toxin, pneumolysin on brain ependymal cilia. *Microbial pathogenesis.* **27,** 303-309.

Molyneux, E.M., Walsh, A.L., Forsyth, H., Tembo, M., Mwenechanya, J., Kayira, K., Bwanaisa, L., Njobvu, A., Rogerson, S., Malenga, G., 2002. Dexamethasone treatment in childhood bacterial meningitis in Malawi: A randomised controlled trial. *Lancet.* **360,** 211-218.

Morgan, P.J., Hyman, S.C., Byron, O., Andrew, P.W., Mitchell, T.J., Rowe, A.J., 1994. Modeling the bacterial protein toxin, pneumolysin, in its monomeric and oligomeric form. *Journal of Biological Chemistry.* **269,** 25315-25320.

Morton, D.B. & Griffiths, P.H., 1985. Guidelines on the recognition of pain, distress and discomfort in experimental animals and an hypothesis for assessment. *Veterinary Record.* **116,** 431-436.

Mullen, L.M., Nair, S.P., Ward, J.M., Rycroft, A.N., Henderson, B., 2006. Phage display in the study of infectious diseases. *Trends in microbiology.* **14,** 141-147.

Musher, D.M., 1992.
Infections caused by Streptococcus pneumoniae: clinical spectrum, pathogenesis, immunity, and treatment. **14,** 801-807.

NCBI - National Centre for Biotechnology Information, 2010. *The PubChem Project.* [online]. Available at: http://pubchem.ncbi.nlm.nih.gov/ [2010].

NEB, 2007. *FAQs For Phage Display Peptide Libraries, NEB.* [online]. Available at: http://www.neb.com/nebecomm/tech_reference/protein_tools/phdFaq.asp#1.1 [2010].

NFID, 2009. *Facts About Pneumococcal Disease.* [online]. Available at: http://www.nfid.org/factsheets/pneumofacts.shtml [2010].

Nicholson, J.K., Lindon, J.C., Scarfe, G.B., Wilson, I.D., Abou-Shakra, F., Sage, A.B., Castro-Perez, J., 2001. High-Performance Liquid Chromatography Linked to Inductively Coupled Plasma Mass Spectrometry and Orthogonal Acceleration Time-of-Flight Mass Spectrometry for the Simultaneous Detection and Identification of Metabolites of 2-Bromo-4- trifluoromethyl-[13C]-acetanilide in Rat Urine. *Analytical Chemistry.* **73,** 1491-1494.

Niederman, M.S., Mandell, L.A., Anzueto, A., Bass, J.B., Broughton, W.A., Campbell, G.D., Dean, N., File, T., Fine, M.J., Gross, P.A., Martinez, F., Marrie, T.J., Plouffe, J.F., Ramirez, J., Sarosi, G.A., Torres, A., Wilson, R., Yu, V.L., 2001. Guidelines for the management of adults with community-acquired pneumonia diagnosis, assessment of severity, antimicrobial therapy, and prevention. *American Journal of Respiratory and Critical Care Medicine.* **163,** 1730-1754.

Nollmann, M., Gilbert, R., Mitchell, T., Sferrazza, M., Byron, O., 2004. The Role of Cholesterol in the Activity of Pneumolysin, a Bacterial Protein Toxin. *Biophysical journal.* **86,** 3141-3151.

O'Brien, K.L., Millar, E.V., Zell, E.R., Bronsdon, M., Weatherholtz, R., Reid, R., Becenti, J., Kvamme, S., Whitney, C.G., Santosham, M., 2007. Effect of pneumococcal conjugate vaccine on nasopharyngeal colonization among immunized and unimmunized children in a community-randomized trial. *Journal of Infectious Diseases.* **196,** 1211-1220.

O'Brien, K.L., Wolfson, L.J., Watt, J.P., Henkle, E., Deloria-Knoll, M., McCall, N., Lee, E., Mulholland, K., Levine, O.S., Cherian, T., 2009. Burden of disease caused by Streptococcus pneumoniae in children younger than 5 years: global estimates. *The Lancet.* **374,** 893-902.

Owen, R.H., Boulnois, G.J., Andrew, P.W., Mitchell, T.J., 1994. A role in cell-binding for the C-terminus of pneumolysin, the thiol-activated toxin of Streptococcus pneumoniae. *FEMS microbiology letters.* **121,** 217-221.

Palmer, M., 2001. The family of thiol-activated, cholesterol-binding cytolysins. *Toxicon.* **39,** 1681-1689.

Palmer, M., Harris, R., Freytag, C., Kehoe, M., Tranum-Jensen, J., Bhakdi, S., 1998. Assembly mechanism of the oligomeric streptolysin O pore: The early membrane lesion is lined by a free edge of the lipid membrane and is extended gradually during oligomerization. *EMBO Journal.* **17,** 1598-1605.

Palmer, M., Saweljew, P., Vulicevic, I., Valeva, A., Kehoe, M., Bhakdi, S., 1996. Membrane-penetrating domain of streptolysin O identified by cysteine scanning mutagenesis. *Journal of Biological Chemistry.* **271,** 26664-26667.

Parker, M.W., Buckley, J.T., Postma, J.P.M., Tucker, A.D., Leonard, K., Pattus, F., Tsernoglou, D., 1994. Structure of the Aeromonas toxin proaerolysin in its water-soluble and membrane-channel states. *Nature.* **367,** 292-295.

Porath, J., Carlsson, J., Olsson, I., Belfrage, G., 1975. Metal chelate affinity chromatography, a new approach to protein fractionation. *Nature.* **258,** 598-599.

Pasqualini, R., Koivunen, E., Kain, R., Lahdenranta, J., Sakamoto, M., Stryhn, A., Ashmun, R.A., Shapiro, L.H., Arap, W., Ruoslahti, E., 2000. Aminopeptidase N is a receptor for tumor-homing peptides and a target for inhibiting angiogenesis. *Cancer research.* **60,** 722-727.

Paton, J.C., Andrew, P.W., Boulnois, G.J., Mitchell, T.J., 1993. Molecular analysis of the pathogenicity of Streptococcus pneumoniae: The role of pneumococcal proteins. *Annual Review of Microbiology.* **47,** ate of Pubaton: 1993.

Paton, J.C., Berry, A.M., Lock, R.A., 1986. Cloning and expression in Escherichia coli of the Streptococcus pneumoniae gene encoding pneumolysin. *Infection and immunity.* **54,** 50-55.

Paton, J.C. & Ferrante, A., 1983. Inhibition of human polymorphonuclear leukocyte respiratory burst, bactericidal activity, and migration by pneumolysin. **41,** 1212-1216.

Paton, J.C., Lock, R.A., Hansman, D.J., 1983. Effect of immunization with pneumolysin on survival time of mice challenged with Streptococcus pneumoniae. *Infection and immunity.* **40,** 548-552.

Pericone, C.D., Overweg, K., Hermans, P.W.M., Weiser, J.N., 2000. Inhibitory and bactericidal effects of hydrogen peroxide production by Streptococcus pneumoniae on other inhabitants of the upper respiratory tract. *Infection and immunity.* **68,** 3990-3997.

Pericone, C.D., Park, S., Imlay, J.A., Weiser, J.N., 2003. Factors Contributing to Hydrogen Peroxide Resistance in Streptococcus pneumoniae Include Pyruvate Oxidase (SpxB) and Avoidance of the Toxic Effects of the Fenton Reaction. *Journal of Bacteriology.* **185,** 6815-6825.

Perlman, D. & Bodanszky, M., 1971. Biosynthesis of peptide antibiotics. *Annual Review of Biochemistry.* **40,** 449-464.

Pettigrew, M.M., Fennie, K.P., York, M.P., Daniels, J., Ghaffar, F., 2006. Variation in the presence of neuraminidase genes among Streptococcus pneumoniae isolates with identical sequence types. *Infection and immunity.* **74,** 3360-3365.

Pillutla, R.C., Hsiao, K.-., Beasley, J.R., Brandt, J., Ostergaard, S., Hansen, P.H., Spetzler, J.C., Danielsen, G.M., Andersen, A.S., Brissette, R.E., Lennick, M., Fletcher, P.W., Blume, A.J., Schaffer, L., Goldstein, N.I., 2002. Peptides identify the critical hotspots involved in the biological activation of the insulin receptor. *Journal of Biological Chemistry.* **277,** 22590-22594.

Plotkowski, M.C., Puchelle, E., Beck, G., Jacquot, J., Hannoun, C., 1986. Adherence of type I *Streptococcus pneumoniae* to tracheal epithelium of mice infected with influenza A/PR8 virus. **134,** 1040-1044.

Price, K.E. & Camilli, A., 2009. Pneumolysin localizes to the cell wall of streptococcuspneumoniae. *Journal of Bacteriology.* **191,** 2163-2168.

Quin, L.R., Carmicle, S., Dave, S., Pangburn, M.K., Evenhuis, J.P., McDaniel, L.S., 2005. In vivo binding of complement regulator factor H by Streptococcus pneumoniae. *Journal of Infectious Diseases.* **192,** 1996-2003.

Rajotte, D. & Ruoslahti, E., 1999. Membrane dipeptidase is the receptor for a lung-targeting peptide identified by in vivo phage display. *Journal of Biological Chemistry.* **274,** 11593-11598.

Rani, G.R., Victor, A., Usha, R., 2005. Invasive Pneumococcal Disease; Current Management Challenges in a case of severe infection. **37,** 113-115.

Rautio, J., Kumpulainen, H., Heimbach, T., Oliyai, R., Oh, D., Jarvinen, T., Savolainen, J., 2008. Prodrugs: Design and clinical applications. *Nature Reviews Drug Discovery.* **7,** 255-270.

Reinert, R.R., 2009. The antimicrobial resistance profile of Streptococcus pneumoniae. *Clinical Microbiology and Infection.* **15,** 7-11.

Reinert, R.R., Al-Lahham, A., Lemperle, M., Tenholte, C., Briefs, C., Haupts, S., Gerards, H.H., Lutticken, R., 2002. Emergence of macrolide and penicillin resistance among invasive pneumococcal isolates in Germany. *Journal of Antimicrobial Chemotherapy.* **49,** 61-68.

Richard B. Johnston, Jr., 1991. Pathogenesis of pneumococcal pneumonia. *Reviews of infectious diseases.* **13,** S509-S517.

Riesenfeld-Orn, I., Wolpe, S., Garcia-Bustos, J.F., Hoffmann, M.K., Tuomanen, E., 1989. Production of interleukin-1 but not tumor necrosis factor by human monocytes stimulated with pneumococcal cell surface components. *Infection and immunity.* **57,** 1890-1893.

Riley, P., 2000. Pneumococcal infections. *Primary care update for Ob/Gyns.* **7,** 20-25.

Rodriguez-Tudela, J.L., de Felipe, F.L., Martinez-Suarez, J.V., Fenoll, A., 1992. Comparative in-vitro activity of four peptide antibiotics against penicillin-resistant Streptococcus pneumoniae isolated from cerebrospinal fluid (CSF). *J.Antimicrob.Chemother.* **29,** 299-302.

Roe, S., ed, 2001. *Protein purification techniques - A pratical approach.* 2nd edition ed. New York: Oxford University Press.

Rosenow, C., Ryan, P., Weiser, J.N., Johnson, S., Fontan, P., Ortqvist, A., Masure, H.R., 1997. Contribution of novel choline-binding proteins to adherence, colonization and immunogenicity of Streptococcus pneumoniae. *Molecular microbiology.* **25,** 819-829.

Rossjohn, J., Feil, S.C., McKinstry, W.J., Tweten, R.K., Parker, M.W., 1997. Structure of a cholesterol-binding, thiol-activated cytolysin and a model of its membrane form. *Cell.* **89,** 685-692.

Rossjohn, J., Gilbert, R.J.C., Crane, D., Morgan, P.J., Mitchell, T.J., Rowe, A.J., Andrew, P.W., Paton, J.C., Tweten, R.K., Parker, M.W., 1998. The molecular mechanism of pneumolysin, a virulence factor from Streptococcus pneumoniae. *Journal of Molecular Biology.* **284,** 449-461.

Rubins, J.B., Charboneau, D., Fasching, C., Berry, A.M., Paton, J.C., Alexander, J.E., Andrew, P.W., Mitchell, T.J., Janoff, E.N., 1996. Distinct roles for pneumolysin's cytotoxic and complement activities in the pathogenesis of pneumococcal pneumonia. *American Journal of Respiratory and Critical Care Medicine.* **153,** 1339-1346.

Rubins, J.B., Duane, P.G., Clawson, D., Charboneau, D., Young, J., Niewoehner, D.E., 1993. Toxicity of pneumolysin to pulmonary alveolar epithelial cells. *Infection and immunity.* **61,** 1352-1358.

Russel, M., Lowman, H.B. and Clackson, T., 2004. Introduction to phage biology and phage display. In Lowman, H. B. & Clackson, T., eds, *Phage Display: A Practical Approach.* New York, USA: Oxford University Press. 1-26.

RxList Inc., 2007. *Relafen (Nabumetone) Drug Information: Uses, Side Effects, Drug Interactions and Warnings at RxList.* [online]. Available at: http://www.rxlist.com/relafen-drug.htm [2010].

Saha, S.K., Khan, N.Z., Ahmed, A.S.M.N.U., Amin, M.R., Hanif, M., Mahbub, M., Anwar, K.S., Qazi, S.A., Kilgore, P., Baqui, A.H., 2009. Neurodevelopmental sequelae in pneumococcal meningitis cases in Bangladesh: A comprehensive follow-up study. *Clinical Infectious Diseases.* **48,** S90-S96.

Saiki, R.K., Gelfand, D.H., Stoffel, S., Scharf, S.J., Higuchi, R., Horn, G.T., Mullis, K.B., Erlich, H.A., 1988. Primer-directed enzymatic amplification of DNA with a thermostable DNA polymerase. *Science.* **239,** 487-491.

Sambrook, J. and Russel, D.W., eds, 2001. *Molecular Cloning: A Laboratory Manual.* 3rd Edition ed. New York: Cold Spring Harbor Laboratory Press, Cold Spring Harbor.

Santana-Arciaga, R., 1996. Corticosteroids as adjunctive therapy in bacterial meningitis: a systematic review of clinical trials. **25,** 48-60.

Saunders, F.K., Mitchell, T.J., Walker, J.A., Andrew, P.W., Boulnois, G.J., 1989. Pneumolysin, the thiol-activated toxin of Streptococcus pneumoniae, does not require a thiol group for in vitro activity. *Infection & Immunity.* **57,** 2547-2552.

Scarborough, M., Gordon, S.B., Whitty, C.J.M., French, N., Njalale, Y., Chitani, A., Peto, T.E.A., Lalloo, D.G., Zijlstra, E.E., 2007. Corticosteroids for bacterial meningitis in adults in sub-Saharan Africa. *New England Journal of Medicine.* **357,** 2441-2450.

Schepetkin, I.A., Khlebnikov, A.I., Kirpotina, L.N., Quinn, M.T., 2006. Novel small-molecule inhibitors of anthrax lethal factor identified by high-throughput screening. *Journal of medicinal chemistry.* **49,** 5232-5244.

Schrag, S., Bealle, B. and Dowell, S., 2001. Resistant Pneumococcal Infections: the Burden of Disease and Challenges in Monitoring and Controlling Antimicrobial Resistance. WHO/CDS/CSR/DRS/2001.6 ed. Geneva, Switzerland: World Health Organization.

Scott, J.A.G., Hall, A.J., Dagan, R., Dixon, J.M.S., Eykyn, S.J., Fenoll, A., Hortal, M., Jette, L.P., Jorgensen, J.H., Lamothe, F., Latorre, C., Macfarlane, J.T., Shlaes, D.M., Smart, L.E., Taunay, A., 1996. Serogroup-specific epidemiology of Streptococcus pneumoniae: Associations with age, sex, and geography in 7,000 episodes of invasive disease. *Clinical Infectious Diseases.* **22,** 973-981.

Shaper, M., Hollingshead, S.K., Benjamin, J., W.H, Briles, D.E., 2004. PspA protects Streptococcus pneumoniae from killing by apolactoferrin, and antibody to PspA enhances killing of pneumococci by apolactoferrin. *Infection and immunity.* **72,** 5031-5040.

Shapiro, E.D., Berg, A.T., Austrian, R., Schroeder, D., Parcelis, V., Margolis, A., Adair, R.K., Clemens, J.D., 1991. The protective efficacy of polyvalent pneumococcal polysaccharide vaccine. *New England Journal of Medicine.* **325,** 1453-1460.

Shepard, L.A., Heuck, A.P., Hamman, B.D., Rossjohn, J., Parker, M.W., Ryan, K.R., Johnson, A.E., Tweten, R.K., 1998. Identification of a membrane-spanning domain of the thiol-activated pore-forming toxin Clostridium perfringens perfringolysin O: An alpha-helical to beta-sheet transition identified by fluorescence spectroscopy. *Biochemistry.* **37,** 14563-14574.

Shepard, L.A., Shatursky, O., Johnson, A.E., Tweten, R.K., 2000. The mechanism of pore assembly for a cholesterol-dependent cytolysin: Formation of a large prepore complex precedes the insertion of the transmembrane beta-hairpins. *Biochemistry.* **39,** 10284-10293.

Shire, S.J., Gombotz, W., Bechtold-Peters, K. and Andya, J., eds, 2010. *Current trends in monoclonal antibody development and manufacturing, Vol. 11 (Biotechnology: Pharmaceutical Aspects).* New York: Springer-Verlag New York Inc.

Siber, G.R., Klugman, K.P. and Mäkelä, P.H., eds, 2008. *Pneumococcal vaccines: the impact of conjugate vaccine.* Washington, DC: ASM Press.

Slatin, S.L., Abrams, C.K., English, L., 1990. Delta-endotoxins form cation-selective channels in planar lipid bilayers. *Biochemical and biophysical research communications.* **169,** 765-772.

Smith, B.L. & Hostetter, M.K., 2000. C3 As substrate for adhesion of Streptococcus pneumoniae. *Journal of Infectious Diseases.* **182,** 497-508.

Smith, C.M., 2005. *Development of a new vaccine strategy against Streptococcus pneumoniae.* Ph. D. Department of Infection, Immunity and Inflammation; University of Leicester.

Smith, C.M., Passo, C.L., Scuderi, A., Kolberg, J., Baxendale, H., Goldblatt, D., Oggioni, M.R., Felici, F., Andrew, P.W., 2009. Peptide mimics of two pneumococcal capsular polysaccharide serotypes (6B and 9V) protect mice from a lethal challenge with *Streptococcus pneumoniae*. *European journal of immunology.* **39,** 1527-1535.

Smith, G.P., 1985. Filamentous fusion phage: Novel expression vectors that display cloned antigens on the virion surface. *Science.* **228,** 1315-1317.

Solovyova, A.S., Nöllmann, M., Mitchell, T.J., Byron, O., 2004. The Solution Structure and Oligomerization Behavior of Two Bacterial Toxins: Pneumolysin and Perfringolysin O. *Biophysical journal.* **87,** 540-552.

Soltero, R., 2005. Oral Protein and Peptide Drug Delivery. In Binghe Wang, Teruna J. Siahaan,Richard Soltero, ed, *Drug Delivery.* 189-200.

Sowdhamini, R., Mitchell, T.J., Andrew, P.W., Morgan, P.J., 1997. Structural and functional analogy between pneumolysin and proaerolysin. *Protein engineering.* **10,** 207-215.

Srivastava, A., Henneke, P., Visintin, A., Morse, S.C., Martin, V., Watkins, C., Paton, J.C., Wessels, M.R., Golenbock, D.T., Malley, R., 2005. The apoptotic response to pneumolysin is toll-like receptor 4 dependent and protects against pneumococcal disease. *Infection and immunity.* **73,** 6479-6487.

Thompson, J.D., Higgins, D.G., Gibson, T.J., 1994. CLUSTAL W: Improving the sensitivity of progressive multiple sequence alignment through sequence weighting, position-specific gap penalties and weight matrix choice. *Nucleic acids research.* **22,** 4673-4680.

Tilley, S.J., Orlova, E.V., Gilbert, R.J.C., Andrew, P.W., Saibil, H.R., 2005. Structural basis of pore formation by the bacterial toxin pneumolysin. *Cell.* **121,** 247-256.

Trappetti, C., Kadioglu, A., Carter, M., Hayre, J., Iannelli, F., Pozzi, G., Andrew, P.W., Oggioni, M.R., 2009. Sialic acid: A preventable signal for pneumococcal biofilm formation, colonization, and invasion of the host. *Journal of Infectious Diseases.* **199,** 1497-1505.

Trepel, M., Arap, W., Pasqualini, R., 2002. In vivo phage display and vascular heterogeneity: Implications for targeted medicine. *Current opinion in chemical biology.* **6,** 399-404.

Tu, A.H.T., Fulgham, R.L., Mccrory, M.A., Briles, D.E., Szalai, A.J., 1999. Pneumococcal surface protein A inhibits complement activation by Streptococcus pneumoniae. *Infection and immunity.* **67,** 4720-4724.

Tuomanen, E.I., Mitchell, T.J., Morrison, D.A. and Spratt, B.G., eds, 2004. *The Pneumococcus.* Washington, D.C.: American Society for Microbiology.

Tweten, R.K., 2005. Cholesterol-dependent cytolysins, a family of versatile pore-forming toxins. *Infection and immunity.* **73,** 6199-6209.

Van Dam, J.E.G., Fleer, A., Snippe, H., 1990. Immunogenicity and immunochemistry of Streptococcus pneumoniae capsular polysaccharides. *Antonie van Leeuwenhoek, International Journal of General and Molecular Microbiology.* **58,** 1-47.

Van De Beek, D., De Gans, J., McIntyre, P., Prasad, K., 2007. Corticosteroids for acute bacterial meningitis. *Cochrane Database of Systematic Reviews.* Arte Number: 004405. ate of Pubaton: 2007.

Waheed, A.A., Shimada, Y., Heijnen, H.F.G., Nakamura, M., Inomata, M., Hayashi, M., Iwashita, S., Slot, J.W., Ohno-Iwashita, Y., 2001. Selective binding of perfringolysin O derivative to cholesterol-rich membrane microdomains (rafts). *Proceedings of the National Academy of Sciences of the United States of America.* **98,** 4926-4931.

Walker, J.A., Allen, R.L., Falmagne, P., 1987. Molecular cloning, characterization, and complete nucleotide sequence of the gene for pneumolysin, the sulfhydryl-activated toxin of Streptococcus pneumoniae. *Infection and immunity.* **55,** 1184-1189.

Watson, D.A. & Musher, D.M., 1990. Interruption of capsule production in *Streptococcus pneumonia* serotype 3 by insertion of transposon Tn916. **58,** 3135-3138.

WHO, 2009. *WHO | Acute Respiratory Infections (September 2009).* [online]. Available at: http://www.who.int/vaccine_research/diseases/ari/en/index3.html [2009].

WHO, 2008. *Weekly epidemiological record: No.42, 2008, 83rd year* [online]. Available at: http://www.who.int/wer/2008/wer8342.pdf [2009].

WHO, 2007. *Weekly epidemiological record: No.12, 2007, 82nd year.* [online]. Available at: http://www.who.int/wer/2007/wer8212.pdf [2009].

Wilken, J. & Kent, S.B., 1998. Chemical protein synthesis. *Current opinion in biotechnology.* **9,** 412-426.

Willats, W.G.T., 2002. Phage display: practicalities and prospects. *Plant Molecular Biology.* **50,** 837-854.

Winkelstein, J.A. & Tomasz, A., 1978. Activation of the Alternative Complement Pathway by Pneumococcal Cell Wall Teichoic Acid. **120,** 174-178.

Zacharakis, G., Kambara, H., Shih, H., Ripoll, J., Grimm, J., Saeki, Y., Weissleder, R., Ntziachristos, V., 2005. Volumetric tomography of fluorescent proteins through small animals in vivo. *Proceedings of the National Academy of Sciences of the United States of America.* **102,** 18252-18257.

Zdanovsky, A.G., Karassina, N.V., Simpson, D., Zdanovskaia, M.V., 2001. Peptide phage display library as source for inhibitors of clostridial neurotoxins. *Journal of protein chemistry.* **20,** 73-80.

Zhang, J.R., Mostov, K.E., Lamm, M.E., Nanno, M., Shimida, S., Ohwaki, M., Tuomanen, E., 2000a. The polymeric immunoglobulin receptor translocates pneumococci across nasopharyngeal human epithelial cells. *Cell.* **102,** 827-837.

Zhang, L., Dhillon, P., Yan, H., Farmer, S., Hancock, R.E.W., 2000b. Interactions of bacterial cationic peptide antibiotics with outer and cytoplasmic membranes of Pseudomonas aeruginosa. *Antimicrobial Agents and Chemotherapy.* **44,** 3317-3321.